

© 2006 by Thomas James McElmurry. All rights reserved.

COLLINEAR SINGULARITIES AND THE FACTORIZATION SCALE IN  
PERTURBATIVE QCD

BY

THOMAS JAMES MCELMURRY

B.S., Bethel College, 2001

B.A., Bethel College, 2001

DISSERTATION

Submitted in partial fulfillment of the requirements  
for the degree of Doctor of Philosophy in Physics  
in the Graduate College of the  
University of Illinois at Urbana-Champaign, 2006

Urbana, Illinois

# Abstract

We discuss several issues related to collinear singularities and the choice of the factorization scale in perturbative QCD calculations. First, we argue in favor of the use of a bottom-quark distribution function, which sums collinear logarithms, in the calculation of the cross section for Higgs-boson production in association with bottom quarks. As a testing ground for Higgs searches, we propose a measurement of  $Z$ -boson production in association with heavy quarks, using an inclusive heavy-quark tagging technique. Next, we present a calculation of the next-to-leading-order QCD corrections to Drell-Yan production of a  $W$  boson, regulating the collinear singularities with a nonzero quark mass and the infrared and ultraviolet singularities with dimensional regularization. Finally, we present the collinear factorization scheme, in which only collinear physics is absorbed into the parton distribution functions. We provide a physically motivated method for choosing the factorization scale in this scheme, and show, for the case of Drell-Yan production of an electroweak gauge boson, that the next-to-leading-order QCD corrections are very small for this choice of factorization scale.

# Acknowledgments

Most things begin with family, and I must thank mine. My parents, who read to me until I could read to them, and somehow taught me a desire for learning that no amount of education has yet been able to extinguish. My sister, Katie, who continually reminds me—as well as anyone can—that there is life outside of physics. My grandparents, whose lives have shown a strength of character that I can never hope to equal, but maybe I can die trying.

I must thank many great teachers, in physics and in other fields. At Irondale High School: Bill Beck, Fred Dressler, Bob Iverson, Danny Meyer, and Beth Weaver. At Bethel College: R. A. Carlsen, Brian Beecken, Tom Greenlee, and Richard Peterson in the Physics Department; Bill Kinney and David Wetzell in the Math Department; and others including Don Alexander, Thomas Becknell, Greg Boyd, Joey Horstman, and Don Postema.

I must thank my adviser, Scott Willenbrock, for sage advice, for a keen understanding of physics and a talent for explaining it, for almost always knowing where to look, for finding the right things to say at all the key moments, and for understanding the importance of Ebertfest.

I must thank my collaborator, Fabio Maltoni, for his excellent ideas and his patience with a naïve graduate student.

I must thank J. Collins, D. Soper, and G. Sterman for valuable comments and discussions pertaining to the work presented in Chapter 4.

The life of a student would not be the same without other students, and I must thank my fellow students for making it a life worth remembering. My friends at Bethel, too many

to name here, but especially Mike, Will, MJ, Reggie, and Jeremy, who in ways large and small changed the way I look at the world. My fellow physics students at UIUC: Dave, for keeping this theorist in his place; Rahul, for knowing the questions when I didn't know the answers; Sean, for knowing the answers when I didn't know the questions; David, for always being interested in everything. Jeremy, for clarity, obscurity, and whimsy, inseparably bound together; William, for being William; Damian, for breathing Unix and ably demonstrating what I would become as a senior graduate student; Aaron, for calling all those games, listening to my rants, and being my advance scout in Madison. And the next generation: Josh, for a stealthy wit and general imperturbability; and Putty, for old-school panache, and for catching all my mistakes. I know I'm leaving the office in good hands.

Speaking of which, I must thank Debbie, not only for keeping Loomis cleaner than any of us have a right to expect, but also for many doses of much-needed late-night perspective.

I must thank the good folks at Boardman's Art Theatre, That's Rentertainment, and Roger Ebert's Overlooked Film Festival. I would not now be sane, if sane is what I am, without them.

I must thank those who pay the bills. This work was supported in part by the Department of Physics at the University of Illinois at Urbana-Champaign, and in part by the U. S. Department of Energy under contract No. DE-FG02-91ER40677.

At the end of all things may I thank the Creator for letting me play in His Universe.

# Table of Contents

List of Tables . . . . .	vii
List of Figures . . . . .	viii
Chapter 1 Introduction . . . . .	1
Chapter 2 Inclusive Production of a Higgs or $Z$ Boson in Association with Heavy Quarks . . . . .	3
2.1 Introduction . . . . .	3
2.2 Higgs production in association with heavy quarks . . . . .	5
2.3 $Z$ production in association with heavy quarks . . . . .	9
2.4 Conclusions . . . . .	13
Chapter 3 QCD Corrections to the Drell-Yan Cross Section . . . . .	15
3.1 $q\bar{q} \rightarrow W$ (tree level) . . . . .	16
3.2 $q\bar{q} \rightarrow W$ (one loop) . . . . .	17
3.2.1 Vertex correction . . . . .	18
3.2.2 Wavefunction renormalization . . . . .	25
3.3 $q\bar{q} \rightarrow gW$ (tree level) . . . . .	32
3.4 $gq \rightarrow qW$ (tree level) . . . . .	45
Chapter 4 Choosing the Factorization Scale in Perturbative QCD . . . . .	50
4.1 Introduction . . . . .	50
4.2 The collinear region . . . . .	52
4.2.1 Initial gluons . . . . .	54
4.2.2 Real and virtual gluons . . . . .	59
4.3 Results . . . . .	71
4.4 Discussion . . . . .	73
References . . . . .	80
Author's Biography . . . . .	83

# List of Tables

2.1	The factorization scale relative to the Higgs mass, $\mu_F/m_h$ , at the Tevatron and the LHC. The factorization scale is determined by the point at which the curves in Fig. 2.2 reach 85% of their values on the collinear plateau. . . . .	7
2.2	Cross sections (pb) for the various contributions to $Z$ production in association with heavy quarks. We use the MRST2002 NNLO parton distribution functions [35] with $\mu_F = \mu_R = M_Z/3$ . . . . .	13
4.1	Couplings of the quarks to electroweak gauge bosons. Here $s_W = \sin\theta_W$ , $c_W = \cos\theta_W$ , and $V_{ij}$ denotes an element of the Cabibbo-Kobayashi-Maskawa matrix. . . . .	54

# List of Figures

2.1	$\sigma(\tilde{b}\tilde{b} \rightarrow h)/\sigma(gg \rightarrow hb\bar{b})$ vs. $m_h$ at the Tevatron and the LHC, using MRST2001 LO parton distribution functions [34], $m_b = 4.7$ GeV, and $\mu_F (= \mu_R) = m_h/4$ .	6
2.2	$-t d\sigma/dt$ vs. $\sqrt{-t}/m_h$ for $gb \rightarrow hb$ at the Tevatron and the LHC. The factorization scale for $b\bar{b} \rightarrow h$ should be chosen near the end of the collinear plateau. . . . .	8
2.3	$\sigma(\tilde{b}\tilde{b} \rightarrow h)/\sigma(gg \rightarrow hb\bar{b})$ vs. $m_h$ at the Tevatron and the LHC, using MRST2001 LO parton distribution functions [34], $m_b = 4.7$ GeV, and $\mu_F (= \mu_R)$ determined from the end of the collinear plateau in Fig. 2.2 (listed in Table 2.1). .	9
2.4	Feynman diagram for $Q\bar{Q} \rightarrow Z$ ( $Q = c, b$ ). The presence of heavy quarks in the final state is implied by the initial-state heavy quarks. . . . .	9
2.5	Feynman diagrams for $q\bar{q} \rightarrow ZQ\bar{Q}$ , where the $Z$ couples to the light quarks.	10
2.6	Feynman diagrams for $qQ \rightarrow ZqQ$ , where the $Z$ couples to the light quarks .	10
2.7	Factorization-scale dependence of $b\bar{b} \rightarrow Z$ at LO, NLO, and NNLO at the Tevatron and the LHC. Only processes in which the $Z$ couples to the heavy quarks are included. Also shown is $gg \rightarrow Zb\bar{b}$ at LO, using $m_b = 4.7$ GeV. We use the LO, NLO, and NNLO parton distribution functions MRST2001 LO [34] and MRST2002 [35]. . . . .	11
2.8	Same as Fig. 2.7, but for $c\bar{c} \rightarrow Z$ . For $gg \rightarrow Zc\bar{c}$ , we use $m_c = 1.4$ GeV. . . . .	12
3.1	The tree-level Feynman diagram for $q\bar{q} \rightarrow W$ . . . . .	16
3.2	The vertex correction to $q\bar{q} \rightarrow W$ . . . . .	18
3.3	The wavefunction-renormalization corrections to $q\bar{q} \rightarrow W$ . . . . .	25
3.4	Feynman diagrams for the real-gluon-emission process $q\bar{q} \rightarrow gW$ . . . . .	32
3.5	Feynman diagrams for the initial-gluon process $gq \rightarrow qW$ . . . . .	45
4.1	Drell-Yan production of an electroweak gauge boson $V$ . . . . .	53
4.2	Correction to the production of an electroweak gauge boson $V$ due to initial gluons. . . . .	54
4.3	The quantity $-t d\tilde{\sigma}_{g\bar{q}+qg}^{(1)}/dt$ defined in Eq. (4.14), normalized to its limiting value as $t \rightarrow 0$ , for the case of real $Z$ -boson production at the Tevatron. The curve passes through 0.5 when $\sqrt{-t} = 0.53Q$ . . . . .	58
4.4	The factorization-scale dependence in the collinear scheme of the LO and initial-gluon NLO contributions to real $Z$ -boson production at the Tevatron. The factorization scale indicated by the plateau is $0.53Q$ . . . . .	59

4.5	Correction to the production of an electroweak gauge boson $V$ due to real gluon emission. . . . .	60
4.6	Vertex correction to the production of an electroweak gauge boson $V$ . . . . .	61
4.7	Wavefunction renormalization correction to the production of an electroweak gauge boson $V$ . . . . .	62
4.8	The region of Feynman-parameter space bounded by $x = 0$ , $y = 0$ , and $z = 0$ is mapped by Eq. (4.26) onto the region of Mandelstam-variable space bounded by $s = \infty$ , $t = 0$ , and $u = 0$ . The real-gluon contribution is bounded by $s = S$ (or $z = z_0$ ), while the virtual-gluon contribution extends all the way to $z = 0$ (or $s = \infty$ ). The heavy lines represent the collinear singularities, and the black dots represent the infrared singularity. . . . .	65
4.9	The counterterms corresponding to the $t$ - and $u$ -channel collinear singularities are formed by integrating over the shaded strips. We must be careful to avoid double-counting in the region where the two strips overlap. . . . .	67
4.10	The quantities $-t d\tilde{\sigma}_{g\bar{q}+q\bar{q}}^{(1)}/dt$ , defined in Eq. (4.14), and $-t d\tilde{\sigma}_{q\bar{q}}^{(1)}/dt$ , defined in Eq. (4.37), normalized to their respective limiting values as $t \rightarrow 0$ , for the case of real $Z$ -boson production at the Tevatron. The initial-gluon curve passes through 0.5 when $\sqrt{-t} = 0.53Q$ , and the real- and virtual-gluon curve when $\sqrt{-t} = 0.57Q$ . . . . .	69
4.11	The factorization-scale dependence in the collinear scheme of the LO and NLO contributions to real $Z$ -boson production at the Tevatron. The factorization scales indicated by the plateaux are $0.53Q$ for initial gluons and $0.57Q$ for real and virtual gluons. . . . .	70
4.12	The factorization-scale dependence in the collinear scheme of the LO and NLO contributions to virtual $Z$ -boson production at the LHC, with $Q = 650$ GeV. The factorization scales indicated by the plateaux are $0.52Q$ for initial gluons and $0.61Q$ for real and virtual gluons. . . . .	71
4.13	The factorization-scale dependence in the collinear scheme of the LO and NLO contributions to virtual $Z$ -boson production at the Tevatron, with $Q = 280$ GeV. The factorization scales indicated by the plateaux are $0.44Q$ for initial gluons and $0.64Q$ for real and virtual gluons. . . . .	72
4.14	The factorization-scale dependence in the collinear scheme of the LO and NLO contributions to virtual $Z$ -boson production at the LHC, with $Q = 2$ TeV. The factorization scales indicated by the plateaux are $0.43Q$ for initial gluons and $0.62Q$ for real and virtual gluons. . . . .	72
4.15	The factorization-scale dependence in the collinear scheme of the LO and NLO contributions to virtual $Z$ -boson production at the Tevatron, with $Q = 490$ GeV. The factorization scales indicated by the plateaux are $0.37Q$ for initial gluons and $0.63Q$ for real and virtual gluons. . . . .	74
4.16	The factorization-scale dependence in the collinear scheme of the LO and NLO contributions to virtual $Z$ -boson production at the LHC, with $Q = 3.5$ TeV. The factorization scales indicated by the plateaux are $0.37Q$ for initial gluons and $0.58Q$ for real and virtual gluons. . . . .	74

4.17	The factorization-scale dependence in the collinear scheme of the LO and NLO contributions to virtual $Z$ -boson production at the Tevatron, with $Q = 700$ GeV. The factorization scales indicated by the plateaux are $0.33Q$ for initial gluons and $0.58Q$ for real and virtual gluons. . . . .	75
4.18	The factorization-scale dependence in the collinear scheme of the LO and NLO contributions to virtual $Z$ -boson production at the LHC, with $Q = 5$ TeV. The factorization scales indicated by the plateaux are $0.32Q$ for initial gluons and $0.53Q$ for real and virtual gluons. . . . .	75
4.19	The factorization-scale dependence in the collinear scheme of the LO and NLO contributions to virtual $Z$ -boson production at the Tevatron, with $Q = 910$ GeV. The factorization scales indicated by the plateaux are $0.28Q$ for initial gluons and $0.53Q$ for real and virtual gluons. . . . .	76
4.20	The factorization-scale dependence in the collinear scheme of the LO and NLO contributions to virtual $Z$ -boson production at the LHC, with $Q = 6.5$ TeV. The factorization scales indicated by the plateaux are $0.28Q$ for initial gluons and $0.49Q$ for real and virtual gluons. . . . .	76
4.21	The factorization-scale dependence in the collinear scheme of the LO and NLO contributions to virtual photon production in $pp$ collisions at $\sqrt{S} = 38.8$ GeV, with $Q = 5$ GeV. The factorization scales indicated by the plateaux are $0.48Q$ for initial gluons and $0.64Q$ for real and virtual gluons. . . . .	77
4.22	The factorization-scale dependence in the collinear scheme of the LO and NLO contributions to virtual photon production in $pp$ collisions at $\sqrt{S} = 38.8$ GeV, with $Q = 20$ GeV. The factorization scales indicated by the plateaux are $0.27Q$ for initial gluons and $0.48Q$ for real and virtual gluons. . . . .	77
4.23	The factorization-scale dependence in the collinear scheme of the LO and real- and virtual-gluon NLO contributions to virtual photon production in $pp$ collisions at $\sqrt{S} = 38.8$ GeV, with $Q = 20$ GeV. The terms proportional to $[1/(1-z)]_+$ and $[\ln(1-z)/(1-z)]_+$ are plotted separately. The factorization scale indicated by the real- and virtual-gluon plateau is $0.48Q$ . . . . .	79

# Chapter 1

## Introduction

Cross sections for scattering processes at hadron colliders are calculated using the parton model, in which a hadron is thought of as a collection of quarks, antiquarks, and gluons (collectively called “partons”), each carrying some fraction of the hadron’s momentum. The number density of particles of species  $i$  with momentum fraction  $x$  ( $0 \leq x \leq 1$ ) is given by the parton distribution function  $f_i(x)$ . At present there is no way to predict the forms of these functions theoretically, and they must therefore be extracted from experimental data.

The cross section  $\sigma$  for a hadronic scattering process is given by a convolution integral of the form

$$\sigma = \sum_{i,j} \int_0^1 dx_1 \int_0^1 dx_2 f_i(x_1) f_j(x_2) \hat{\sigma}_{ij}(x_1, x_2),$$

where  $\hat{\sigma}_{ij}$  denotes the partonic cross section with partons  $i$  and  $j$  in the initial state. At sufficiently high energies, such as those found at hadron colliders, this partonic cross section can be calculated using perturbation theory, while the nonperturbative physics involved in the hadronic structure is encapsulated in the parton distribution functions.

Higher-order corrections in parton-model calculations often involve large logarithms of the form  $\ln(Q/m)$ , where  $m$  is the mass of a parton and  $Q$  is a mass scale characterizing the process being studied (e.g.  $M_Z$  in the case of  $Z$ -boson production). These logarithms arise from regions of phase space where two partons’ momenta are nearly collinear, and degrade the convergence of the perturbation series. In fact, since quark masses are often neglected (and gluons really are massless), they produce collinear divergences, which must be dealt

with if we are to obtain sensible results from parton-model calculations beyond the leading order.

Fortunately, these collinear divergences can be thought of as corresponding to corrections to the parton distribution functions due to the splitting of one parton into a pair of collinear partons. They can thus be absorbed by a renormalization of the parton distribution functions, leaving only finite corrections to the hard-scattering cross section. This requires the introduction of a factorization scale  $\mu$ , which can be a source of uncertainty in theoretical predictions. Exact cross sections (to all orders in perturbation theory) must be independent of  $\mu$ , but fixed-order results need not be. Leading-order and next-to-leading-order results often exhibit significant dependence on  $\mu$ . Hence one must either report a sizable theoretical uncertainty due to factorization-scale choice, or (preferably) choose  $\mu$  in such a way that one can have confidence in the validity of the results.

In this thesis we discuss several issues related to collinear divergences and the factorization scale. In Chapter 2 we argue for the use of a bottom-quark distribution function in the calculation of associated production of a Higgs boson with bottom quarks, and, as a test case for Higgs searches, propose a measurement of associated production of a  $Z$  boson with heavy quarks. In Chapter 3 we present a calculation of the next-to-leading-order QCD corrections to Drell-Yan production of a  $W$  boson, using a nonzero quark mass in order to distinguish the collinear divergences from the infrared and ultraviolet divergences. In Chapter 4 we present a factorization scheme in which only collinear physics is absorbed into the parton distribution functions, and provide a physically motivated method for choosing the factorization scale in this scheme.

# Chapter 2

## Inclusive Production of a Higgs or $Z$ Boson in Association with Heavy Quarks<sup>1</sup>

We calculate the cross section for the production of a  $Z$  boson in association with heavy quarks. We suggest that this cross section can be measured using an inclusive heavy-quark tagging technique. This could be used as a feasibility study for the search for a Higgs boson produced in association with bottom quarks. We argue that the best formalism for calculating that cross section is based on the leading-order process  $b\bar{b} \rightarrow h$ , and that it is valid for all Higgs masses of interest at both the Fermilab Tevatron and the CERN Large Hadron Collider.

### 2.1 Introduction

In the standard model, the Higgs boson has a very weak coupling to bottom quarks. However, in a two-Higgs-doublet model, the coupling of some or all of the physical Higgs particles to bottom quarks can be greatly enhanced. For example, this occurs in the minimal supersymmetric model for large values of  $\tan\beta \equiv v_2/v_1$ , where  $v_1$  and  $v_2$  are the vacuum expectation values of the Higgs doublets that couple to bottom and top quarks, respectively. If the coupling is sufficiently enhanced, the production of Higgs bosons in association with bottom quarks can be an important process at the Fermilab Tevatron ( $p\bar{p}$ ,  $\sqrt{S} = 1.96$  TeV) and the CERN Large Hadron Collider (LHC) ( $pp$ ,  $\sqrt{S} = 14$  TeV). A great deal of attention has been directed towards this process [2, 3, 4, 5, 6, 7, 8, 9, 10, 11, 12, 13, 14, 15, 16, 17, 18, 19, 20, 21, 22, 23, 24, 25, 26, 27].

---

<sup>1</sup>This chapter includes material previously published in Ref. [1].

In order to separate the signal from the background, and also to identify the production process, it is advantageous to tag one or more of the bottom quarks produced along with the Higgs boson (in addition to the bottom quarks that might result from Higgs decay). Up until now, this has been discussed as the identification of a high- $p_T$   $b$ -tagged jet. However, there exist more inclusive means to identify bottom quarks in the final state at hadron colliders, such as identifying a secondary vertex without requiring the reconstruction of a high- $p_T$  jet [28]. In this paper we would like to lay the groundwork for such a measurement.

As a testing ground for the Higgs, we propose a measurement of the inclusive production of a  $Z$  boson in association with heavy quarks.<sup>2</sup> This is more complicated than the Higgs case for three reasons. First, the  $Z$  boson is produced in association with both bottom and charm quarks, so both possibilities must be taken into account. Second,  $Z$  bosons are dominantly produced in association with light quarks, which can fake a heavy quark. Third, the processes  $q\bar{q} \rightarrow ZQ\bar{Q}$  and  $qQ \rightarrow ZqQ$  ( $Q = c, b$ ), where the  $Z$  couples to the light quarks, are contributions that have no analogue in the Higgs case.

There is a second motivation for this paper. There exist two different formalisms for the calculation of inclusive Higgs production in association with bottom quarks. The first is based on the leading-order (LO) process  $gg \rightarrow hb\bar{b}$ , the second on the LO process  $b\bar{b} \rightarrow h$ .<sup>3</sup> The advantage of the latter formalism is that it resums, to all orders in perturbation theory, collinear logarithms of the form  $\ln(m_h/m_b)$  that arise in the calculation based on  $gg \rightarrow hb\bar{b}$  [31, 32]. It has recently been suggested that both formalisms may be unreliable for Higgs bosons at the Tevatron [33]. We will show evidence that the calculation based on  $b\bar{b} \rightarrow h$  is reliable for Higgs masses of experimental interest, and argue for its superiority. However, we also find evidence that the formalism fails as the Higgs mass approaches the machine energy, in agreement with Ref. [33].

The paper is organized as follows. We first discuss, in Section 2.2, the calculation of

---

<sup>2</sup>The production of a  $Z$  boson in association with a heavy-quark jet is dealt with in Refs. [29, 30].

<sup>3</sup>When a  $b$  distribution function is used, it is implicit that there is a spectator  $\bar{b}$  in the final state.

$b\bar{b} \rightarrow h$ , and argue that it is reliable for all Higgs masses of interest at the Tevatron and LHC. We then turn in Section 2.3 to inclusive production of a  $Z$  boson with heavy quarks. Readers who are only interested in the latter topic may skip directly to that section. We conclude with a discussion of our results.

## 2.2 Higgs production in association with heavy quarks

Inclusive Higgs production in association with bottom quarks may be calculated in two different schemes. One may work in a four-flavor scheme, where the leading-order (LO) process is  $gg \rightarrow hb\bar{b}$ . This approach yields collinear logarithms of the form  $\ln(m_h/m_b)$ , which degrade the convergence of the perturbation series. Alternatively, one may work in a five-flavor scheme, where the LO process is  $b\bar{b} \rightarrow h$  [31, 32]. The calculation based on  $b\bar{b} \rightarrow h$  yields a more convergent perturbation series, since the collinear logarithms are summed into the  $b$ -quark distribution functions via the Dokshitzer-Gribov-Lipatov-Altarelli-Parisi (DGLAP) equations. As one calculates to higher and higher order in perturbation theory, the two calculations should approach each other, since they are simply different orderings of the same terms.

The collinear logarithms that arise in  $gg \rightarrow hb\bar{b}$  at LO can be captured by an approximate  $b$ -quark distribution function,

$$\tilde{b}(x, \mu_F) = \frac{\alpha_S(\mu_F)}{2\pi} \ln\left(\frac{\mu_F^2}{m_b^2}\right) \int_x^1 \frac{dy}{y} P_{qg}\left(\frac{x}{y}\right) g(y, \mu_F),$$

where  $P_{qg}(x) = \frac{1}{2}[x^2 + (1-x)^2]$  is the LO DGLAP splitting function and  $\mu_F$  is the factorization scale, of order  $m_h$ . Unlike the exact  $b$  distribution function, the approximate  $b$  distribution function does not sum the collinear logarithms. Thus the calculations  $gg \rightarrow hb\bar{b}$  and  $\tilde{b}\bar{b} \rightarrow h$  should approximately agree if the terms enhanced by collinear logarithms in  $gg \rightarrow hb\bar{b}$  are

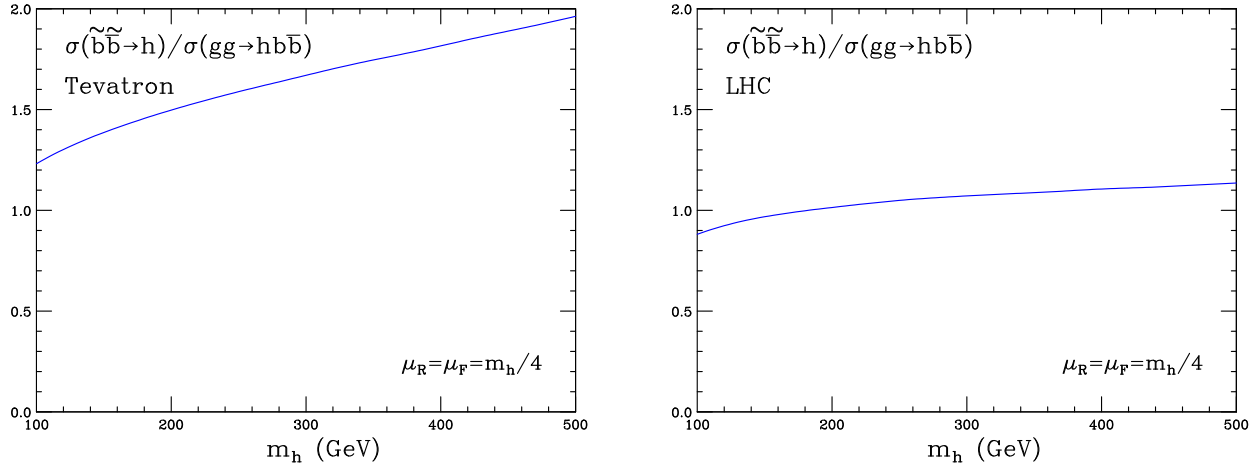


Figure 2.1:  $\sigma(\tilde{b}\tilde{b} \rightarrow h)/\sigma(gg \rightarrow hb\bar{b})$  vs.  $m_h$  at the Tevatron and the LHC, using MRST2001 LO parton distribution functions [34],  $m_b = 4.7$  GeV, and  $\mu_F (= \mu_R) = m_h/4$ .

dominant.

Recently it was noted that the calculations  $gg \rightarrow hb\bar{b}$  and  $\tilde{b}\tilde{b} \rightarrow h$  differ substantially at LO for heavy Higgs bosons ( $m_h > 100$  GeV) at the Tevatron, the discrepancy increasing with increasing Higgs mass [33]. In contrast, the two calculations agree fairly well at the LHC for  $m_h = 100 - 500$  GeV as well as at the Tevatron for  $m_h < 100$  GeV. Ref. [33] concludes that both calculations are suspect at the Tevatron for  $m_h > 100$  GeV.

We show in Fig. 2.1 the ratio of  $\tilde{b}\tilde{b} \rightarrow h$  to  $gg \rightarrow hb\bar{b}$  at both the Tevatron and the LHC. These results agree closely with those of Ref. [33]. We see that the ratio is about 1.5 for  $m_h = 200$  GeV at the Tevatron, increasing to nearly 2 for  $m_h = 500$  GeV.

Implicit in this argument is the choice of the factorization scale. It was argued in Ref. [21] that the appropriate factorization scale is  $\mu_F \approx m_h/4$ , and this is the scale that was used in Ref. [33] and Fig. 2.1. We show below that for heavy Higgs bosons at the Tevatron, a slightly lower scale is more appropriate, and that this partially resolves the large discrepancy between the LO calculations of  $gg \rightarrow hb\bar{b}$  and  $\tilde{b}\tilde{b} \rightarrow h$ .

The argument for the factorization scale made in Ref. [21] is based on an analysis of the collinear logarithm that arises at next-to-leading order (NLO) in the calculation of  $b\bar{b} \rightarrow h$ ,

$m_h$ [GeV]	Tevatron	LHC
100	0.203	0.227
200	0.188	0.219
300	0.176	0.215
400	0.166	0.210
500	0.157	0.206

Table 2.1: The factorization scale relative to the Higgs mass,  $\mu_F/m_h$ , at the Tevatron and the LHC. The factorization scale is determined by the point at which the curves in Fig. 2.2 reach 85% of their values on the collinear plateau.

and is in the same spirit as the argument of Refs. [36, 37]. In the collinear region, the NLO differential hadronic cross section scales like  $d\sigma/dt \sim 1/t$ , where  $t$  is the usual Mandelstam variable. We show in Fig. 2.2 the quantity  $-t d\sigma/dt$  vs.  $\sqrt{-t}/m_h$  for the NLO process  $gb \rightarrow hb$  at both the Tevatron and the LHC for  $m_h = 100 - 500$  GeV.<sup>4</sup> The factorization scale should be chosen near the end of the collinear plateau. At the LHC this plateau ends around  $m_h/4$  for the Higgs-boson masses considered. However, at the Tevatron the end of the plateau slowly creeps below  $m_h/4$  as the Higgs-boson mass increases (this is also true at the LHC, but much less so).

To be consistent, we choose the factorization scale to be where  $-t d\sigma/dt$  reaches 85% of its value on the collinear plateau. The resulting factorization scale at both the Tevatron and the LHC is given in Table 2.1. We show in Fig. 2.3 the ratio of  $b\bar{b} \rightarrow h$  to  $gg \rightarrow hb\bar{b}$  at both the Tevatron and the LHC with this choice of factorization scale. The ratio approaches unity for large Higgs masses at the LHC, as would be expected if the collinear logarithms dominate. The situation at the Tevatron is more complicated. The ratio is near unity for Higgs masses of experimental interest, indicating that the calculation is reliable. However, as the Higgs mass increases the ratio grows, and continues to grow as the mass approaches the machine energy. This suggests that the calculation based on  $b\bar{b} \rightarrow h$  may be unreliable for very heavy Higgs bosons at the Tevatron.

---

<sup>4</sup>Since this is a NLO process, we use NLO parton distribution functions [35]. We use  $\mu_F = m_h$  (the default value), as this graph is being used to determine  $\mu_F$ . We subsequently check that the curves are not very sensitive to the choice of  $\mu_F$ .

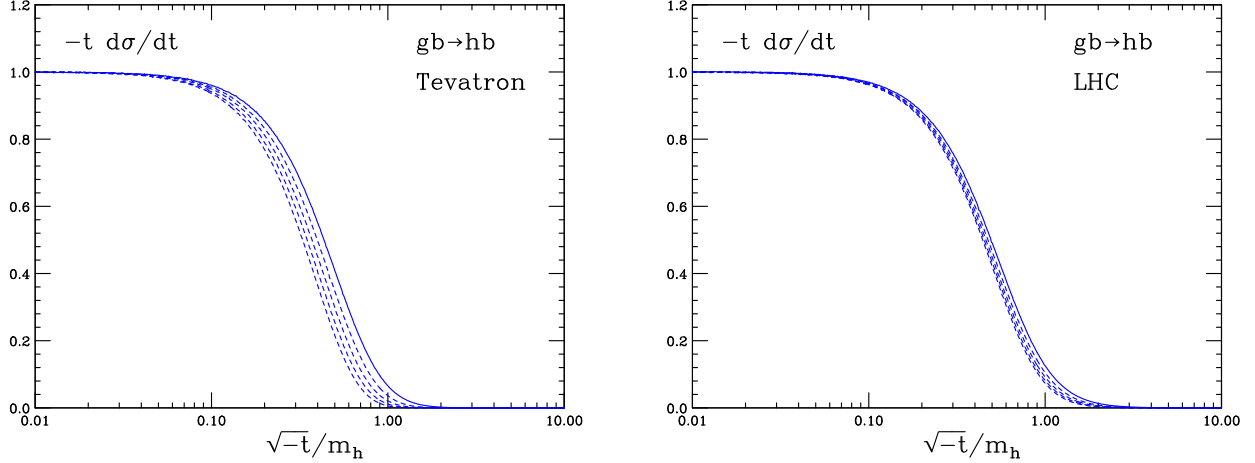


Figure 2.2:  $-t d\sigma/dt$  vs.  $\sqrt{-t}/m_h$  for  $gb \rightarrow hb$  at the Tevatron and the LHC. The factorization scale for  $b\bar{b} \rightarrow h$  should be chosen near the end of the collinear plateau.

In the full calculation of  $b\bar{b} \rightarrow h$  (using the exact  $b$  distribution function) it is important to choose the factorization scale near the end of the collinear plateau, but not very important exactly how that is defined. A less-than-optimal choice will be corrected by higher orders. Indeed, the next-to-next-to-leading-order (NNLO) calculation of  $b\bar{b} \rightarrow h$  has very little factorization-scale dependence for values of  $\mu_F$  near the end of the collinear plateau [22].

The advantage of the calculation based on the LO process  $b\bar{b} \rightarrow h$  is actually twofold. As already discussed, it gives a more convergent perturbation series. In addition, it allows for a higher-order calculation than  $gg \rightarrow hb\bar{b}$ , since it is a simpler LO process. Indeed,  $b\bar{b} \rightarrow h$  is known at NNLO [22], while  $gg \rightarrow hb\bar{b}$  is known only at NLO [23, 24, 25]. Thus the NNLO calculation of  $b\bar{b} \rightarrow h$  is the most accurate existing calculation of inclusive Higgs-boson production in association with bottom quarks. This is reflected by the very mild dependence of the NNLO calculation of  $b\bar{b} \rightarrow h$  on the factorization scale in comparison with that of the NLO calculation of  $gg \rightarrow hb\bar{b}$  [26]. It would be interesting to study the behavior of the NNLO calculation for very heavy Higgs bosons at the Tevatron.

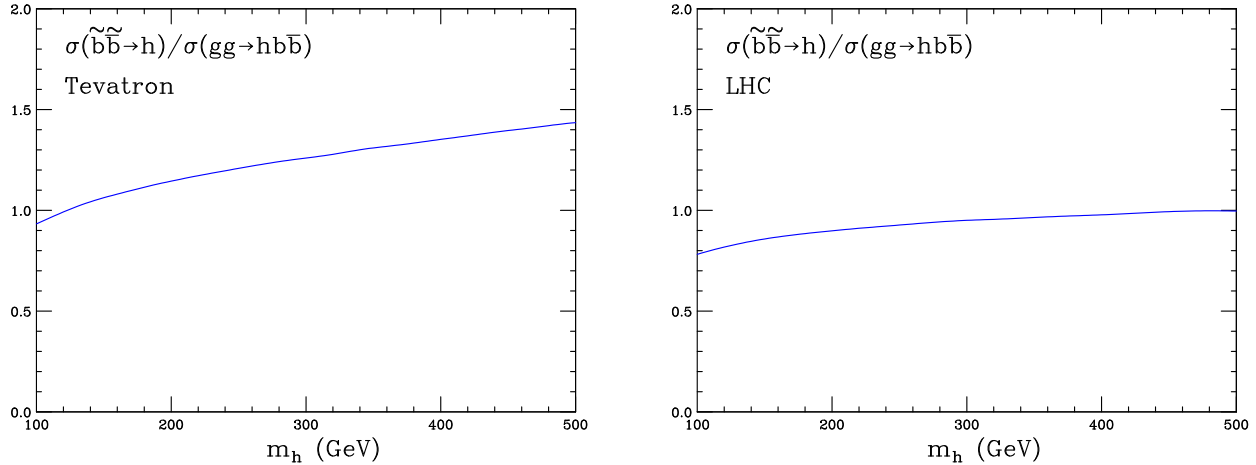


Figure 2.3:  $\sigma(\tilde{b}\tilde{b} \rightarrow h)/\sigma(gg \rightarrow hb\bar{b})$  vs.  $m_h$  at the Tevatron and the LHC, using MRST2001 LO parton distribution functions [34],  $m_b = 4.7$  GeV, and  $\mu_F (= \mu_R)$  determined from the end of the collinear plateau in Fig. 2.2 (listed in Table 2.1).

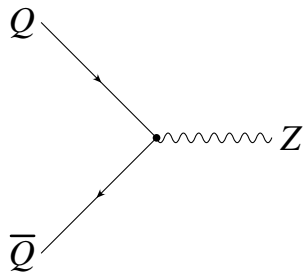


Figure 2.4: Feynman diagram for  $Q\bar{Q} \rightarrow Z$  ( $Q = c, b$ ). The presence of heavy quarks in the final state is implied by the initial-state heavy quarks.

## 2.3 $Z$ production in association with heavy quarks

Unlike the case of the Higgs boson, there are a variety of contributions to the inclusive production of a  $Z$  boson with heavy quarks. The analogue of the Higgs case is  $b\bar{b} \rightarrow Z$ , shown in Fig. 2.4. In the case of the  $Z$  boson, one must also consider  $c\bar{c} \rightarrow Z$  and  $q\bar{q} \rightarrow Z$  ( $q = u, d, s$ ), since both charm quarks and light quarks can fake a  $b$  quark. Finally, there are the processes  $q\bar{q} \rightarrow ZQ\bar{Q}$  and  $qQ \rightarrow ZqQ$  ( $Q = c, b$ ), shown in Figs. 2.5 and 2.6, where the  $Z$  boson couples to the light quarks. As we will show, these last two processes are more important at the Tevatron than at the LHC.

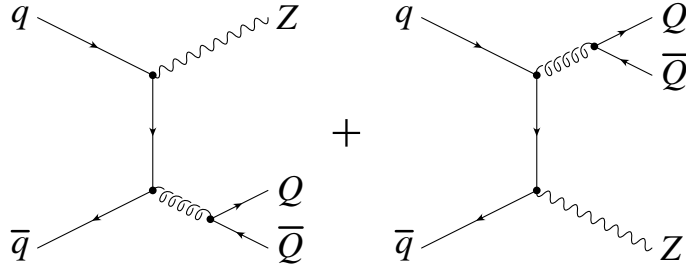


Figure 2.5: Feynman diagrams for  $q\bar{q} \rightarrow ZQ\bar{Q}$ , where the  $Z$  couples to the light quarks.

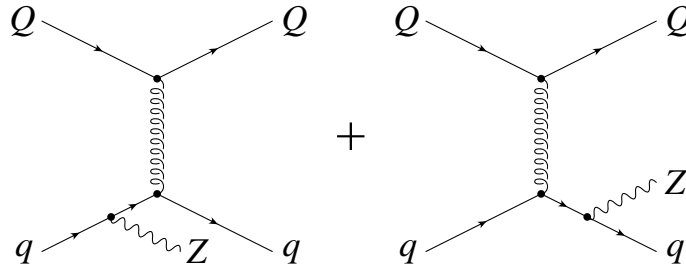


Figure 2.6: Feynman diagrams for  $qQ \rightarrow ZqQ$ , where the  $Z$  couples to the light quarks

Let us begin by considering only processes in which the  $Z$  boson couples to the heavy quarks. This is completely analogous to the case of the Higgs boson discussed in the previous section. We will then include processes in which the  $Z$  boson couples to light quarks, which have no analogue in the Higgs case.

The process  $q\bar{q} \rightarrow Z$  has been calculated at next-to-next-to-leading order (NNLO) [38, 39, 40]. We modified this code to extract  $Q\bar{Q} \rightarrow Z$  ( $Q = c, b$ ) at NNLO, neglecting the heavy-quark mass, which is a small effect of order  $(m_Q/M_Z)^2 \times 1/\ln^2(M_Z/m_Q)$ . We keep (for the moment) only diagrams in which the  $Z$  couples to the heavy quarks.<sup>5</sup> We show in Fig. 2.7 the factorization-scale dependence of the cross section for  $b\bar{b} \rightarrow Z$  at both the Tevatron and the LHC at LO, NLO, and NNLO. The renormalization scale has been set equal to the factorization scale, although this hardly matters as it first enters only at NLO,

<sup>5</sup>This includes NNLO processes with four external heavy quarks of the same flavor. However, we do not include processes with two external charm and two external bottom quarks. These processes contribute less than 1% of the LO cross section.

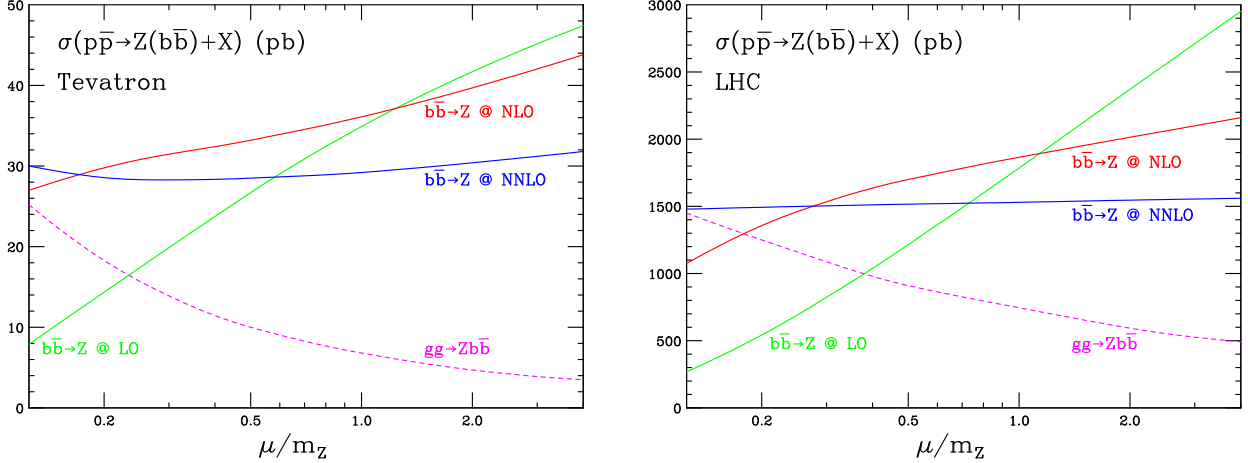


Figure 2.7: Factorization-scale dependence of  $b\bar{b} \rightarrow Z$  at LO, NLO, and NNLO at the Tevatron and the LHC. Only processes in which the  $Z$  couples to the heavy quarks are included. Also shown is  $gg \rightarrow Zb\bar{b}$  at LO, using  $m_b = 4.7$  GeV. We use the LO, NLO, and NNLO parton distribution functions MRST2001 LO [34] and MRST2002 [35].

via the argument of  $\alpha_S(\mu_R)$ . As expected, the scale dependence decreases with increasing order, to the point where there is almost no scale dependence at NNLO. Similar results are obtained for  $c\bar{c} \rightarrow Z$ , as shown in Fig. 2.8.

Also shown on the same plot is the LO cross section in the four-flavor scheme,  $gg \rightarrow Zb\bar{b}$ . If we were to choose  $\mu_F = \mu_R = M_Z$ , this calculation would underestimate the true cross section by a factor of 4 at the Tevatron. If we choose the scale as in the previous section, by finding the end of the collinear plateau in  $gb \rightarrow Zb$ , we find that the appropriate factorization scale is around  $M_Z/3$  at both the Tevatron and the LHC. With this choice of scale, the factor of 4 is reduced to 2. For charm, the corresponding factor is 5 at the Tevatron, reduced to 3. These results mirror a similar result that was obtained in the case of the Higgs [21].

We list in Table 2.2 the NNLO cross sections for  $b\bar{b} \rightarrow Z$  and  $c\bar{c} \rightarrow Z$  at both the Tevatron and the LHC. These cross sections have very little theoretical uncertainty.

We now include processes in which the  $Z$  couples to light quarks, shown in Figs. 2.5 and 2.6.<sup>6</sup> Here it is essential to keep the heavy-quark mass nonzero in order to regulate collinear

<sup>6</sup>We also consider the process  $Q\bar{Q} \rightarrow Zq\bar{q}$ , where the  $Z$  couples to the light quarks. We find this to be numerically negligible. The interference with the same process, but where the  $Z$  couples to the heavy

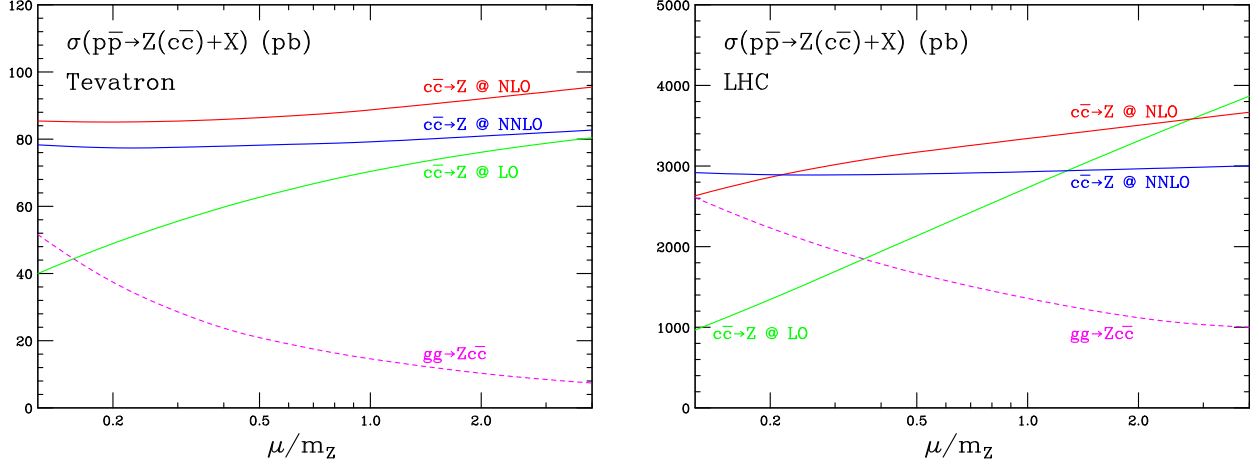


Figure 2.8: Same as Fig. 2.7, but for  $c\bar{c} \rightarrow Z$ . For  $gg \rightarrow Zc\bar{c}$ , we use  $m_c = 1.4$  GeV.

singularities.<sup>7</sup> While these processes are NNLO with respect to inclusive  $Z$  production,  $q\bar{q} \rightarrow ZQ\bar{Q}$  is LO with respect to  $Z$  production in association with heavy quarks, and  $qQ \rightarrow ZqQ$  is NLO. The correct power counting is obtained when one recalls that a heavy-quark distribution function is intrinsically of order  $\alpha_S \ln(\mu_F/m_Q)$  [41]. The analogous processes for heavy-quark structure functions in deep-inelastic scattering,  $F_i^Q$ , have been discussed in Ref. [42].

There are two serious drawbacks to the calculations of these processes. First, the cross sections contain factors of  $\ln(M_Z/m_Q)$ , due to the collinear singularities, which are not resummed. This is related to the fact that we are calculating a semi-inclusive quantity, namely  $Z$  production in association with heavy quarks. If we were instead calculating the inclusive  $Z$  cross section, this issue would not arise. Fracture functions may be useful in this context [43]. Second, and more importantly, these processes are only known at LO at this time (with a nonzero quark mass).<sup>8</sup> The NLO calculation is an important missing result for this as well as many other analyses (the same holds true of  $q\bar{q} \rightarrow WQ\bar{Q}$ ). Thus our quarks, is also negligible.

<sup>7</sup>We also evaluate the interference of these processes with the similar processes in which the  $Z$  is radiated from the heavy quark. This may be done in the limit of vanishing heavy-quark mass, since there are no collinear singularities. We find that these interference contributions are numerically negligible.

<sup>8</sup>The process  $q\bar{q} \rightarrow ZQ\bar{Q}$  is known at NLO with a vanishing quark mass, which is relevant when the heavy quarks are produced at high  $p_T$  [44].

Process		Tevatron	LHC
$Z(b\bar{b})$	$b\bar{b} \rightarrow Z$ (NNLO)	28.3	1500
	$q\bar{q} \rightarrow Zb\bar{b}$ (LO)	19	120
	$qb \rightarrow Zqb$ (LO)	5.9	430
$Z(c\bar{c})$	$c\bar{c} \rightarrow Z$ (NNLO)	77.7	2890
	$q\bar{q} \rightarrow Zc\bar{c}$ (LO)	69	430
	$qc \rightarrow Zqc$ (LO)	21	1200
Inclusive $Z$		7510	56700

Table 2.2: Cross sections (pb) for the various contributions to  $Z$  production in association with heavy quarks. We use the MRST2002 NNLO parton distribution functions [35] with  $\mu_F = \mu_R = M_Z/3$ .

calculation of these processes is relatively crude. This is a serious problem at the Tevatron, but less so at the LHC, where these processes are relatively less important. It is desirable both to obtain NLO results for  $q\bar{q} \rightarrow ZQ\bar{Q}$  and  $qQ \rightarrow ZqQ$  (with finite  $m_Q$ ) and to develop a formalism that allows the resummation of the collinear logarithms.<sup>9</sup>

We give in Table 2.2 the cross sections for the various processes that contribute to  $Z$  production in association with heavy quarks. We also give the inclusive  $Z$  cross section at NNLO. Although this cross section is two orders of magnitude larger than that of any of the processes that produce a  $Z$  in association with heavy quarks, the mistag rate for light quarks and gluons is on the order of 1%, so this background is not overwhelming.

## 2.4 Conclusions

Our results for  $Z$  production in association with heavy quarks are summarized in Table 2.2. The final row is the inclusive  $Z$  cross section calculated at next-to-next-to-leading order (NNLO). Each row above that corresponds to some subset of this calculation, with heavy

---

<sup>9</sup>The collinear logarithm that occurs in  $qQ \rightarrow ZqQ$  also occurs in the process  $qg \rightarrow ZqQ\bar{Q}$ , where the initial gluon splits to  $Q\bar{Q}$ . Thus the same issues arise in a calculation that does not make use of a heavy-quark distribution function.

quarks in the final state, either implicitly (such as  $Q\bar{Q} \rightarrow Z$ ) or explicitly (such as  $q\bar{q} \rightarrow ZQ\bar{Q}$ ). We see that there are a large variety of processes that contribute to  $Z$  production in association with heavy quarks. Taken together, they constitute 3% of the inclusive  $Z$  cross section at the Tevatron, and 12% at the LHC. The measurement of these fractions will require simulation of the acceptances and tagging efficiencies of the various processes. We advocate using an inclusive tagging technique to maximize the number of signal events.

The measurement of  $Z$  production in association with heavy quarks is interesting in its own right, but also as a feasibility study for Higgs production in association with bottom quarks. In this paper we have argued that the best formalism for the calculation of the latter process is based on the leading-order process  $b\bar{b} \rightarrow h$ , and that this calculation is valid for all Higgs masses of interest at both the Tevatron and the LHC. The most accurate calculation of this process is the NNLO cross section given in Ref. [22]. We also showed evidence that this formalism fails as the Higgs mass approaches the machine energy.

# Chapter 3

## QCD Corrections to the Drell-Yan Cross Section

The next-to-leading-order (NLO) QCD corrections to the hadronic cross section for Drell-Yan production of an electroweak gauge boson involve ultraviolet, infrared, and collinear divergences, all of which must be regulated in some way. The ultraviolet divergences cancel among the Feynman diagrams involving virtual gluons, while the infrared divergences cancel between the virtual-gluon and real-gluon-emission processes. The collinear divergences do not cancel, and are absorbed into the parton distribution functions.

The first calculations of the NLO QCD corrections to the Drell-Yan cross section were published in 1979. One of these [45] used a quark mass to regulate the collinear divergences, and a gluon mass to regulate the infrared divergences. The other calculation [46] used dimensional regularization throughout. The latter approach has the advantage of greater simplicity; however, when all divergences are regulated in the same way, it can be difficult to identify the nature of the various divergent terms.

In order to better understand the collinear divergences involved in the NLO QCD corrections to the Drell-Yan cross section, we present in this chapter a calculation of these corrections using a quark mass  $m$  to regulate the collinear divergences, and using dimensional regularisation with  $4 - 2\epsilon$  spacetime dimensions to regulate the infrared and ultraviolet divergences. We consider the production of an on-shell  $W^\pm$  boson; the generalization to production of a photon or  $Z$  boson, or of a lepton pair resulting from the decay of the electroweak gauge boson, is straightforward. Also, we consider only partonic cross sections; the hadronic cross section is formed by convolving the partonic cross sections with parton distribution functions in the usual way.

### 3.1 $q\bar{q} \rightarrow W$ (tree level)

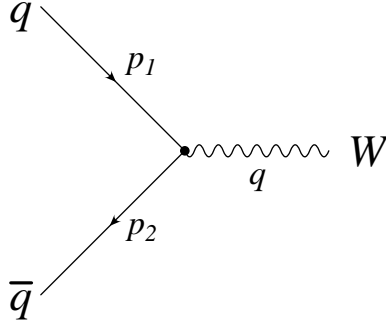


Figure 3.1: The tree-level Feynman diagram for  $q\bar{q} \rightarrow W$ .

Since the tree-level process  $q\bar{q} \rightarrow W$ , shown in Fig. 3.1, has no infrared or ultraviolet divergences, we can work in four dimensions. We parametrize the momenta as follows:

$$\begin{aligned}
 p_1 &= \left( \frac{\sqrt{s}}{2}, \frac{\sqrt{s}}{2}\beta, 0, 0 \right), \\
 p_2 &= \left( \frac{\sqrt{s}}{2}, -\frac{\sqrt{s}}{2}\beta, 0, 0 \right), \\
 q &= (\sqrt{s}, 0, 0, 0),
 \end{aligned}$$

where  $s \equiv (p_1 + p_2)^2$ ,  $\rho \equiv m^2/s$ , and  $\beta \equiv \sqrt{1 - 4\rho}$ .

The one-body phase space integration is quite simple:

$$\begin{aligned}
 \int d\Phi &= \int \frac{d^4k}{(2\pi)^4} \theta(k^0) 2\pi \delta(k^2 - M_W^2) (2\pi)^4 \delta^4(p_1 + p_2 - k) \\
 &= 2\pi \delta(s - M_W^2) \\
 &= \frac{2\pi}{M_W^2} \delta(1 - \tau),
 \end{aligned}$$

where  $\tau \equiv M_W^2/s$ .

Now the tree-level graph has no collinear divergence, so that we can neglect the quark mass altogether. It follows that we can neglect the longitudinal term in the sum over  $W$

polarizations, since the vector-coupling piece of this term vanishes due to the Ward identity, while the axial-vector piece is suppressed by a factor of  $m$ . The amplitude, then, is given by:

$$i\mathcal{M} = \varepsilon_\mu^*(k)\bar{v}(p_2)\frac{-ig}{2\sqrt{2}}\gamma^\mu(1-\gamma_5)u(p_1).$$

Squaring, averaging over quark spins and colors, and summing over  $W$  polarizations, we find

$$\begin{aligned} |\overline{\mathcal{M}}|^2 &= \frac{1}{2}\frac{1}{3}\frac{1}{2}\frac{1}{3}(-g_{\mu\nu})\frac{g^2}{8}\text{Tr}\mathbf{1}_F\text{Tr}[\not{p}_1(1+\gamma_5)\gamma^\nu\not{p}_2\gamma^\mu(1-\gamma_5)] \\ &= \frac{-g^2}{96}\text{Tr}[\not{p}_1\gamma_\mu\not{p}_2\gamma^\mu 2(1-\gamma_5)] \\ &= \frac{-g^2}{48}\text{Tr}[-2\not{p}_1\not{p}_2] \\ &= \frac{g^2}{6}p_1\cdot p_2 \\ &= \frac{4\pi\alpha}{6s_W^2}\frac{M_W^2}{2} \\ &= \frac{\pi\alpha M_W^2}{3s_W^2}. \end{aligned}$$

The cross section, then, is

$$\begin{aligned} \hat{\sigma} &= \frac{1}{2s}\frac{2\pi}{M_W^2}\delta(1-\tau)\frac{\pi\alpha M_W^2}{3s_W^2} \\ &= \frac{\pi^2\alpha}{3s_W^2 M_W^2}\delta(1-\tau). \end{aligned}$$

## 3.2 $q\bar{q} \rightarrow W$ (one loop)

The virtual-gluon diagrams feature ultraviolet divergences, which will cancel among these diagrams, and infrared divergences, which will survive for a while. These will be regulated by working in  $4-2\epsilon$  dimensions. There are also collinear divergences, which will be regulated by the quark mass. However, the interference between the tree-level and virtual-gluon diagrams

does not produce any terms of order  $1/m^2$ ; thus we can neglect the quark mass in the numerator. Also we can neglect the longitudinal  $W$  polarization, as in Section 3.1.

### 3.2.1 Vertex correction

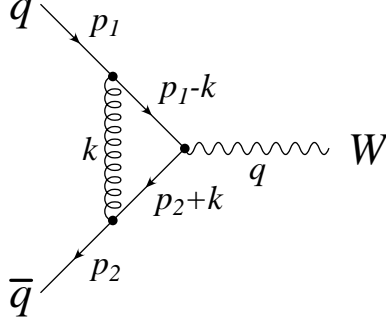


Figure 3.2: The vertex correction to  $q\bar{q} \rightarrow W$ .

The amplitude for the vertex correction, shown in Fig. 3.2, is given by

$$\begin{aligned}
i\mathcal{M} &= \int \frac{d^{4-2\epsilon}k}{(2\pi)^{4-2\epsilon}} \varepsilon_\mu^*(q) \bar{v}(p_2) (-ig_s) \gamma^\lambda t^A \frac{i(\not{k} - \not{p}_2)}{(k - p_2)^2 - m^2} \frac{-ig}{2\sqrt{2}} \gamma^\mu (1 - \gamma_5) \\
&\quad \times \frac{i(\not{k} + \not{p}_1)}{(k + p_1)^2 - m^2} (-ig_s) \gamma^\nu t^B u(p_1) \frac{-ig_{\lambda\nu} \delta_{AB}}{k^2} \\
&\equiv i\varepsilon_\mu^*(q) \bar{v}(p_2) \Gamma^\mu u(p_1),
\end{aligned}$$

where

$$\Gamma^\mu = \frac{igg_s^2}{2\sqrt{2}} C_F (1 + \gamma_5) \int \frac{d^{4-2\epsilon}k}{(2\pi)^d} \frac{\gamma_\nu (\not{k} - \not{p}_2) \gamma^\mu (\not{k} + \not{p}_1) \gamma^\nu}{k^2 ((k + p_1)^2 - m^2) ((k - p_2)^2 - m^2)}.$$

#### Loop integrals

We introduce Feynman parameters  $x$  and  $y$  to rewrite the denominator:

$$\text{Den.} = \frac{1}{k^2 ((k + p_1)^2 - m^2) ((k - p_2)^2 - m^2)}$$

$$\begin{aligned}
&= \int_0^1 dx \int_0^{1-x} dy \frac{2}{[(1-x-y)k^2 + x((k+p_1)^2 - m^2) + y((k-p_2)^2 - m^2)]^3} \\
&= \int_0^1 dx \int_0^{1-x} dy \frac{2}{[k^2 + 2(xp_1 - yp_2) \cdot k]^3} \\
&= \int_0^1 dx \int_0^{1-x} dy \frac{2}{[\ell^2 - (xp_1 - yp_2)^2]^3} \\
&= \int_0^1 dx \int_0^{1-x} dy \frac{2}{[\ell^2 + xyM_W^2 - (x+y)^2m^2]^3},
\end{aligned}$$

where  $\ell \equiv k + xp_1 - yp_2$ .

The numerator can also be simplified. As the denominator is an even function of  $\ell$ , any terms odd in  $\ell$  will vanish in the loop integration and can safely be neglected. Also, we can take advantage of the Dirac equations  $\not{p}_1 u(p_1) = 0$  and  $\bar{v}(p_2) \not{p}_2 = 0$ . The symbol  $\sim$  will denote equality modulo such terms.

$$\begin{aligned}
\text{Num.} &= \gamma_\nu (\not{q} - \not{p}_2) \gamma^\mu (\not{q} + \not{p}_1) \gamma^\nu \\
&= -2(\not{q} + \not{p}_1) \gamma^\mu (\not{q} - \not{p}_2) + 2\epsilon (\not{q} - \not{p}_2) \gamma^\mu (\not{q} + \not{p}_1) \\
&= -2(\not{\ell} + (1-x)\not{p}_1 + y\not{p}_2) \gamma^\mu (\not{\ell} - x\not{p}_1 - (1-y)\not{p}_2) \\
&\quad + 2\epsilon (\not{\ell} - x\not{p}_1 - (1-y)\not{p}_2) \gamma^\mu (\not{\ell} + (1-x)\not{p}_1 + y\not{p}_2) \\
&\sim -2(\not{\ell} + (1-x)\not{p}_1) \gamma^\mu (\not{\ell} - (1-y)\not{p}_2) + 2\epsilon (\not{\ell} - x\not{p}_1) \gamma^\mu (\not{\ell} + y\not{p}_2) \\
&= -2(1-\epsilon)\not{\ell} \gamma^\mu \not{\ell} + 2[(1-x)(1-y) - \epsilon xy] \not{p}_1 \gamma^\mu \not{p}_2.
\end{aligned}$$

Now  $\not{p}_1 \gamma^\mu \not{p}_2 \sim \not{q} \gamma^\mu \not{q} = 2q^\mu \not{q} - M_W^2 \gamma^\mu \sim -M_W^2 \gamma^\mu$ , so that the numerator can be replaced by

$$\text{Num.} \sim -2[(1-\epsilon)\not{\ell} \gamma^\mu \not{\ell} + ((1-x)(1-y) - \epsilon xy) M_W^2 \gamma^\mu].$$

Putting things together, then, we have:

$$\begin{aligned}
\Gamma^\mu &= \frac{igg_s^2}{2\sqrt{2}} \frac{4}{3} 2(-2)(1+\gamma_5) \int_0^1 dx \int_0^{1-x} dy \int \frac{d^{4-2\epsilon}\ell}{(2\pi)^{4-2\epsilon}} \\
&\quad \times \frac{(1-\epsilon)\ell\gamma^\mu\ell + [(1-x)(1-y) - \epsilon xy]M_W^2\gamma^\mu}{[\ell^2 + xyM_W^2 - (x+y)^2m^2]^3} \\
&= \frac{-4\sqrt{2}igg_s^2}{3}(1+\gamma_5) \int_0^1 dx \int_0^{1-x} dy \\
&\quad \times \left[ (1-\epsilon)\gamma^\lambda\gamma^\mu\gamma^\nu \frac{i}{(4\pi)^{2-\epsilon}} \frac{g_{\lambda\nu}}{2} \frac{\Gamma(\epsilon)}{\Gamma(3)} [-xyM_W^2 + (x+y)^2m^2]^{-\epsilon} \right. \\
&\quad \left. + [(1-x)(1-y) - \epsilon xy]M_W^2\gamma^\mu \frac{-i}{(4\pi)^{2-\epsilon}} \frac{\Gamma(1+\epsilon)}{\Gamma(3)} \right. \\
&\quad \left. [-xyM_W^2 + (x+y)^2m^2]^{-1-\epsilon} \right] \\
&= \frac{-4\sqrt{2}igg_s^2}{3} \frac{i}{(4\pi)^2} \frac{1}{2} \left( \frac{4\pi}{-M_W^2} \right)^\epsilon (1+\gamma_5) \\
&\quad \times \left[ \frac{1}{2}(1-\epsilon)(-2)(1-\epsilon)\gamma^\mu \frac{1}{\epsilon} \Gamma(1+\epsilon) \int_0^1 dx \int_0^{1-x} dy (xy - \rho(x+y)^2)^{-\epsilon} \right. \\
&\quad \left. + \gamma^\mu \Gamma(1+\epsilon) \int_0^1 dx \int_0^{1-x} dy [(1-x)(1-y) - \epsilon xy] (xy - \rho(x+y)^2)^{-1-\epsilon} \right] \\
&= \frac{g\alpha_s}{3\pi\sqrt{2}} \left( \frac{4\pi}{-M_W^2} \right)^\epsilon \Gamma(1+\epsilon)\gamma^\mu(1-\gamma_5) \\
&\quad \times \left[ \left( -\frac{1}{\epsilon} + 2 \right) \int_0^1 dx \int_0^{1-x} dy (xy - \rho(x+y)^2)^{-\epsilon} \right. \\
&\quad \left. + \int_0^1 dx \int_0^{1-x} dy \frac{(1-x)(1-y) - \epsilon xy}{(xy - \rho(x+y)^2)^{1+\epsilon}} \right].
\end{aligned}$$

The term proportional to  $1/\epsilon$  is an ultraviolet divergence.

### Parametric integrals

To perform the parametric integrals, it will be useful to change variables. Let

$$u = x + y, \quad v = \frac{x - y}{x + y},$$

so that

$$\int_0^1 dx \int_0^{1-x} dy = \frac{1}{2} \int_0^1 u du \int_{-1}^1 dv.$$

The variables  $u$  and  $v$  are closely related to polar coordinates in the  $(\sqrt{x}, \sqrt{y})$  plane;  $\sqrt{u}$  is the radial coordinate, while  $\frac{1}{2} \cos^{-1} v$  is the angular coordinate.

Now we have two integrals to do, one from each of the scalar and tensor loop integrals. We will encounter terms involving  $\ln(-\rho)$ , which has an imaginary part. However, only the real part is relevant for the cross section we're trying to calculate, so we can safely ignore the imaginary part, except in products of logarithms of negative quantities. We will treat  $m$  and  $M_W$  as having infinitesimal negative and positive imaginary parts, respectively.

The parametric integral resulting from the tensor loop integral is

$$\begin{aligned} & \int_0^1 dx \int_0^{1-x} dy (xy - \rho(x+y)^2)^{-\epsilon} \\ &= \frac{1}{2} \int_0^1 u du \int_{-1}^1 dv \left[ \frac{1}{4} u^2 (1-v^2) - u^2 \rho \right]^{-\epsilon} \\ &= \frac{1}{2} 4^\epsilon \int_0^1 du u^{1-2\epsilon} \int_{-1}^1 dv [1 - \epsilon \ln(\beta^2 - v^2) + \mathcal{O}(\epsilon^2)] \\ &= \frac{1}{2} 4^\epsilon \frac{1}{2-2\epsilon} \left[ 2 - 2\epsilon \int_{-1}^1 dv \ln(\beta + v) \right] \\ &= \frac{1}{2} (1 + \epsilon)(1 + \epsilon \ln 4) \left[ 1 - \epsilon (\beta + v)(\ln(\beta + v) - 1) \Big|_{-1}^1 \right] + \mathcal{O}(\epsilon^2) \\ &= \frac{1}{2} (1 + \epsilon)(1 + \epsilon \ln 4) \\ &\quad \times \left[ 1 - \epsilon \left( (1 + \beta) \ln(1 + \beta) - (1 + \beta) - (\beta - 1) \ln(\beta - 1) + (\beta - 1) \right) \right] \\ &= \frac{1}{2} (1 + \epsilon)(1 + \epsilon \ln 4) [1 - \epsilon(2 \ln 2 - 2 + \mathcal{O}(\rho \ln \rho))] \\ &= \frac{1}{2} (1 + 3\epsilon) + \mathcal{O}(\epsilon^2). \end{aligned}$$

The parametric integral resulting from the scalar loop integral is more complicated:

$$\begin{aligned}
& \int_0^1 dx \int_0^{1-x} dy \frac{(1-x)(1-y) - \epsilon xy}{[xy - \rho(x+y)^2]^{1+\epsilon}} \\
&= \frac{1}{2} \int_0^1 u du \int_{-1}^1 dv \frac{1-u + \frac{1}{4}(1-\epsilon)u^2(1-v)^2}{[\frac{1}{4}u^2(1-v^2) - u^2\rho]^{1+\epsilon}} \\
&= \frac{1}{2} 4^{1+\epsilon} \left[ \int_0^1 du (u^{-1-2\epsilon} - u^{-2\epsilon}) \int_{-1}^1 dv \frac{1 - \epsilon \ln(\beta^2 - v^2) + \mathcal{O}(\epsilon^2)}{\beta^2 - v^2} \right. \\
&\quad \left. + \frac{1}{4} \int_0^1 du u \int_{-1}^1 dv \frac{1-v^2}{\beta^2 - v^2} + \mathcal{O}(\epsilon) \right] \\
&= 2(4^\epsilon) \left( \frac{1}{-2\epsilon} - \frac{1}{1-2\epsilon} \right) \int_{-1}^1 dv \frac{1 - \epsilon \ln(\beta^2 - v^2)}{\beta^2 - v^2} + \frac{1}{4} \int_{-1}^1 dv \frac{1-v^2}{\beta^2 - v^2}.
\end{aligned}$$

The term proportional to  $1/\epsilon$  arises from an infrared singularity at  $u = 0$ . This leaves us with several integrals over  $v$  to perform. First,

$$\begin{aligned}
\int_{-1}^1 \frac{dv}{\beta^2 - v^2} &= \frac{1}{2\beta} \int_{-1}^1 dv \left[ \frac{1}{\beta + v} + \frac{1}{\beta - v} \right] \\
&= \frac{1}{\beta} \int_{-1}^1 \frac{dv}{\beta + v} \\
&= \frac{1}{\beta} \ln \left( \frac{1 + \beta}{\beta - 1} \right) \\
&= \ln \left( \frac{2}{-2\rho} + \mathcal{O}(1) \right) \\
&= -\ln(-\rho) + \mathcal{O}(\rho) \\
&= -\ln \rho - i\pi.
\end{aligned}$$

Next,

$$\begin{aligned}
\int_{-1}^1 dv \frac{\ln(\beta^2 - v^2)}{\beta^2 - v^2} &= \int_{-1}^1 dv [\ln(\beta + v) + \ln(\beta - v)] \left[ \frac{1}{\beta + v} + \frac{1}{\beta - v} \right] \frac{1}{2\beta} \\
&= \frac{1}{\beta} \int_{-1}^1 dv \frac{\ln(\beta + v) + \ln(\beta - v)}{\beta + v}.
\end{aligned}$$

Now

$$\begin{aligned}
\int_{-1}^1 dv \frac{\ln(\beta + v)}{\beta + v} &= \frac{1}{2} \ln^2(\beta + v) \Big|_{-1}^1 \\
&= \frac{1}{2} \ln^2(1 + \beta) - \frac{1}{2} \ln^2(\beta - 1) \\
&= \frac{1}{2} \ln^2 2 - \frac{1}{2} \ln^2(-2\rho) + \mathcal{O}(\rho) \\
&= \frac{1}{2} \ln^2 2 - \frac{1}{2} \ln^2 2\rho + \frac{\pi^2}{2} + \text{imag.} \\
&= -\frac{1}{2} \ln^2 \rho - \ln 2 \ln \rho + \frac{\pi^2}{2}
\end{aligned}$$

and

$$\begin{aligned}
\int_{-1}^1 dv \frac{\ln(\beta - v)}{\beta + v} &= \int_{\beta-1}^{1+\beta} \frac{dw}{w} \ln(2\beta - w) \\
&= \ln 2\beta \int_{\beta-1}^{1+\beta} \frac{dw}{w} + \int_{\beta-1}^{1+\beta} \frac{dw}{w} \ln \left( 1 - \frac{w}{2\beta} \right) \\
&= \ln 2\beta \ln \frac{1 + \beta}{\beta - 1} + \int_{\frac{\beta-1}{2\beta}}^{\frac{1+\beta}{2\beta}} \frac{dz}{z} \ln(1 - z) \\
&= \ln 2\beta \ln \frac{1 + \beta}{\beta - 1} - \text{Li}_2 \left( \frac{1 + \beta}{2\beta} \right) + \text{Li}_2 \left( \frac{\beta - 1}{2\beta} \right) \\
&= -\ln 2 \ln(-\rho) - \text{Li}_2(1) + \mathcal{O}(\rho) \\
&= -\ln 2 \ln \rho - \frac{\pi^2}{6} + \text{imag.},
\end{aligned}$$

so that

$$\begin{aligned}
\int_{-1}^1 dv \frac{1 - \epsilon \ln(\beta^2 - v^2)}{\beta^2 - v^2} &= -\ln \rho + \epsilon \left[ \frac{1}{2} \ln^2 \rho + \ln 2 \ln \rho - \frac{\pi^2}{2} + \ln 2 \ln \rho + \frac{\pi^2}{6} \right] \\
&= -\ln \rho + \epsilon \left[ \frac{1}{2} \ln^2 \rho + \ln 4 \ln \rho - \frac{\pi^2}{3} \right].
\end{aligned}$$

Finally,

$$\int_{-1}^1 dv \frac{1-v^2}{\beta^2-v^2} = \int_{-1}^1 dv (1 + \mathcal{O}(\rho)) = 2.$$

Combining these results, we find that the scalar loop integral is

$$\begin{aligned} & \int_0^1 dx \int_0^{1-x} dy \frac{(1-x)(1-y) - \epsilon xy}{[xy - (x+y)^2 \rho]^{1+\epsilon}} \\ &= \left( -\frac{1}{\epsilon} - 2 \right) (1 + \epsilon \ln 4) \left[ -\ln \rho - i\pi + \epsilon \left( \frac{1}{2} \ln^2 \rho + \ln 4 \ln \rho - \frac{\pi^2}{3} \right) \right] + \frac{1}{4}(2) \\ &= \left( \frac{1}{\epsilon} + 2 \right) (1 + \epsilon \ln 4) \left[ \ln \rho + i\pi - \epsilon \left( \frac{1}{2} \ln^2 \rho + \ln 4 \ln \rho - \frac{\pi^2}{3} \right) \right] + \frac{1}{2} \\ &= \frac{1}{\epsilon} (\ln \rho + i\pi) + (2 + \ln 4) \ln \rho - \left( \frac{1}{2} \ln^2 \rho + \ln 4 \ln \rho - \frac{\pi^2}{3} \right) + \frac{1}{2} + \mathcal{O}(\epsilon) + \text{imag.} \\ &= \frac{1}{\epsilon} (\ln \rho + i\pi) - \frac{1}{2} \ln^2 \rho + 2 \ln \rho + \frac{\pi^2}{3} + \frac{1}{2}. \end{aligned}$$

The vertex correction is then

$$\begin{aligned} \Gamma^\mu &= \frac{-4\sqrt{2}igg_s^2}{3} \frac{i}{(4\pi)^2} \frac{1}{2} \left( \frac{4\pi}{-M_W^2} \right)^\epsilon \Gamma(1+\epsilon) \gamma^\mu (1-\gamma_5) \\ &\quad \times \left[ -\frac{1}{\epsilon} (1-2\epsilon) \frac{1}{2} (1+3\epsilon) + \frac{1}{\epsilon} (\ln \rho + i\pi) - \frac{1}{2} \ln^2 \rho + 2 \ln \rho + \frac{\pi^2}{3} + \frac{1}{2} \right] \\ &= \frac{g}{2\sqrt{2}} \gamma^\mu (1-\gamma_5) \frac{2\alpha_s}{3\pi} \left( 1 - \gamma\epsilon + \epsilon \ln \frac{4\pi}{M_W^2} + \epsilon i\pi \right) \\ &\quad \times \left[ -\frac{1}{2\epsilon} (1+\epsilon) + \frac{1}{\epsilon} (\ln \rho + i\pi) - \frac{1}{2} \ln^2 \rho + 2 \ln \rho + \frac{\pi^2}{3} + \frac{1}{2} \right] + \mathcal{O}(\epsilon) \\ &= \frac{-g}{2\sqrt{2}} \gamma^\mu (1-\gamma_5) \frac{\alpha_s}{3\pi} \\ &\quad \times \left[ \left( \frac{1}{\epsilon} - \gamma + \ln \frac{4\pi}{M_W^2} + i\pi \right) (-2 \ln \rho + 1 - 2\pi i) + \ln^2 \rho - 4 \ln \rho - \frac{2\pi^2}{3} \right] + \mathcal{O}(\epsilon) \\ &= \frac{-g}{2\sqrt{2}} \gamma^\mu (1-\gamma_5) \frac{\alpha_s}{3\pi} \\ &\quad \times \left[ \left( \frac{1}{\epsilon} - \gamma + \ln \frac{4\pi}{M_W^2} \right) (-2 \ln \rho + 1) + 2\pi^2 + \ln^2 \rho - 4 \ln \rho - \frac{2\pi^2}{3} \right] + \text{imag.} \end{aligned}$$

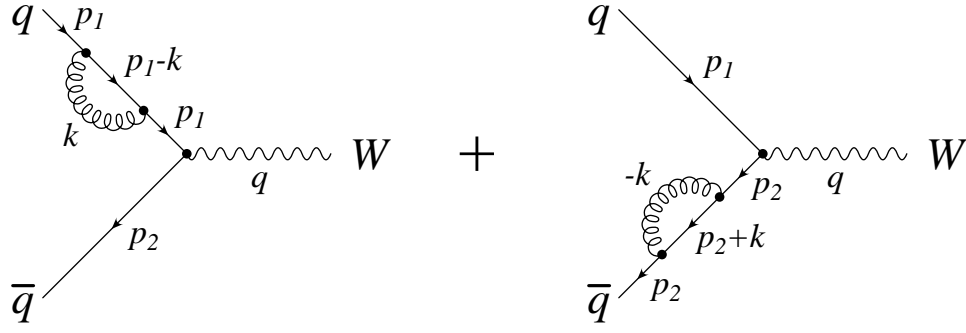


Figure 3.3: The wavefunction-renormalization corrections to  $q\bar{q} \rightarrow W$ .

$$= \frac{-g}{2\sqrt{2}} \gamma^\mu (1 - \gamma_5) \frac{\alpha_s}{3\pi} \left[ \left( \frac{1}{\epsilon} - \gamma + \ln \frac{4\pi}{M_W^2} \right) (-2 \ln \rho + 1) + \ln^2 \rho - 4 \ln \rho + \frac{4\pi^2}{3} \right]. \quad (3.1)$$

This result contains several divergent terms. The terms involving  $\ln \rho$  arise from collinear singularities at  $v = \pm 1$ . The term proportional to  $(1/\epsilon) \ln \rho$  contains both infrared and collinear divergences, while the term proportional to  $1/\epsilon$  without a factor of  $\ln \rho$  is the ultraviolet divergence.

### 3.2.2 Wavefunction renormalization

We must also consider the effect of wavefunction renormalization of the initial quark and antiquark, shown in Fig. 3.3. This involves the geometric series which is the sum of self-energy corrections to the quark propagator:

$$\frac{i}{\not{p} - m_0} + \frac{i}{\not{p} - m_0} i\Sigma(p) \frac{i}{\not{p} - m_0} + \dots$$

$$\begin{aligned}
&= \frac{i}{\not{p} - m_0} \left( 1 - \frac{\Sigma(p)}{\not{p} - m_0} + \dots \right) \\
&= \frac{i}{\not{p} - m_0} \frac{1}{1 + \Sigma(p)/(\not{p} - m_0)} \\
&= \frac{i}{\not{p} - m_0 + \Sigma(p)} \\
&= \frac{i}{\not{p} - m_0 + \Sigma(m) + (\not{p} - m_0)\Sigma'(m) + \dots} \\
&= \frac{i}{(\not{p} - m)(1 + \Sigma'(m) + \dots)} \\
&= \frac{i}{\not{p} - m} (1 - \Sigma'(m) + \dots),
\end{aligned}$$

where  $m_0$  is the bare quark mass,  $m$  is the renormalized quark mass,  $\Sigma(p)$  is the quark self-energy, and  $\Sigma'(p) \equiv d\Sigma/d\not{p}$ .

Now we must evaluate the quark self-energy:

$$\begin{aligned}
i\Sigma(p) &= \int \frac{d^{4-2\epsilon}k}{(2\pi)^{4-2\epsilon}} (-ig_s) \gamma^\mu t^A \frac{i(\not{p} - \not{k} + m)}{(p-k)^2 - m^2} (-ig_s) \gamma^\nu t^B \frac{-ig_{\mu\nu} \delta_{AB}}{k^2} \\
&= -g_s^2 C_F \int \frac{d^{4-2\epsilon}k}{(2\pi)^d} \frac{\gamma^\mu (\not{p} - \not{k} + m) \gamma_\mu}{k^2 ((p-k)^2 - m^2)}.
\end{aligned}$$

We rewrite the denominator using a Feynman parameter:

$$\begin{aligned}
\frac{1}{k^2 [(p-k)^2 - m^2]} &= \int_0^1 dx \frac{1}{[(1-x)k^2 + x((p-k)^2 - m^2)]^2} \\
&= \int_0^1 dx \frac{1}{[k^2 - 2x k \cdot p + x(p^2 - m^2)]^2} \\
&= \int_0^1 dx \frac{1}{[\ell^2 - x^2 p^2 + x(p^2 - m^2)]^2},
\end{aligned}$$

where  $\ell \equiv k - xp$ . The numerator can also be simplified:

$$\gamma^\mu (\not{p} - \not{k} + m) \gamma_\mu = -2(1 - \epsilon)(\not{p} - \not{k}) + (4 - 2\epsilon)m$$

$$\begin{aligned}
&\sim 2[(1-\epsilon)(\ell - (1-x)\not{p}) + (2-\epsilon)m] \\
&= -2[(1-\epsilon)(1-x)\not{p} - (2-\epsilon)m],
\end{aligned}$$

where we have neglected terms odd in  $\ell$ .

Thus the self-energy is given by

$$i\Sigma(p) = -\frac{4}{3}g_s^2 \int_0^1 dx \int \frac{d^d\ell}{(2\pi)^d} \frac{-2[(1-\epsilon)(1-x)\not{p} - (2-\epsilon)m]}{[\ell^2 - x^2p^2 + x(p^2 - m^2)]^2}. \quad (3.2)$$

For our purposes we need only  $\Sigma'(m)$ . We can evaluate this expression in two different ways.

### Method 1: Integrating before differentiating

Following the method of Ref. [47], we now expand the self-energy near the mass shell:

$$\begin{aligned}
i\Sigma(p) &= -\frac{4}{3}g_s^2 \int_0^1 dx \int \frac{d^{4-2\epsilon}\ell}{(2\pi)^{4-2\epsilon}} \frac{-2[(1-\epsilon)(1-x)\not{p} - (2-\epsilon)m]}{[\ell^2 - x^2p^2 + x(p^2 - m^2)]^2} \\
&= \frac{8}{3}g_s^2 \frac{i}{(4\pi)^{2-\epsilon}} \frac{\Gamma(\epsilon)}{\Gamma(2)} \int_0^1 dx [(1-\epsilon)(1-x)\not{p} - (2-\epsilon)m] [x^2p^2 - x(p^2 - m^2)]^{-\epsilon} \\
&= \frac{8}{3}i \frac{\alpha_s}{4\pi} (4\pi)^\epsilon \Gamma(\epsilon) \int_0^1 dx [(1-\epsilon)(1-x)\not{p} - (2-\epsilon)m] (x^2p^2)^{-\epsilon} \\
&\quad \times \left[ 1 + \epsilon \frac{p^2 - m^2}{xm^2} + \mathcal{O}((p^2 - m^2)^2) \right].
\end{aligned}$$

The factor of  $\Gamma(\epsilon)$  is an ultraviolet divergence. The integrand also features a singularity at  $x = 0$ , which yields an infrared divergence. Simplifying the integrand and performing the integration, we obtain:

$$\begin{aligned}
i\Sigma(p) &= \frac{2i\alpha_s}{3\pi} (4\pi)^\epsilon \Gamma(\epsilon) (p^2)^{-\epsilon} \int_0^1 dx \left[ (1-\epsilon)\not{p}x^{-2\epsilon}(1-x) - (2-\epsilon)m x^{-2\epsilon} \right. \\
&\quad \left. + \epsilon(1-\epsilon)\not{p} \frac{p^2 - m^2}{m^2} x^{-1-2\epsilon}(1-x) \right. \\
&\quad \left. - \epsilon(2-\epsilon)m \frac{p^2 - m^2}{m^2} x^{-1-2\epsilon} \right]
\end{aligned}$$

$$\begin{aligned}
&= \frac{2i\alpha_s}{3\pi}(4\pi)^\epsilon \Gamma(\epsilon)(p^2)^{-\epsilon} \left[ (1-\epsilon)\not{p} \frac{\Gamma(1-2\epsilon)\Gamma(2)}{\Gamma(3-2\epsilon)} - \frac{(2-\epsilon)m}{1-2\epsilon} \right. \\
&\quad \left. + \epsilon(1-\epsilon)\not{p} \left( \frac{p^2}{m^2} - 1 \right) \frac{\Gamma(-2\epsilon)\Gamma(2)}{\Gamma(2-2\epsilon)} \right. \\
&\quad \left. - \epsilon(2-\epsilon)m \left( \frac{p^2}{m^2} - 1 \right) \frac{1}{-2\epsilon} \right] \\
&= \frac{2i\alpha_s}{3\pi}(4\pi)^\epsilon \Gamma(\epsilon)(p^2)^{-\epsilon} \left[ \frac{1-\epsilon}{(1-2\epsilon)(2-2\epsilon)}\not{p} - \frac{2-\epsilon}{1-2\epsilon} \right. \\
&\quad \left. - \frac{1-\epsilon}{2(1-2\epsilon)} \left( \frac{p^2}{m^2} - 1 \right) \not{p} + \frac{2-\epsilon}{2} \left( \frac{p^2}{m^2} - 1 \right) m \right].
\end{aligned}$$

Therefore

$$\begin{aligned}
\Sigma'(p) &= \frac{2\alpha_s}{3\pi}(4\pi)^\epsilon \Gamma(\epsilon) \left\{ -2\epsilon(p^2)^{-1-\epsilon} \not{p} \left[ \frac{1}{2(1-2\epsilon)}\not{p} - \frac{2-\epsilon}{1-2\epsilon}m - \frac{1-\epsilon}{2(1-2\epsilon)} \left( \frac{p^2}{m^2} - 1 \right) \not{p} \right. \right. \\
&\quad \left. \left. + \left( 1 - \frac{1}{2}\epsilon \right) \left( \frac{p^2}{m^2} - 1 \right) m \right] \right. \\
&\quad \left. + (p^2)^{-\epsilon} \left[ \frac{1}{2(1-2\epsilon)} - \frac{1-\epsilon}{2(1-2\epsilon)} \left( \frac{p^2}{m^2} - 1 \right) \right. \right. \\
&\quad \left. \left. - \frac{1-\epsilon}{2(1-2\epsilon)} \frac{2p^2}{m^2} + \left( 1 - \frac{1}{2}\epsilon \right) \frac{2\not{p}}{m} \right] \right\}
\end{aligned}$$

and

$$\begin{aligned}
\Sigma'(m) &= \frac{2\alpha_s}{3\pi}(4\pi)^\epsilon \Gamma(\epsilon)m^{-2\epsilon} \left\{ -2\epsilon \left[ \frac{1}{2(1-2\epsilon)} - \frac{2-\epsilon}{1-2\epsilon} \right] \right. \\
&\quad \left. + \left[ \frac{1}{2(1-2\epsilon)} - \frac{1-\epsilon}{1-2\epsilon} + 2 \left( 1 - \frac{1}{2}\epsilon \right) \right] \right\} \\
&= \frac{2\alpha_s}{3\pi} \left( \frac{1}{\epsilon} - \gamma + \ln \frac{4\pi}{m^2} \right) \left\{ -2\epsilon \left[ \frac{1}{2} - 2 \right] + \left[ \frac{1}{2}(1+2\epsilon) - (1+\epsilon) + (2-\epsilon) \right] \right\} \\
&\quad + \mathcal{O}(\epsilon) \\
&= \frac{2\alpha_s}{3\pi} \left( \frac{1}{\epsilon} - \gamma + \ln \frac{4\pi}{m^2} \right) \left( \frac{3}{2} + 2\epsilon \right) \\
&= \frac{\alpha_s}{\pi} \left( \frac{1}{\epsilon} - \gamma + \ln \frac{4\pi}{m^2} + \frac{4}{3} \right). \tag{3.3}
\end{aligned}$$

One third of the term involving  $1/\epsilon$  can be attributed to the ultraviolet divergence of the loop integral, and the other two thirds to the infrared singularity at  $x = 0$ . The term involving  $\ln m^2$  is a collinear divergence.

## Method 2: Differentiating before integrating

We can obtain a cleaner derivation by observing that the self-energy, as written in Eq. (3.2), depends only on  $\not{p}$  and can therefore be safely differentiated:

$$\Sigma'(p) = -\frac{8}{3}ig_s^2 \int_0^1 dx \int \frac{d^{4-2\epsilon}\ell}{(2\pi)^{4-2\epsilon}} \left\{ \frac{(1-\epsilon)(1-x)}{[\ell^2 - x^2p^2 + x(p^2 - m^2)]^2} - \frac{4x(1-x)\not{p}[(1-\epsilon)(1-x)\not{p} - (2-\epsilon)m]}{[\ell^2 - x^2p^2 + x(p^2 - m^2)]^3} \right\}.$$

Now we can put the quark on shell and perform the loop integration:

$$\begin{aligned} \Sigma'(m) &= \frac{8}{3}ig_s^2 \int_0^1 dx \int \frac{d^{4-2\epsilon}\ell}{(2\pi)^{4-2\epsilon}} \left\{ \frac{(1-\epsilon)(1-x)}{(\ell^2 - x^2m^2)^2} - \frac{4x(1-x)[(1-\epsilon)(1-x) - (2-\epsilon)]m^2}{(\ell^2 - x^2m^2)^3} \right\} \\ &= -\frac{8}{3}ig_s^2 \int_0^1 dx \left\{ \frac{i}{(4\pi)^{2-\epsilon}} \frac{\Gamma(\epsilon)}{\Gamma(2)} (x^2m^2)^{-\epsilon} (1-\epsilon)(1-x) \right. \\ &\quad \left. + \frac{i}{(4\pi)^{2-\epsilon}} \frac{\Gamma(1+\epsilon)}{\Gamma(3)} (x^2m^2)^{-1-\epsilon} \right. \\ &\quad \left. \times 4x(1-x)[(1-\epsilon)(1-x) - (2-\epsilon)]m^2 \right\} \\ &= \frac{8}{3} \frac{\alpha_s}{4\pi} \Gamma(1+\epsilon) \left( \frac{4\pi}{m^2} \right)^\epsilon \int_0^1 dx \left\{ \frac{1}{\epsilon} (1-\epsilon)x^{-2\epsilon}(1-x) \right. \\ &\quad \left. + 2[(1-\epsilon)(1-x) - (2-\epsilon)]x^{-1-2\epsilon}(1-x) \right\} \end{aligned}$$

The factor of  $1/\epsilon$  in the first term of the integrand is an ultraviolet divergence. The second term in the integrand contains an infrared singularity at  $x = 0$ . The factor of  $m^{-2\epsilon}$  will

produce a collinear divergence in the form of  $\ln m^2$ . Continuing the evaluation, we obtain:

$$\begin{aligned}
&= \frac{2\alpha_s}{3\pi} \Gamma(1 + \epsilon) \left( \frac{4\pi}{m^2} \right)^\epsilon \int_0^1 dx \left[ \frac{1}{\epsilon} (1 - \epsilon) x^{-2\epsilon} (1 - x) + 2(1 - \epsilon) x^{-1-2\epsilon} (1 - x)^2 \right. \\
&\quad \left. - 2(2 - \epsilon) x^{-1-2\epsilon} (1 - x) \right] \\
&= \frac{2\alpha_s}{3\pi} \Gamma(1 + \epsilon) \left( \frac{4\pi}{m^2} \right)^\epsilon \left[ \frac{1}{\epsilon} (1 - \epsilon) \frac{\Gamma(1 - 2\epsilon) \Gamma(2)}{\Gamma(3 - 2\epsilon)} + 2(1 - \epsilon) \frac{\Gamma(-2\epsilon) \Gamma(3)}{\Gamma(3 - 2\epsilon)} \right. \\
&\quad \left. - 2(2 - \epsilon) \frac{\Gamma(-2\epsilon) \Gamma(2)}{\Gamma(2 - 2\epsilon)} \right] \\
&= \frac{2\alpha_s}{3\pi} \Gamma(1 + \epsilon) \left( \frac{4\pi}{m^2} \right)^\epsilon \left[ \frac{1}{\epsilon} (1 - \epsilon) \frac{1}{(1 - 2\epsilon)(2 - 2\epsilon)} \right. \\
&\quad \left. + 2(1 - \epsilon) \frac{2}{-2\epsilon(1 - 2\epsilon)(2 - 2\epsilon)} \right. \\
&\quad \left. - 2(2 - \epsilon) \frac{1}{-2\epsilon(1 - 2\epsilon)} \right] \\
&= \frac{2\alpha_s}{3\pi} \Gamma(1 + \epsilon) \left( \frac{4\pi}{m^2} \right)^\epsilon \left[ \frac{1}{2\epsilon(1 - 2\epsilon)} - \frac{1}{\epsilon(1 - 2\epsilon)} + \frac{2 - \epsilon}{\epsilon(1 - 2\epsilon)} \right] \\
&= \frac{2\alpha_s}{3\pi} \Gamma(1 + \epsilon) \left( \frac{4\pi}{m^2} \right)^\epsilon \frac{1}{\epsilon(1 - 2\epsilon)} \left( \frac{1}{2} - 1 + 2 - \epsilon \right) \\
&= \frac{2\alpha_s}{3\pi} \left( 1 - \gamma\epsilon + \epsilon \ln \frac{4\pi}{m^2} \right) \frac{1}{\epsilon} (1 + 2\epsilon) \left( \frac{3}{2} - \epsilon \right) + \mathcal{O}(\epsilon) \\
&= \frac{\alpha_s}{\pi} \left( \frac{1}{\epsilon} - \gamma + \ln \frac{4\pi}{m^2} \right) (1 + 2\epsilon) \left( 1 - \frac{2\epsilon}{3} \right) \\
&= \frac{\alpha_s}{\pi} \left( \frac{1}{\epsilon} - \gamma + \ln \frac{4\pi}{m^2} + \frac{4}{3} \right) + \mathcal{O}(\epsilon). \tag{3.4}
\end{aligned}$$

The two methods yield the same result, given by Eqs. (3.3) and (3.4).

We must multiply the tree-level amplitude by a factor of  $1/\sqrt{1 + \Sigma'(m)} = 1 - \frac{1}{2}\Sigma'(m) + \mathcal{O}(\alpha_s^2)$  for the external quark, and by the same factor for the external antiquark. Combining this with the vertex correction given in Eq. (3.1), we find that the NLO amplitude for

$q\bar{q} \rightarrow W$  is given by

$$\begin{aligned}
i\mathcal{M} &= \frac{-ig}{2\sqrt{2}}\varepsilon_\mu^*(k)\bar{v}(p_2)\gamma^\mu(1-\gamma_5)u(p_1) \\
&\quad \times \left\{ 1 + \frac{\alpha_s}{3\pi} \left[ \left( \frac{1}{\epsilon} - \gamma + \ln \frac{4\pi}{M_W^2} \right) (-2\ln\rho + 1) + \ln^2\rho - 4\ln\rho \right. \right. \\
&\quad \quad \left. \left. + \frac{4\pi^2}{3} - 3 \left( \frac{1}{\epsilon} - \gamma + \ln \frac{4\pi}{m^2} + \frac{4}{3} \right) \right] \right\} \\
&= \frac{-ig}{2\sqrt{2}}\varepsilon_\mu^*(k)\bar{v}(p_2)\gamma^\mu(1-\gamma_5)u(p_1) \\
&\quad \times \left\{ 1 + \frac{\alpha_s}{3\pi} \left[ \left( \frac{1}{\epsilon} - \gamma + \ln 4\pi \right) (-2\ln\rho - 2) + (2\ln\rho - 1)\ln M_W^2 + 3\ln m^2 \right. \right. \\
&\quad \quad \left. \left. + \ln^2\rho - 4\ln\rho + \frac{4\pi^2}{3} - 4 \right] \right\}.
\end{aligned}$$

Therefore the  $q\bar{q} \rightarrow W$  cross section, including the virtual-gluon diagrams, is simply given by the tree-level cross section times the square of the quantity in braces, except that the Dirac trace must now be evaluated in  $4 - 2\epsilon$  dimensions:

$$\begin{aligned}
\text{Tr}[\not{p}_1\gamma_\mu\not{p}_2\gamma^\mu] &= \text{Tr}[-2(1-\epsilon)\not{p}_1\not{p}_2] \\
&= -8(1-\epsilon)p_1 \cdot p_2,
\end{aligned}$$

i.e. there is an additional factor of  $(1-\epsilon)$ . To first order in  $\alpha_s$ , the cross section is

$$\begin{aligned}
\hat{\sigma} &= \frac{\pi^2\alpha}{3s_W^2M_W^2}(1-\epsilon)\delta(1-\tau) \\
&\quad \times \left\{ 1 + \frac{2\alpha_s}{3\pi} \left[ -2 \left( \frac{1}{\epsilon} - \gamma + \ln 4\pi \right) (\ln\rho + 1) + (2\ln\rho - 1)\ln M_W^2 \right. \right. \\
&\quad \quad \left. \left. + 3\ln m^2 + \ln^2\rho - 4\ln\rho + \frac{4\pi^2}{3} - 4 \right] \right\} \\
&= \frac{\pi^2\alpha}{3s_W^2M_W^2}\delta(1-\tau) \left\{ 1 + \frac{2\alpha_s}{3\pi} \left[ -2 \left( \frac{1}{\epsilon} - \gamma + \ln 4\pi \right) (\ln\rho + 1) + (2\ln\rho - 1)\ln M_W^2 \right. \right. \\
&\quad \quad \left. \left. + 3\ln m^2 + \ln^2\rho - 2\ln\rho + \frac{4\pi^2}{3} - 2 \right] \right\} + \mathcal{O}(\epsilon).
\end{aligned} \tag{3.5}$$

The ultraviolet divergences have cancelled between the vertex and wavefunction-renormalization corrections; the remaining term involving  $1/\epsilon$  is the infrared divergence. The collinear divergences are contained in the various terms involving  $\ln m^2$ .

### 3.3 $q\bar{q} \rightarrow gW$ (tree level)

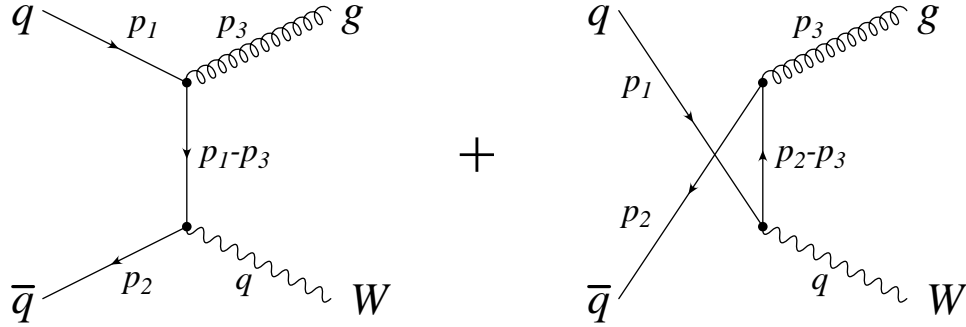


Figure 3.4: Feynman diagrams for the real-gluon-emission process  $q\bar{q} \rightarrow gW$ .

The real-gluon-emission process, shown in Fig. 3.4, features an infrared divergence, which cancels against that from the virtual-gluon diagrams; thus we continue to work in  $4 - 2\epsilon$  dimensions. Also, the  $t$ - and  $u$ -channel diagrams both contain collinear singularities. In fact, the squares of these diagrams involve double poles, which yield factors of  $1/m^2$ , so that we need to keep the quark mass in the numerator.

We parametrize the momenta as follows:

$$\begin{aligned}
 p_1 &= \left( \frac{\sqrt{s}}{2}, \frac{\sqrt{s}}{2}\beta, 0, 0 \right) \\
 p_2 &= \left( \frac{\sqrt{s}}{2}, -\frac{\sqrt{s}}{2}\beta, 0, 0 \right) \\
 p_3 &= \left( \frac{\sqrt{s}}{2}(1-\tau), \frac{\sqrt{s}}{2}(1-\tau)\cos\theta, \frac{\sqrt{s}}{2}(1-\tau)\sin\theta, 0 \right) \\
 k &= \left( \frac{\sqrt{s}}{2}(1+\tau), -\frac{\sqrt{s}}{2}(1-\tau)\cos\theta, -\frac{\sqrt{s}}{2}(1-\tau)\sin\theta, 0 \right)
 \end{aligned}$$

where  $\tau \equiv M_W^2/s$ ,  $\rho \equiv m^2/s$ , and  $\beta \equiv \sqrt{1-4\rho}$ .

Two-body phase space in  $(4-2\epsilon)$  dimensions is rather interesting. It is convenient to express it in terms of the variable  $z$ , the cosine of the scattering angle  $\theta$ .

$$\begin{aligned}
\int d\Phi &= \int \frac{d^{4-2\epsilon} p_3}{(2\pi)^{4-2\epsilon}} \theta(p_3^0) 2\pi \delta(p_3^2) \int \frac{d^{4-2\epsilon} q}{(2\pi)^{4-2\epsilon}} \theta(q^0) 2\pi \delta(q^2 - M_W^2) \\
&\quad \times (2\pi)^{4-2\epsilon} \delta^{4-2\epsilon}(p_1 + p_2 - p_3 - q) \\
&= \frac{1}{(2\pi)^{2-2\epsilon}} \int_0^{\sqrt{s}} dq^0 \int d^{3-2\epsilon} \vec{q} \delta(q^2 - M_W^2) \delta((p_1 + p_2 - q)^2) \\
&= \frac{1}{(4\pi^2)^{1-\epsilon}} \int_0^{\sqrt{s}} dq^0 \int d^{3-2\epsilon} \vec{q} \delta(q^2 - M_W^2) \delta(s - 2(p_1 + p_2) \cdot q + M_W^2) \\
&= \frac{1}{(4\pi^2)^{1-\epsilon}} \int_0^{\sqrt{s}} dq^0 \int d^{3-2\epsilon} \vec{q} \delta(q^2 - M_W^2) \frac{1}{2\sqrt{s}} \delta\left(q^0 - \frac{\sqrt{s}}{2}(1+\tau)\right) \\
&= \frac{1}{(4\pi^2)^{1-\epsilon} 2\sqrt{s}} \int d^{3-2\epsilon} \vec{q} \delta\left(\frac{s}{4}(1+\tau)^2 - \vec{q}^2 - M_W^2\right) \\
&= \frac{1}{(4\pi^2)^{1-\epsilon} 2\sqrt{s}} \int_0^\infty |\vec{q}|^{2-2\epsilon} d|\vec{q}| \int_0^\pi \sin^{1-2\epsilon} \theta d\theta \int d^{1-2\epsilon} \Omega \delta\left(\vec{q}^2 - \frac{s}{4}(1-\tau)^2\right) \\
&= \frac{1}{(4\pi^2)^{1-\epsilon} 2\sqrt{s}} \frac{2\pi^{1-\epsilon}}{\Gamma(1-\epsilon)} \int_0^\infty d|\vec{q}| \frac{|\vec{q}|^{2-2\epsilon}}{2|\vec{q}|} \delta\left(|\vec{q}| - \frac{\sqrt{s}}{2}(1-\tau)\right) \\
&\quad \times \int_{-1}^1 dz \left(\sqrt{1-z^2}\right)^{-2\epsilon} \\
&= \frac{1}{(4\pi)^{1-\epsilon}} \frac{1}{2\sqrt{s}} \frac{1}{\Gamma(1-\epsilon)} \left(\frac{\sqrt{s}}{2}(1-\tau)\right)^{1-2\epsilon} \int_{-1}^1 dz (1-z^2)^{-\epsilon} \\
&= \frac{1}{\Gamma(1-\epsilon)} \frac{1}{(16\pi)^{1-\epsilon}} \frac{1}{s^\epsilon} (1-\tau)^{1-2\epsilon} \int_{-1}^1 dz (1-z^2)^{-\epsilon} \\
&= \frac{1}{16\pi\Gamma(1-\epsilon)} \left(\frac{16\pi}{M_W^2}\right)^\epsilon \tau^\epsilon (1-\tau)^{1-2\epsilon} \int_{-1}^1 dz (1-z^2)^{-\epsilon} \\
&= \frac{1}{16\pi} \left(1 - \gamma\epsilon + \epsilon \ln \frac{16\pi\tau}{M_W^2}\right) (1-\tau)^2 \left(-\frac{1}{2\epsilon} \delta(1-\tau) + \frac{1}{(1-\tau)_+}\right) \\
&\quad \times \int_{-1}^1 dz (1 - \epsilon \ln(1-z^2)) + \mathcal{O}(\epsilon) \\
&= -\frac{1}{32\pi} (1-\tau)^2 \left[ \left(\frac{1}{\epsilon} - \gamma + \ln \frac{16\pi}{M_W^2}\right) \delta(1-\tau) - \frac{2}{(1-\tau)_+} \right] \\
&\quad \times \int_{-1}^1 dz (1 - \epsilon \ln(1-z^2)). \tag{3.6}
\end{aligned}$$

The distribution  $1/(1-\tau)_+$  is defined by

$$\int_0^1 d\tau \frac{f(\tau)}{(1-\tau)_+} \equiv \int_0^1 d\tau \frac{f(\tau) - f(1)}{1-\tau}$$

for any sufficiently smooth function  $f$ . The form of the phase space integral in Eq. (3.6) will be useful when we combine the real- and virtual-gluon contributions.

The amplitude for  $q\bar{q} \rightarrow gW$  is given by

$$\begin{aligned} i\mathcal{M} &= \varepsilon_{\mu A}^*(p_3)\varepsilon_{\nu}^*(q)\bar{v}(p_2) \left[ \frac{-ig}{2\sqrt{2}}\gamma^\nu(1-\gamma_5)\frac{i(\not{p}_1-\not{p}_3+m)}{t-m^2}(-ig_s)\gamma^\mu t^A \right. \\ &\quad \left. - ig_s\gamma^\mu t^A\frac{i(\not{p}_3-\not{p}_2+m)}{u-m^2}\frac{-ig}{2\sqrt{2}}\gamma^\nu(1-\gamma_5) \right] u(p_1) \\ &\equiv i\varepsilon_{\nu}^*(q)\mathcal{M}^\nu. \end{aligned}$$

We cannot *a priori* neglect the longitudinal  $W$  polarization, since the squares of the  $t$ - and  $u$ -channel diagrams feature double poles. By the Ward identity,

$$\begin{aligned} q_\nu\mathcal{M}^\nu &= \frac{gg_s}{2\sqrt{2}}t^A\varepsilon_{\mu A}^*(p_3)\bar{v}(p_2) \left[ \not{q}\gamma_5\frac{\not{p}_1-\not{p}_3+m}{t-m^2}\gamma^\mu + \gamma^\mu\frac{\not{p}_3-\not{p}_2+m}{u-m^2}\not{q}\gamma_5 \right] u(p_1) \\ &= \frac{gg_s}{2\sqrt{2}}t^A\varepsilon_{\mu A}^*(p_3)\bar{v}(p_2) \left[ (\not{p}_1-\not{p}_3-m)\gamma_5\frac{\not{p}_1-\not{p}_3+m}{t-m^2}\gamma^\mu \right. \\ &\quad \left. - \gamma^\mu\frac{\not{p}_3-\not{p}_2+m}{u-m^2}\gamma_5(\not{p}_2-\not{p}_3+m) \right] u(p_1) \\ &= \frac{gg_s}{s\sqrt{2}}t^A\varepsilon_{\mu A}^*(p_3)\bar{v}(p_2) \left[ \frac{(\not{p}_1-\not{p}_3-m)^2}{t-m^2}\gamma^\mu\gamma_5 - \gamma^\mu\gamma_5\frac{(\not{p}_2-\not{p}_3+m)^2}{u-m^2} \right] u(p_1) \\ &= \frac{gg_s}{2\sqrt{2}}t^A\varepsilon_{\mu A}^*(p_3)\bar{v}(p_2) \left[ \frac{t-2m(\not{p}_1-\not{p}_3)+m^2}{t-m^2}\gamma^\mu\gamma_5 \right. \\ &\quad \left. - \gamma^\mu\gamma_5\frac{u+2m(\not{p}_2-\not{p}_3)+m^2}{u-m^2} \right] u(p_1) \\ &= 2m\frac{gg_s}{2\sqrt{2}}t^A\varepsilon_{\mu A}^*(p_3)\bar{v}(p_2) \left[ \frac{\not{p}_3-\not{p}_1+m}{t-m^2}\gamma^\mu\gamma_5 - \gamma^\mu\gamma_5\frac{\not{p}_2-\not{p}_3+m}{u-m^2} \right] u(p_1). \end{aligned}$$

The squared amplitude can then be written as

$$|\overline{\mathcal{M}}|^2 = \frac{1}{2} \frac{1}{3} \frac{1}{2} \frac{1}{3} \frac{g^2 g_s^2}{8} \text{Tr}[t^A t_A] (L_{tt} + L_{uu} + T_{tt} + T_{uu} + 2 \text{Re} T_{tu}), \quad (3.7)$$

where

$$\begin{aligned} L_{tt} &= -\frac{4m^2}{M_W^2} \text{Tr} \left[ \not{p}_1 (-\gamma_5) \gamma_\mu \frac{\not{p}_3 - \not{p}_1}{t - m^2} \not{p}_2 \frac{\not{p}_3 - \not{p}_1}{t - m^2} \gamma^\mu \gamma_5 \right], \\ L_{uu} &= -\frac{4m^2}{M_W^2} \text{Tr} \left[ \not{p}_1 \frac{\not{p}_2 - \not{p}_3}{u - m^2} (-\gamma_5) \gamma_\mu \not{p}_2 \gamma^\mu \gamma_5 \frac{\not{p}_2 - \not{p}_3}{u - m^2} \right], \\ T_{tt} &= \text{Tr} \left[ (\not{p}_1 + m) \gamma_\mu \frac{\not{p}_1 - \not{p}_3 + m}{t - m^2} (1 + \gamma_5) \gamma_\nu (\not{p}_2 - m) \gamma^\nu (1 - \gamma_5) \frac{\not{p}_2 - \not{p}_3 + m}{t - m^2} \gamma^\mu \right], \\ T_{uu} &= \text{Tr} \left[ (\not{p}_1 + m) (1 + \gamma_5) \gamma_\nu \frac{\not{p}_3 - \not{p}_2 + m}{u - m^2} \gamma_\mu (\not{p}_2 - m) \gamma^\mu \frac{\not{p}_3 - \not{p}_2 + m}{u - m^2} \gamma^\nu (1 - \gamma_5) \right], \end{aligned}$$

and

$$T_{tu} = \text{Tr} \left[ \not{p}_1 \gamma_\mu \frac{\not{p}_1 - \not{p}_3}{t - m^2} (1 + \gamma_5) \gamma_\nu \not{p}_2 \gamma^\mu \frac{\not{p}_3 - \not{p}_2}{u - m^2} \gamma^\nu (1 - \gamma_5) \right].$$

Note that the longitudinal terms  $L_{tt}$  and  $L_{uu}$  are already suppressed by a factor of  $m^2$ , so that we can neglect  $m$  in the numerators of these terms. We can neglect the interference term  $L_{tu}$  altogether, since only a double pole can produce a factor of  $1/m^2$ . For the same reason, we can neglect  $m$  in the numerator of the transverse interference term  $T_{tu}$ .

Now

$$\begin{aligned} L_{tt} &= -\frac{4m^2}{M_W^2} \text{Tr} \left[ \not{p}_1 (-\gamma_5) \gamma_\mu \frac{\not{p}_3 - \not{p}_1}{t - m^2} \not{p}_2 \frac{\not{p}_3 - \not{p}_1}{t - m^2} \gamma^\mu \gamma_5 \right] \\ &= -\frac{4\rho}{\tau (t - m^2)^2} \text{Tr} \left[ \gamma^\mu \not{p}_1 \gamma_\mu (\not{p}_3 - \not{p}_1) \not{p}_2 (\not{p}_3 - \not{p}_1) \right] \\ &= -\frac{4\rho}{\tau (t - m^2)^2} \text{Tr} \left[ -2(1 - \epsilon) \not{p}_2 (\not{p}_3 - \not{p}_1) \not{p}_2 (\not{p}_3 - \not{p}_1) \right] \\ &= \frac{8\rho(1 - \epsilon)}{\tau (t - m^2)^2} \text{Tr} \not{p}_2 \not{p}_3 \not{p}_1 \not{p}_3 + \mathcal{O}(m^4) \end{aligned}$$

$$\begin{aligned}
&= \frac{8\rho(1-\epsilon)}{\tau(p_1 \cdot p_3)^2} 2 p_1 \cdot p_3 p_2 \cdot p_3 \\
&= 16(1-\epsilon) \frac{\rho p_2 \cdot p_3}{\tau p_1 \cdot p_3}.
\end{aligned}$$

One of the poles has been cancelled, so that this term's contribution to the cross section will be  $\mathcal{O}(\rho \ln \rho)$ , which vanishes in the limit  $\rho \rightarrow 0$ . Thus we can neglect this term, and likewise

$L_{uu}$ .

Now

$$\begin{aligned}
T_{tt} &= \text{Tr} \left[ (\not{p}_1 + m) \gamma_\mu \frac{\not{p}_1 - \not{p}_3 + m}{t - m^2} (1 + \gamma_5) \gamma_\nu (\not{p}_2 - m) \gamma^\nu (1 - \gamma_5) \frac{\not{p}_1 - \not{p}_3 + m}{t - m^2} \gamma^\mu \right] \\
&= \frac{1}{(t - m^2)^2} \text{Tr} [(\not{p}_1 - \not{p}_3 + m) \gamma^\mu (\not{p}_1 + m) \gamma_\mu (\not{p}_1 - \not{p}_3 + m) \gamma_\nu \not{p}_2 \gamma^\nu 2(1 - \gamma_5)] \\
&= \frac{2}{(t - m^2)^2} \text{Tr} [(\not{p}_1 - \not{p}_3 + m) (-2(1 - \epsilon) \not{p}_1 + (4 - 2\epsilon)m) \\
&\quad \times (\not{p}_1 - \not{p}_3 + m) (-2)(1 - \epsilon) \not{p}_2] \\
&= \frac{8(1 - \epsilon)}{(t - m^2)^2} \text{Tr} [(1 - \epsilon)(\not{p}_1 - \not{p}_3 + m) ((1 - \epsilon) \not{p}_1 - (2 - \epsilon)m) (\not{p}_1 - \not{p}_3 + m) \not{p}_2] \\
&= \frac{8(1 - \epsilon)}{(t - m^2)^2} \text{Tr} [(1 - \epsilon)(\not{p}_1 - \not{p}_3) \not{p}_1 (\not{p}_1 - \not{p}_3) \not{p}_2 \\
&\quad + m^2 ((1 - \epsilon) \not{p}_1 - 2(2 - \epsilon)(\not{p}_1 - \not{p}_3)) \not{p}_2] \\
&= \frac{8(1 - \epsilon)}{(t - m^2)^2} \text{Tr} [(1 - \epsilon)(m^2 - \not{p}_3 \not{p}_1) (\not{p}_1 - \not{p}_3) \not{p}_2 + m^2 \not{p}_2 ((4 - 2\epsilon) \not{p}_3 - (3 - \epsilon) \not{p}_1)] \\
&= \frac{8(1 - \epsilon)}{(t - m^2)^2} \text{Tr} [(1 - \epsilon) \not{p}_3 (\not{p}_1 \not{p}_3 - m^2) \not{p}_2 + m^2 \not{p}_2 ((3 - \epsilon) \not{p}_3 - 2 \not{p}_1)] \\
&= \frac{8(1 - \epsilon)}{(t - m^2)^2} \text{Tr} [(1 - \epsilon) \not{p}_3 \not{p}_1 \not{p}_3 \not{p}_2 + 2m^2 \not{p}_2 (\not{p}_3 - \not{p}_1)] \\
&= \frac{8(1 - \epsilon)}{(p_1 \cdot p_3)^2} [2(1 - \epsilon) p_1 \cdot p_3 p_2 \cdot p_3 + 2m^2 p_2 \cdot (p_2 - k)] \\
&= 16(1 - 2\epsilon) \frac{p_2 \cdot p_3}{p_1 \cdot p_3} - 16(1 - \epsilon) \frac{m^2 p_2 \cdot k}{(p_1 \cdot p_3)^2} \\
&= 16(1 - 2\epsilon) \frac{1 + \beta z}{1 - \beta z} - 64(1 - \epsilon) \rho \frac{1 + \tau - (1 - \tau)\beta z}{(1 - \tau)^2 (1 - \beta z)^2} \\
&= 16(1 - 2\epsilon) \frac{2 - (1 - \beta z)}{1 - \beta z} - \frac{64(1 - \epsilon) \rho 2\tau + (1 - \tau)(1 - \beta z)}{(1 - \tau)^2 (1 - \beta z)^2}
\end{aligned}$$

$$= \frac{32(1-2\epsilon)}{1-\beta z} - 16(1-2\epsilon) - \frac{128(1-\epsilon)\tau\rho}{(1-\tau)^2(1-\beta z)^2},$$

where we have neglected terms proportional to  $\rho$  without a double pole. Similarly

$$T_{uu} = \frac{32(1-2\epsilon)}{1+\beta z} - 16(1-2\epsilon) - \frac{128(1-\epsilon)\tau\rho}{(1-\tau)^2(1+\beta z)^2}.$$

Finally,

$$\begin{aligned} T_{tu} &= \text{Tr} \left[ \not{p}_1 \gamma_\mu \frac{\not{p}_1 - \not{p}_3}{t - m^2} (1 + \gamma_5) \gamma_\nu \not{p}_2 \gamma^\mu \frac{\not{p}_3 - \not{p}_2}{u - m^2} \gamma^\nu (1 - \gamma_5) \right] \\ &= \frac{1}{(t - m^2)(u - m^2)} \text{Tr} \left[ \not{p}_1 \gamma_\mu (\not{p}_1 - \not{p}_3) \gamma_\nu \not{p}_2 \gamma^\mu (\not{p}_3 - \not{p}_2) \gamma^\nu 2(1 - \gamma_5) \right] \\ &= \frac{2}{(t - m^2)(u - m^2)} \text{Tr} \left[ \not{p}_1 (-2) (\not{p}_2 \gamma_\nu (\not{p}_1 - \not{p}_3) \right. \\ &\quad \left. - \epsilon (\not{p}_1 - \not{p}_3) \gamma_\nu \not{p}_2) (\not{p}_3 - \not{p}_2) \gamma^\nu (1 - \gamma_5) \right] \\ &= \frac{-4}{(t - m^2)(u - m^2)} \text{Tr} \left[ (\not{p}_3 - \not{p}_2) (\gamma^\nu \not{p}_1 \not{p}_2 \gamma_\nu (\not{p}_1 - \not{p}_3) \right. \\ &\quad \left. - \epsilon \gamma^\nu \not{p}_1 (\not{p}_1 - \not{p}_3) \gamma_\nu \not{p}_2) (1 - \gamma_5) \right] \\ &= \frac{-4}{(t - m^2)(u - m^2)} \text{Tr} \left[ (\not{p}_3 - \not{p}_2) (\gamma^\nu \not{p}_1 \not{p}_2 \gamma_\nu (\not{p}_1 - \not{p}_3) + \epsilon \gamma^\nu \not{p}_1 \not{p}_3 \gamma_\nu \not{p}_2) (1 - \gamma_5) \right] \\ &= \frac{-4}{(t - m^2)(u - m^2)} \text{Tr} \left[ (\not{p}_3 - \not{p}_2) 2((2p_1 \cdot p_2 - \epsilon \not{p}_1 \not{p}_2) (\not{p}_1 - \not{p}_3) + 2\epsilon p_1 \cdot p_3 \not{p}_2) \right] \\ &= \frac{-8}{(t - m^2)(u - m^2)} \text{Tr} \left[ 2p_1 \cdot p_2 (\not{p}_3 - \not{p}_2) (\not{p}_1 - \not{p}_3) + 2\epsilon p_1 \cdot p_3 \not{p}_2 \not{p}_3 \right. \\ &\quad \left. - \epsilon \not{p}_1 \not{p}_2 (\not{p}_1 - \not{p}_3) (\not{p}_3 - \not{p}_2) \right] \\ &= \frac{-8}{p_1 \cdot p_3 p_2 \cdot p_3} \left[ 2p_1 \cdot p_2 (p_3 - p_2) \cdot (p_1 - p_3) + 2\epsilon p_1 \cdot p_3 p_2 \cdot p_3 \right. \\ &\quad \left. - \epsilon p_1 \cdot p_2 (p_1 - p_3) \cdot (p_3 - p_2) - \epsilon p_1 \cdot p_3 p_2 \cdot p_3 \right. \\ &\quad \left. - \epsilon p_1 \cdot (p_1 - q) p_2 \cdot (q - p_2) \right] \\ &= \frac{-8}{p_1 \cdot p_3 p_2 \cdot p_3} \left[ 2p_1 \cdot p_2 (p_1 \cdot (p_1 - q) - p_3 \cdot (p_3 - p_2)) \right. \\ &\quad \left. - \epsilon p_1 \cdot p_2 (p_1 \cdot (p_1 - q) - p_3 \cdot (p_3 - p_2)) + 2\epsilon p_1 \cdot p_3 p_2 \cdot p_3 \right. \\ &\quad \left. - \epsilon p_1 \cdot p_3 p_2 \cdot p_3 + \epsilon p_1 \cdot q p_2 \cdot q \right] \end{aligned}$$

$$\begin{aligned}
&= \frac{-8}{p_1 \cdot p_3 p_2 \cdot p_3} [(2 - \epsilon) p_1 \cdot p_2 (-p_1 \cdot q + p_2 \cdot p_3) + \epsilon p_1 \cdot p_3 p_2 \cdot p_3 + \epsilon p_1 \cdot q p_2 \cdot q] \\
&= 8(2 - \epsilon) \frac{p_1 \cdot p_2 (p_1 \cdot q - p_2 \cdot p_3)}{p_1 \cdot p_3 p_2 \cdot p_3} - 8\epsilon - 8\epsilon \frac{p_1 \cdot q p_2 \cdot q}{p_1 \cdot p_3 p_2 \cdot p_3} \\
&= 8(2 - \epsilon) \frac{(1 + \beta^2)[1 + \tau + (1 - \tau)\beta z - (1 - \tau)(1 + \beta z)]}{(1 - \tau)(1 - \beta z)(1 - \tau)(1 + \beta z)} - 8\epsilon \\
&\quad - 8\epsilon \frac{[1 + \tau + (1 - \tau)\beta z][1 + \tau - (1 - \tau)\beta z]}{(1 - \tau)(1 - \beta z)(1 - \tau)(1 + \beta z)} \\
&= \frac{16(2 - \epsilon)}{(1 - \tau)^2} \frac{2\tau}{(1 - \beta z)(1 + \beta z)} - 8\epsilon \\
&\quad - \frac{8\epsilon}{(1 - \tau)^2} \frac{[2\tau + (1 - \tau)(1 + \beta z)][2\tau + (1 - \tau)(1 - \beta z)]}{(1 - \beta z)(1 + \beta z)} \\
&= \frac{16(2 - \epsilon)\tau}{(1 - \tau)^2} \left( \frac{1}{1 + \beta z} + \frac{1}{1 - \beta z} \right) - 8\epsilon \\
&\quad - \frac{16\epsilon\tau^2}{(1 - \tau)^2} \left( \frac{1}{1 + \beta z} + \frac{1}{1 - \beta z} \right) - \frac{16\epsilon\tau}{1 - \tau} \left( \frac{1}{1 + \beta z} + \frac{1}{1 - \beta z} \right) - 8\epsilon \\
&= \frac{32(1 - \epsilon)\tau}{(1 - \tau)^2} \left( \frac{1}{1 + \beta z} + \frac{1}{1 - \beta z} \right) - 16\epsilon.
\end{aligned}$$

We must compute three phase-space integrals, for the cases of zero, one, and two poles.

- Zero poles:

$$\begin{aligned}
\int_{-1}^1 dz [1 - \epsilon \ln(1 - z^2)] &= \int_{-1}^1 dz [1 - 2\epsilon \ln(1 + z)] \\
&= 2 - 2\epsilon (1 + z)(\ln(1 + z) - 1) \Big|_{-1}^1 \\
&= 2 - 2\epsilon(2 \ln 2 - 2) \\
&= 2 + 4\epsilon(1 - \ln 2).
\end{aligned}$$

- One pole:

$$\int_{-1}^1 dz \frac{1 - \epsilon \ln(1 - z^2)}{1 \pm \beta z} = \int_{-1}^1 dz \frac{1 - \epsilon \ln(1 + z) - \epsilon \ln(1 - z)}{1 + \beta z}.$$

Now

$$\begin{aligned}
\int_{-1}^1 \frac{dz}{1+\beta z} &= \frac{1}{\beta} \ln \left( 1 + \frac{1+\beta}{1-\beta} \right) \\
&= \ln \left( \frac{2}{2\rho} \right) + \mathcal{O}(\rho) \\
&= -\ln \rho,
\end{aligned}$$

$$\begin{aligned}
\int_{-1}^1 dz \frac{\ln(1+z)}{1+\beta z} &= \frac{1}{\beta} \int_{1-\beta}^{1+\beta} \frac{dx}{x} \ln \left( 1 + \frac{x-1}{\beta} \right) \quad \text{where } x \equiv 1 + \beta z \\
&= \frac{1}{\beta} \int_{1-\beta}^{1+\beta} \frac{dx}{x} \ln \left( \frac{\beta-1}{\beta} + \frac{x}{\beta} \right) \\
&= \frac{1}{\beta} \ln \frac{\beta-1}{\beta} \int_{1-\beta}^{1+\beta} \frac{dx}{x} + \frac{1}{\beta} \int_{1-\beta}^{1+\beta} \frac{dx}{x} \ln \left( 1 - \frac{x}{1-\beta} \right) \\
&= \frac{1}{\beta} \ln \frac{\beta-1}{\beta} \ln \frac{1+\beta}{1-\beta} + \frac{1}{\beta} \int_1^{1+\beta} \frac{dy}{y} \ln(1-y) \quad \text{where } y \equiv \frac{x}{1-\beta} \\
&= \frac{1}{\beta} \ln \frac{\beta-1}{\beta} \ln \frac{1+\beta}{1-\beta} - \frac{1}{\beta} \text{Li}_2 \left( \frac{1+\beta}{1-\beta} \right) + \frac{1}{\beta} \text{Li}_2(1) \\
&= \ln(-2\rho) \ln \frac{1}{\rho} - \text{Li}_2 \left( \frac{1}{\rho} \right) + \frac{\pi^2}{6} + \mathcal{O}(\rho) \\
&= -\ln^2 \rho - \ln 2 \ln \rho - \left( \frac{\pi^2}{3} - \text{Li}_2(\rho) - \frac{1}{2} \ln^2 \rho \right) + \frac{\pi^2}{6} + \text{imag.} \\
&= -\frac{1}{2} \ln^2 \rho - \ln 2 \ln \rho - \frac{\pi^2}{6} + \mathcal{O}(\rho),
\end{aligned}$$

and

$$\begin{aligned}
\int_{-1}^1 dz \frac{\ln(1-z)}{1+\beta z} &= \frac{1}{\beta} \int_{1-\beta}^{1+\beta} \frac{dx}{x} \ln \left( 1 - \frac{x-1}{\beta} \right) \quad \text{where } x \equiv 1 + \beta z \\
&= \frac{1}{\beta} \int_{1-\beta}^{1+\beta} \frac{dx}{x} \ln \left( \frac{1+\beta}{\beta} - \frac{x}{\beta} \right) \\
&= \frac{1}{\beta} \ln \left( \frac{1+\beta}{\beta} \right) \int_{1-\beta}^{1+\beta} \frac{dx}{x} + \frac{1}{\beta} \int_{1-\beta}^{1+\beta} \frac{dx}{x} \ln \left( 1 - \frac{x}{1+\beta} \right)
\end{aligned}$$

$$\begin{aligned}
&= \frac{1}{\beta} \ln \left( \frac{1+\beta}{\beta} \right) \ln \left( \frac{1+\beta}{1-\beta} \right) + \frac{1}{\beta} \int_{\frac{1-\beta}{1+\beta}}^1 \frac{dy}{y} \ln(1-y) \\
&\hspace{20em} \text{where } y \equiv \frac{x}{1+\beta} \\
&= \frac{1}{\beta} \ln \left( \frac{1+\beta}{\beta} \right) \ln \left( \frac{1+\beta}{1-\beta} \right) - \frac{1}{\beta} \text{Li}_2(1) + \frac{1}{\beta} \text{Li}_2 \left( \frac{1-\beta}{1+\beta} \right) \\
&= \ln 2 \ln \left( \frac{1}{\rho} \right) - \frac{\pi^2}{6} + \mathcal{O}(\rho) \\
&= -\ln 2 \ln \rho - \frac{\pi^2}{6}.
\end{aligned}$$

Therefore

$$\int_{-1}^1 dz \frac{1 - \epsilon \ln(1 - z^2)}{1 \pm \beta z} = -\ln \rho + \epsilon \left( \frac{1}{2} \ln^2 \rho + \ln 4 \ln \rho + \frac{\pi^2}{3} \right).$$

- Two poles:

$$\int_{-1}^1 dz \frac{1 - \epsilon \ln(1 - z^2)}{(1 \pm \beta z)^2} = \int_{-1}^1 dz \frac{1 - \epsilon \ln(1 + z) - \epsilon \ln(1 - z)}{(1 + \beta z)^2}.$$

Now

$$\begin{aligned}
\int_{-1}^1 \frac{dz}{(1 + \beta z)^2} &= \frac{1}{\beta} \left( \frac{1}{1 - \beta} - \frac{1}{1 + \beta} \right) \\
&= \frac{2}{1 - \beta^2} \\
&= \frac{1}{2\rho} + \mathcal{O}(1),
\end{aligned}$$

$$\begin{aligned}
\int_{-1}^1 dz \frac{\ln(1 + z)}{(1 + \beta z)^2} &= -\frac{1}{\beta} \int_{-1}^1 dz \ln(1 + z) \frac{d}{dz} \frac{1}{1 + \beta z} \\
&= -\frac{1}{\beta} \int_{-1}^1 dz \left[ \frac{d}{dz} \frac{\ln(1 + z)}{1 + \beta z} - \frac{1}{1 + \beta z} \frac{d}{dz} \ln(1 + z) \right] \\
&= -\frac{1}{\beta} \int_{-1}^1 dz \left[ \frac{d}{dz} \frac{\ln(1 + z)}{1 + \beta z} - \frac{1}{(1 + \beta z)(1 + z)} \right]
\end{aligned}$$

$$\begin{aligned}
&= -\frac{1}{\beta} \int_{-1}^1 dz \left[ \frac{d}{dz} \frac{\ln(1+z)}{1+\beta z} + \frac{\beta}{1-\beta} \frac{1}{1+\beta z} - \frac{1}{1-\beta} \frac{1}{1+z} \right] \\
&= -\frac{1}{\beta} \int_{-1}^1 dz \frac{d}{dz} \left[ \frac{\ln(1+z)}{1+\beta z} + \frac{1}{1-\beta} \ln \frac{1+\beta z}{1+z} \right] \\
&= -\frac{1}{\beta} \left[ \frac{\ln(1+z)}{1+\beta z} + \frac{1}{1-\beta} \ln \frac{1+\beta z}{1+z} \right]_{-1}^1 \\
&= -\frac{1}{\beta} \left[ \frac{\ln 2}{1+\beta} + \frac{1}{1-\beta} \ln \frac{1+\beta}{2} - \frac{\ln(1-\beta)}{1-\beta} \right] \\
&= -\frac{1}{\beta} \left[ -\frac{2\beta}{1-\beta^2} \ln 2 + \frac{1}{1-\beta} \ln \frac{1+\beta}{1-\beta} \right] \\
&= \frac{1}{2\rho} \ln \rho + \frac{1}{2\rho} \ln 2 + \mathcal{O}(\ln \rho) \\
&= \frac{1}{2\rho} \ln 2\rho,
\end{aligned}$$

and

$$\begin{aligned}
\int_{-1}^1 dz \frac{\ln(1-z)}{(1+\beta z)^2} &= -\frac{1}{\beta} \int_{-1}^1 dz \ln(1-z) \frac{d}{dz} \frac{1}{1+\beta z} \\
&= -\frac{1}{\beta} \int_{-1}^1 dz \left[ \frac{d}{dz} \frac{\ln(1-z)}{1+\beta z} - \frac{1}{1+\beta z} \frac{d}{dz} \ln(1-z) \right] \\
&= -\frac{1}{\beta} \int_{-1}^1 dz \left[ \frac{d}{dz} \frac{\ln(1-z)}{1+\beta z} + \frac{\beta}{1+\beta} \frac{1}{1+\beta z} + \frac{1}{1+\beta} \frac{1}{1-z} \right] \\
&= -\frac{1}{\beta} \int_{-1}^1 dz \frac{d}{dz} \left[ \frac{\ln(1-z)}{1+\beta z} + \frac{\beta}{1+\beta} \ln \frac{1+\beta z}{1-z} \right] \\
&= -\frac{1}{\beta} \left[ \frac{\ln(1-z)}{1+\beta z} + \frac{1}{1+\beta} \ln \frac{1+\beta z}{1-z} \right]_{-1}^1 \\
&= -\frac{1}{\beta} \left[ \frac{\ln(1+\beta)}{1+\beta} - \frac{\ln 2}{1-\beta} - \frac{1}{1+\beta} \ln \frac{1-\beta}{2} \right] \\
&= -\frac{1}{\beta} \left[ -\frac{2\beta}{1-\beta^2} \ln 2 + \frac{1}{1+\beta} \ln \frac{1+\beta}{1-\beta} \right] \\
&= \frac{1}{2\rho} \ln 2 + \mathcal{O}(\ln \rho).
\end{aligned}$$

Therefore

$$\int_{-1}^1 dz \frac{1 - \epsilon \ln(1-z^2)}{(1 \pm \beta z)^2} = \frac{1}{2\rho} (1 - \epsilon \ln 4\rho).$$

Using these integrals, we find that

$$\begin{aligned}
\int_{-1}^1 dz (1 - \epsilon \ln(1 - z^2)) T_{tt} &= \int_{-1}^1 dz (1 - \epsilon \ln(1 - z^2)) T_{uu} \\
&= 32(1 - 2\epsilon) \left[ -\ln \rho + \epsilon \left( \frac{1}{2} \ln^2 \rho + \ln 4 \ln \rho + \frac{\pi^2}{3} \right) \right] - 16(1 - 2\epsilon)[2 + 4\epsilon(1 - \ln 2)] \\
&\quad - \frac{128(1 - \epsilon)\tau\rho}{(1 - \tau)^2} \frac{1}{2\rho} (1 - \epsilon \ln 4\rho) \\
&= 32 \left[ -\ln \rho + \epsilon \left( \frac{1}{2} \ln^2 \rho + (2 + \ln 4) \ln \rho + \frac{\pi^2}{3} \right) \right] - 32(1 - \epsilon \ln 4) \\
&\quad - \frac{64\tau}{(1 - \tau)^2} [1 - \epsilon(\ln 4\rho + 1)] + \mathcal{O}(\epsilon^2) \\
&= -\frac{64\tau}{(1 - \tau)^2} - 32(\ln \rho + 1) \\
&\quad + \epsilon \left[ \frac{64\tau}{(1 - \tau)^2} (\ln 4\rho + 1) + 32 \left( \frac{1}{2} \ln^2 \rho + (2 + \ln 4) \ln \rho + \ln 4 + \frac{\pi^2}{3} \right) \right]
\end{aligned}$$

and

$$\begin{aligned}
\int_{-1}^1 dz (1 - \epsilon \ln(1 - z^2)) T_{tu} &= \frac{64(1 - \epsilon)\tau}{(1 - \tau)^2} \left[ -\ln \rho + \epsilon \left( \frac{1}{2} \ln^2 \rho + \ln 4 \ln \rho + \frac{\pi^2}{3} \right) \right] - 16\epsilon[2 + 4\epsilon(1 - \ln 2)] \\
&= \frac{64\tau}{(1 - \tau)^2} \left[ -\ln \rho + \epsilon \left( \frac{1}{2} \ln^2 \rho + (1 + \ln 4) \ln \rho + \frac{\pi^2}{3} \right) \right] - 32\epsilon + \mathcal{O}(\epsilon^2) \\
&= -\frac{64\tau}{(1 - \tau)^2} \ln \rho + \epsilon \left[ \frac{64\tau}{(1 - \tau)^2} \left( \frac{1}{2} \ln^2 \rho + (1 + \ln 4) \ln \rho + \frac{\pi^2}{3} \right) - 32 \right].
\end{aligned}$$

The cross section for  $q\bar{q} \rightarrow gW$  is then

$$\hat{\sigma} = \frac{1}{2s} \frac{2\pi^2 \alpha \alpha_s}{9s_W^2} \int d\Phi (2T_{tt} + 2T_{tu})$$

$$\begin{aligned}
&= -\frac{2\pi^2\alpha\alpha_s}{9s_W^2s} \frac{1}{32\pi} (1-\tau)^2 \left[ \left( \frac{1}{\epsilon} - \gamma + \ln \frac{16\pi}{M_W^2} \right) \delta(1-\tau) - \frac{2}{(1-\tau)_+} \right] \\
&\quad \times \left\{ -\frac{64\tau}{(1-\tau)^2} (\ln \rho + 1) - 32(\ln \rho + 1) \right. \\
&\quad \left. + \epsilon \left[ \frac{64\tau}{(1-\tau)^2} \left( \frac{1}{2} \ln^2 \rho + (2 + \ln 4) \ln \rho + \ln 4 + \frac{\pi^2}{3} + 1 \right) \right. \right. \\
&\quad \left. \left. + 32 \left( \frac{1}{2} \ln^2 \rho + (2 + \ln 4) \ln \rho + \ln 4 + \frac{\pi^2}{3} - 1 \right) \right] \right\} \\
&= \frac{2\pi\alpha\alpha_s}{9s_W^2s} \left\{ 2 \left( \frac{1}{\epsilon} - \gamma + \ln \frac{16\pi}{M_W^2} \right) \right. \\
&\quad \times \left[ \ln \rho + 1 - \epsilon \left( \frac{1}{2} \ln^2 \rho + (2 + \ln 4) \ln \rho + \ln 4 + \frac{\pi^2}{3} + 1 \right) \right] \delta(1-\tau) \\
&\quad \left. - 2 \left[ 2\tau(\ln \rho + 1) + (1-\tau)^2(\ln \rho + 1) \right] \frac{1}{(1-\tau)_+} \right\} \\
&= \frac{4\pi\alpha\alpha_s}{9s_W^2M_W^2} \left\{ \left[ \left( \frac{1}{\epsilon} - \gamma + \ln \frac{16\pi}{M_W^2} \right) (\ln \rho + 1) - \frac{1}{2} \ln^2 \rho \right. \right. \\
&\quad \left. \left. - (2 + \ln 4) \ln \rho - \ln 4 - \frac{\pi^2}{3} - 1 \right] \delta(1-\tau) \right. \\
&\quad \left. - \frac{\tau(1+\tau^2)}{(1-\tau)_+} (\ln \rho + 1) \right\} \\
&= \frac{4\pi\alpha\alpha_s}{9s_W^2M_W^2} \left\{ \left[ \left( \frac{1}{\epsilon} - \gamma + \ln 4\pi \right) (\ln \rho + 1) - (\ln \rho + 1) \ln M_W^2 \right. \right. \\
&\quad \left. \left. - \frac{1}{2} \ln^2 \rho - 2 \ln \rho - \frac{\pi^2}{3} - 1 \right] \delta(1-\tau) \right. \\
&\quad \left. - \frac{\tau(1+\tau^2)}{(1-\tau)_+} (\ln \rho + 1) \right\}. \tag{3.8}
\end{aligned}$$

The term involving  $1/\epsilon$  is an infrared divergence, corresponding to the limit  $\tau \rightarrow 1$  in which the radiated gluon is soft. The terms involving  $\ln \rho$  result from the collinear singularities at  $t = 0$  and at  $u = 0$ .

Adding Eq. (3.8) to the  $q\bar{q} \rightarrow W$  cross section given by Eq. (3.5), we find that

$$\begin{aligned}
\hat{\sigma}(q\bar{q} \rightarrow (g)W) &= \frac{\pi^2\alpha}{3s_W^2 M_W^2} \delta(1-\tau) \\
&\quad + \frac{2\pi\alpha\alpha_s}{9s_W^2 M_W^2} \left\{ \left[ -2 \left( \frac{1}{\epsilon} - \gamma + \ln 4\pi \right) (\ln \rho + 1) + (2 \ln \rho - 1) \ln M_W^2 \right. \right. \\
&\quad \quad \quad \left. \left. + 3 \ln m^2 + \ln^2 \rho - 2 \ln \rho + \frac{4\pi^2}{3} - 2 \right] \delta(1-\tau) \right. \\
&\quad \quad \quad \left. + 2 \left[ \left( \frac{1}{\epsilon} - \gamma + \ln 4\pi \right) (\ln \rho + 1) - (\ln \rho + 1) \ln M_W^2 \right. \right. \\
&\quad \quad \quad \left. \left. - \frac{1}{2} \ln^2 \rho - 2 \ln \rho - \frac{\pi^2}{3} - 1 \right] \delta(1-\tau) \right. \\
&\quad \quad \quad \left. - \frac{2\tau(1+\tau^2)}{(1-\tau)_+} (\ln \rho + 1) \right\} \\
&= \frac{\pi^2\alpha}{3s_W^2 M_W^2} \delta(1-\tau) \\
&\quad + \frac{2\pi\alpha\alpha_s}{9s_W^2 M_W^2} \left[ \left( -3 \ln \rho + \frac{2\pi^2}{3} - 4 \right) \delta(1-\tau) - 2(\ln \rho + 1) \frac{\tau(1+\tau^2)}{(1-\tau)_+} \right] \\
&= \frac{\pi^2\alpha}{3s_W^2 M_W^2} \delta(1-\tau) \\
&\quad + \frac{2\pi\alpha\alpha_s}{9s_W^2 M_W^2} \tau \left[ \left( -3\delta(1-\tau) - \frac{2(1+\tau^2)}{(1-\tau)_+} \right) \ln \rho \right. \\
&\quad \quad \quad \left. + \left( \frac{2\pi^2}{3} - 4 \right) \delta(1-\tau) - \frac{2(1+\tau^2)}{(1-\tau)_+} \right] \\
&= \frac{\pi^2\alpha}{3s_W^2 M_W^2} \delta(1-\tau) \\
&\quad - \frac{\pi\alpha\alpha_s}{3s_W^2 M_W^2} \tau \left[ P_{qq}(\tau) \ln \rho + \left( \frac{8}{3} - \frac{4\pi^2}{9} \right) \delta(1-\tau) + \frac{4}{3} \frac{(1+\tau^2)}{(1-\tau)_+} \right],
\end{aligned} \tag{3.9}$$

where

$$P_{qq}(\tau) = \frac{4}{3} \left[ \frac{1+\tau^2}{(1-\tau)_+} + \frac{3}{2} \delta(1-\tau) \right]$$

is the Dokshitzer-Gribov-Lipatov-Altarelli-Parisi (DGLAP) splitting function corresponding to the collinear splitting  $q \rightarrow qg$ .

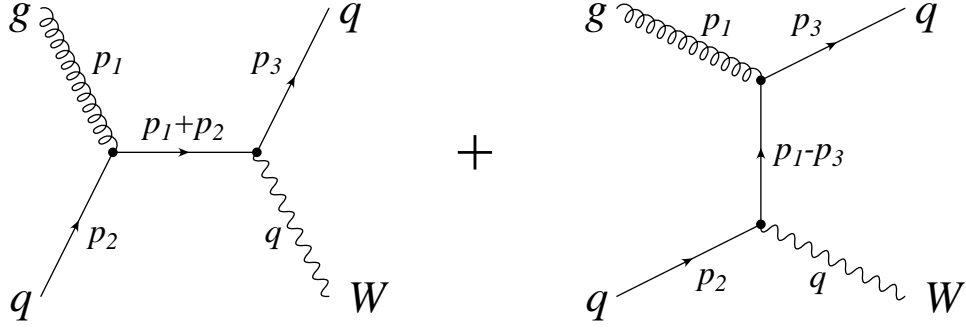


Figure 3.5: Feynman diagrams for the initial-gluon process  $gq \rightarrow qW$ .

Note that Eq. (3.9) does not contain any terms proportional to  $1/\epsilon$ : the infrared divergences have cancelled between the real- and virtual-gluon processes. The terms involving  $\ln^2 \rho$  have cancelled as well. The only divergent term remaining is the collinear divergence  $\ln \rho$ , which can be absorbed into the parton distribution functions by the DGLAP equations.

This result, Eq. (3.9), agrees with Eq. (3.10) of Ref. [45].

### 3.4 $gq \rightarrow qW$ (tree level)

Finally we must calculate the cross section for the initial-gluon correction, shown in Fig. 3.5. We will consider the process  $gq \rightarrow qW$ ; the process  $g\bar{q} \rightarrow qW$  is completely analogous. Here there is no infrared divergence; thus we can safely work in four dimensions.

We parametrize the momenta as follows:

$$\begin{aligned}
 p_1 &= \left( \frac{\sqrt{s}}{2}(1-\rho), \frac{\sqrt{s}}{2}(1-\rho), 0, 0 \right) \\
 p_2 &= \left( \frac{\sqrt{s}}{2}(1+\rho), -\frac{\sqrt{s}}{2}(1-\rho), 0, 0 \right) \\
 p_3 &= \left( \frac{\sqrt{s}}{2}(1-\tau+\rho), \frac{\sqrt{s}}{2}(1-\tau+\rho)\beta \cos \theta, \frac{\sqrt{s}}{2}(1-\tau+\rho)\beta \sin \theta, 0 \right) \\
 k &= \left( \frac{\sqrt{s}}{2}(1+\tau-\rho), -\frac{\sqrt{s}}{2}(1-\tau+\rho)\beta \cos \theta, -\frac{\sqrt{s}}{2}(1-\tau+\rho)\beta \sin \theta, 0 \right)
 \end{aligned}$$

where  $\tau \equiv M_W^2/s$ ,  $\rho \equiv m^2/s$ , and  $\beta \equiv \sqrt{1 - 4\rho/(1 - \tau + \rho)^2}$ .

The 4-dimensional phase space is reasonably simple:

$$\begin{aligned}
\int d\Phi &= \int \frac{d^4 p_3}{(2\pi)^4} \theta(p_3^0) 2\pi \delta(p_3^2 - m^2) \int \frac{d^4 q}{(2\pi)^4} \theta(q^0) 2\pi \delta(q^2 - M_W^2) \\
&\quad \times (2\pi)^4 \delta^4(p_1 + p_2 - p_3 - q) \\
&= \frac{1}{(2\pi)^2} \int_0^{\sqrt{s}} dq^0 \int d^3 \vec{q} \delta(q^2 - M_W^2) \delta((p_1 + p_2 - q)^2 - m^2) \\
&= \frac{1}{4\pi^2} \int_0^{\sqrt{s}} dq^0 \int d^3 \vec{q} \delta(q^2 - M_W^2) \frac{1}{2\sqrt{s}} \delta\left(q^0 - \frac{\sqrt{s}}{2}(1 + \tau - \rho)\right) \\
&= \frac{1}{8\pi^2 \sqrt{s}} \int d^3 \vec{q} \delta\left(\frac{s}{4}(1 + \tau - \rho)^2 - \vec{q}^2 - M_W^2\right) \\
&= \frac{1}{8\pi^2 \sqrt{s}} \int_0^\infty \vec{q}^2 d|\vec{q}| \int_0^\pi \sin \theta d\theta \int_0^{2\pi} d\phi \delta\left(\vec{q}^2 - \frac{s}{4}((1 + \tau - \rho)^2 - 4\tau)\right) \\
&= \frac{1}{4\pi \sqrt{s}} \int_0^\infty d|\vec{q}| \frac{\vec{q}^2}{2|\vec{q}|} \delta\left(|\vec{q}| - \frac{\sqrt{s}}{2}(1 - \tau + \rho)\beta\right) \int_{-1}^1 dz \\
&= \frac{1}{16\pi} (1 - \tau + \rho)\beta \int_{-1}^1 dz.
\end{aligned}$$

We can obtain the squared amplitude  $|\overline{\mathcal{M}}|^2$  from the real-gluon calculation [Eq. (3.7)] by crossing  $p_1 \rightarrow p_2 \rightarrow -p_3 \rightarrow p_1$  (or  $s \rightarrow t \rightarrow u \rightarrow s$ ) and flipping the overall sign (since we have crossed a fermion from the initial state to the final state). Note that we need to keep the quark mass only in the square of the  $t$ -channel diagram.

$$|\overline{\mathcal{M}}|^2 = \frac{1}{2} \frac{1}{8} \frac{1}{2} \frac{1}{3} \frac{g^2 g_s^2}{8} \text{Tr}[t^A t_A] (T_{ss} + T_{tt} + 2 \text{Re} T_{st}),$$

where

$$\begin{aligned}
T_{ss} &= 16 \frac{p_1 \cdot p_3}{p_1 \cdot p_2} \\
&= 16 \frac{(1 - \rho)(1 - \tau + \rho)(1 - \beta z)}{2(1 - \rho)} \\
&= 8(1 - \tau)(1 - z) + \mathcal{O}(\rho),
\end{aligned}$$

$$\begin{aligned}
T_{tt} &= 16 \frac{p_1 \cdot p_2}{p_1 \cdot p_3} + 16 \frac{p_2 \cdot k}{(p_1 \cdot p_3)^2} \\
&= 16 \frac{2(1-\rho)}{(1-\rho)(1-\tau+\rho)(1-\beta z)} + 64\rho \frac{(1+\rho)(1+\tau-\rho) - (1-\rho)(1-\tau+\rho)\beta z}{(1-\rho)^2(1-\tau+\rho)^2(1-\beta z)^2} \\
&= \frac{32}{(1-\tau)(1-\beta z)} + 64\rho \frac{2\tau + (1-\tau)(1-\beta z)}{(1-\tau)^2(1-\beta z)^2} \\
&= \frac{32}{(1-\tau)(1-\beta z)} + \frac{128\tau\rho}{(1-\tau)^2(1-\beta z)^2}
\end{aligned}$$

up to terms which do not contribute in the limit  $\rho \rightarrow 0$ , and

$$\begin{aligned}
T_{st} &= -16 \frac{p_2 \cdot p_3 (p_2 \cdot k - p_1 \cdot p_3)}{p_1 \cdot p_2 p_1 \cdot p_3} \\
&= -16 \frac{p_2 \cdot p_3 (p_1 \cdot p_2 - p_3 \cdot k)}{p_1 \cdot p_2 p_1 \cdot p_3} \\
&= -16 \frac{(1-\tau+\rho)[1+\rho+(1-\rho)\beta z]}{2(1-\rho)(1-\rho)(1-\tau+\rho)(1-\beta z)} \\
&\quad \times [2(1-\rho) - (1-\tau+\rho)(1+\tau-\rho + (1-\tau+\rho)\beta)] \\
&= -8 \frac{(1+\beta z)2\tau}{1-\beta z} + \mathcal{O}(\rho) \\
&= -16\tau \frac{2 - (1-\beta z)}{1-\beta z} \\
&= 16\tau - \frac{32\tau}{1-\beta z}.
\end{aligned}$$

The longitudinal  $W$ -boson polarization can be neglected for the same reason as in the real-gluon calculation.

We must evaluate four simple phase integrals:

$$\int_{-1}^1 dz (1-z) = 2,$$

$$\int_{-1}^1 dz = 2,$$

$$\begin{aligned}\int_{-1}^1 \frac{dz}{1-\beta z} &= -\frac{1}{\beta} \ln \frac{1-\beta}{1+\beta} \\ &= -\ln \frac{\rho}{(1-\tau)^2} + \mathcal{O}(\rho),\end{aligned}$$

and

$$\begin{aligned}\int_{-1}^1 \frac{dz}{(1-\beta z)^2} &= -\frac{1}{\beta} \left( \frac{1}{1+\beta} - \frac{1}{1-\beta} \right) \\ &= \frac{2}{1-\beta^2} \\ &= \frac{(1-\tau)^2}{2\rho} + \mathcal{O}(1).\end{aligned}$$

We find that

$$\begin{aligned}\int_{-1}^1 dz T_{ss} &= 8(1-\tau)(2) \\ &= 16(1-\tau),\end{aligned}$$

$$\begin{aligned}\int_{-1}^1 dz T_{tt} &= -\frac{32}{1-\tau} \ln \frac{\rho}{(1-\tau)^2} + \frac{128\tau\rho}{(1-\tau)^2} \frac{(1-\tau)^2}{2\rho} \\ &= -\frac{32}{1-\tau} \ln \frac{\rho}{(1-\tau)^2} + 64\tau,\end{aligned}$$

and

$$\begin{aligned}\int_{-1}^1 dz T_{st} &= 16\tau(2) - 32\tau \left( -\ln \frac{\rho}{(1-\tau)^2} \right) \\ &= 32\tau \ln \frac{\rho}{(1-\tau)^2} + 32\tau.\end{aligned}$$

Therefore the  $gq \rightarrow qW$  cross section is

$$\hat{\sigma} = \frac{1}{2s} \frac{\pi^2 \alpha \alpha_s}{12s_W^2} \int d\Phi (T_{ss} + T_{tt} + 2T_{st})$$

$$\begin{aligned}
&= \frac{\pi^2 \alpha \alpha_s}{24 s_W^2 s} \frac{1}{16\pi} (1-\tau) \left[ 16(1-\tau) - \frac{32}{1-\tau} \ln \frac{\rho}{(1-\tau)^2} + 64\tau + 64\tau \ln \frac{\rho}{(1-\tau)^2} + 64\tau \right] \\
&= \frac{\pi \alpha \alpha_s}{24 s_W^2 s} \left[ -2(1-2\tau(1-\tau)) \ln \frac{\rho}{(1-\tau)^2} + (1-\tau)(1+7\tau) \right] \\
&= \frac{\pi \alpha \alpha_s}{24 s_W^2 M_W^2} \tau \left[ -2(\tau^2 + (1-\tau)^2) \ln \frac{\rho}{(1-\tau)^2} + (1-\tau)(1+7\tau) \right] \\
&= -\frac{\pi \alpha \alpha_s}{6 s_W^2 M_W^2} \tau \left[ P_{qg}(\tau) \ln \frac{\rho}{(1-\tau)^2} - \frac{1}{4}(1-\tau)(1+7\tau) \right], \tag{3.10}
\end{aligned}$$

where

$$P_{qg}(\tau) \equiv \frac{1}{2} [\tau^2 + (1-\tau)^2]$$

is the DGLAP splitting function corresponding to the collinear splitting  $g \rightarrow q\bar{q}$ . This result, Eq. (3.10), agrees with Eq. (2.2) of Ref. [45].

This concludes the calculation of the NLO QCD corrections to the Drell-Yan cross section. Collinear singularities are present in all portions of these corrections. By using a nonzero quark mass  $m$ , we have been able to separate these collinear singularities from the ultraviolet and infrared singularities that are also present in the real- and virtual-gluon corrections. The collinear divergences manifest themselves as terms involving  $\ln m^2$ , and can be absorbed into the parton distribution functions by means of the DGLAP equations. In Chapter 4, we present a factorization scheme in which a physical understanding of the collinear singularities can be used to ensure that explicit radiative corrections to the Drell-Yan cross section are small.

# Chapter 4

## Choosing the Factorization Scale in Perturbative QCD<sup>1</sup>

We define the collinear factorization scheme, which absorbs only the collinear physics into the parton distribution functions. In this scheme, the factorization scale  $\mu$  has a simple physical interpretation as a collinear cutoff. We present a method for choosing the factorization scale and apply it to the Drell-Yan process; we find  $\mu \approx Q/2$ , where  $Q$  is the vector-boson invariant mass. We show that, for a wide variety of collision energies and  $Q$ , the radiative corrections are very small in the collinear scheme for this choice of factorization scale.

### 4.1 Introduction

In the parton model, a hadron is regarded as a collection of quarks, antiquarks, and gluons, each of which carries some fraction  $x$  of the hadron's momentum, with a number density  $f(x, \mu)$ , where  $\mu$  is the factorization scale. Qualitatively, the factorization scale corresponds to the resolution with which the hadron is being probed. To calculate the cross section for processes in hadron-hadron or lepton-hadron collisions, the partonic cross section is convolved with the corresponding parton distribution functions  $f(x, \mu)$ . At leading order in perturbative QCD, the partonic (hard-scattering) cross section is independent of the factorization scale  $\mu$ , but depends logarithmically on  $\mu$  at next-to-leading order and higher. When calculated to all orders in perturbative QCD, the hadronic cross section is independent of the factorization scale  $\mu$ . However, at any finite order in perturbation theory, the calculated hadronic cross section depends on  $\mu$ . One therefore desires a systematic way to choose the

---

<sup>1</sup>This chapter contains material from Ref. [48].

factorization scale.

Many things are said about the choice of factorization scale, some more sensible than others. If the hard-scattering cross section is characterized by a single scale  $Q$ , then the factorization scale is usually chosen to be of order  $Q$ , simply because there is no other scale in the problem. However, this only reveals the order of magnitude of  $\mu$ , and one desires to do better, as finite-order calculations often have significant dependence on the factorization scale. In a process such as Drell-Yan production of a lepton pair of invariant mass  $Q$ , it is often considered “obvious” that the factorization scale is *exactly*  $Q$ , but there is no good argument for this. In a process such as the production of a pair of heavy quarks of mass  $m_Q$ , there is not even a unique “obvious” choice: both  $m_Q$  and  $2m_Q$  are equally “obvious.” If the hard-scattering cross section depends on more than one scale, then the choice of factorization scale becomes an even murkier issue.

One argument against trying to do better than simply choosing  $\mu \sim Q$  (here and henceforth we use  $\sim$  to denote order-of-magnitude equality) goes as follows. Since the hadronic cross section is a physical quantity that does not depend on any factorization scale, the factorization scale is unphysical, and therefore one cannot make a physical argument for its choice. A more extreme conclusion is that the factorization scale is totally arbitrary, and does not even have to be chosen to be of order  $Q$ . It is in part due to arguments such as these that there has been little effort to try to do better than choosing  $\mu \sim Q$ .

On the other hand, one often hears statements that the factorization scale separates the short-distance physics of the hard-scattering cross section from the long-distance hadronic physics. The qualitative statement made earlier, that  $\mu$  corresponds to the resolution with which the hadron is probed, falls into this class. This is contradictory to the attitude that the factorization scale is unphysical and even arbitrary.

In this paper we put forward a physical argument for the choice of factorization scale. In order to be clear, we restrict our attention to Drell-Yan production, but the argument can and hopefully will be extended to other processes in the future.

The physical argument we advance is that the factorization scale should be chosen such that collinear (long-distance) physics is included in the parton distribution functions, and non-collinear (short-distance) physics in the hard-scattering cross section. This is not a new idea, and goes back to the origins of the parton model.<sup>2</sup> What is new is the implementation of this idea in practice. The method we pursue here was first proposed in the context of Higgs-boson production in association with bottom quarks [36, 37], and was refined and elaborated upon in Ref. [21]. An alternative approach in the same spirit has been developed in Ref. [50].

All of the above studies are in the context of Higgs-boson (both charged and neutral) production via a bottom-quark distribution function, which is a rather exotic process, both in the initial and the final state. However, the ideas developed there are of general validity, and should be applicable to all parton-model calculations. In this paper we further develop the method of Ref. [21] and apply it to one of the most basic processes of perturbative QCD, namely Drell-Yan production [45, 46]. Our hope is that this method can be generalized to all parton-model calculations, finally satisfying the desire for a systematic method of factorization-scale choice.

## 4.2 The collinear region

The parton distribution functions are evolved from one factorization scale to another via the Dokshitzer-Gribov-Lipatov-Altarelli-Parisi (DGLAP) equations. These equations sum collinear logarithms into the parton distribution functions. Our first step is to define a factorization scheme in which the factorization scale  $\mu$  has the interpretation of a cutoff in the integration over the virtuality of a propagator associated with collinear radiation.

Consider the Drell-Yan process, shown in Fig. 4.1. The colliding quark  $q_i$  and antiquark  $\bar{q}_j$  annihilate into an electroweak gauge boson  $V$  of invariant mass  $Q$ ; we do not consider

---

<sup>2</sup>See, for example, Ref. [49].

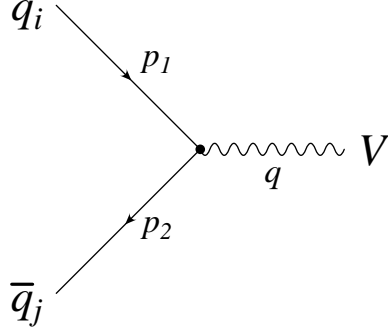


Figure 4.1: Drell-Yan production of an electroweak gauge boson  $V$ .

the subsequent decay of the boson into lepton pairs, which is irrelevant to our discussion. The leading-order (LO) cross section, in dimensional regularization with  $4 - 2\epsilon$  spacetime dimensions, is

$$\sigma_{q\bar{q}}^{(0)} = \frac{4\pi^2\alpha}{3}(1 - \epsilon)\mu_D^{2\epsilon} \sum_{i,j} C_{ij} \int_0^1 dx_1 \int_0^1 dx_2 \times [q_{0i}(x_1)\bar{q}_{0j}(x_2) + \bar{q}_{0j}(x_1)q_{0i}(x_2)]\delta(x_1x_2S - Q^2), \quad (4.1)$$

where  $\mu_D$  is the 't Hooft mass,  $S$  is the hadronic center-of-mass energy squared, and  $C_{ij}$  (shown in Table 4.1) specifies the coupling of the quarks to the boson  $V$ . For the sake of brevity we define the convolution  $f_1 \otimes f_2$  of two functions  $f_1$  and  $f_2$  by

$$(f_1 \otimes f_2)(x) \equiv \int_0^1 dx_1 \int_0^1 dx_2 \delta(x_1x_2 - x)f_1(x_1)f_2(x_2). \quad (4.2)$$

Eq. (4.1) can then be rewritten as

$$\sigma_{q\bar{q}}^{(0)} = \frac{4\pi^2\alpha}{3S}(1 - \epsilon)\mu_D^{2\epsilon} \sum_{i,j} C_{ij}(q_{0i} \otimes \bar{q}_{0j} + \bar{q}_{0j} \otimes q_{0i})(z_0), \quad (4.3)$$

where  $z_0 \equiv Q^2/S$ .

$q_i \bar{q}_j \rightarrow V$	$C_{ij}$
$u_i \bar{u}_j \rightarrow \gamma^*$	$\frac{4}{9} \delta_{ij}$
$d_i \bar{d}_j \rightarrow \gamma^*$	$\frac{1}{9} \delta_{ij}$
$u_i \bar{d}_j \rightarrow W^+$	$\frac{1}{4s_W^2}  V_{ij} ^2$
$d_i \bar{u}_j \rightarrow W^-$	$\frac{1}{4s_W^2}  V_{ji} ^2$
$u_i \bar{u}_j \rightarrow Z$	$\frac{1}{8s_W^2 c_W^2} (1 - \frac{8}{3} s_W^2 + \frac{32}{9} s_W^4) \delta_{ij}$
$d_i \bar{d}_j \rightarrow Z$	$\frac{1}{8s_W^2 c_W^2} (1 - \frac{4}{3} s_W^2 + \frac{8}{9} s_W^4) \delta_{ij}$

Table 4.1: Couplings of the quarks to electroweak gauge bosons. Here  $s_W = \sin \theta_W$ ,  $c_W = \cos \theta_W$ , and  $V_{ij}$  denotes an element of the Cabibbo-Kobayashi-Maskawa matrix.

### 4.2.1 Initial gluons

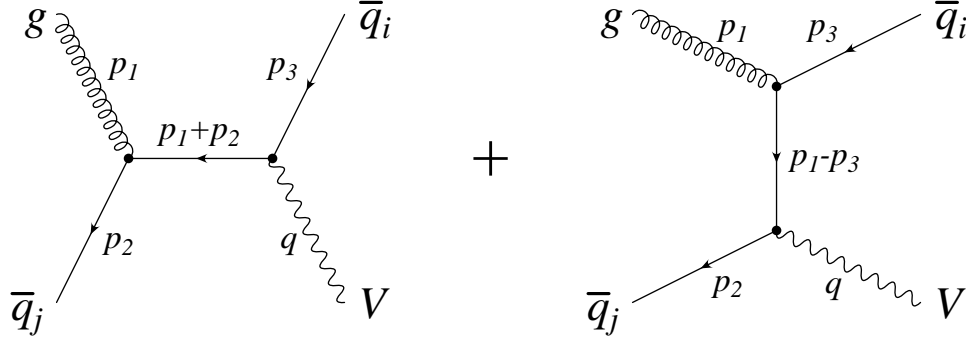


Figure 4.2: Correction to the production of an electroweak gauge boson  $V$  due to initial gluons.

The quark distribution function  $q_i(x)$  receives corrections due to the splitting of a parton into a pair of collinear partons, one of which is a quark. In order to find the correction to  $q_i(x)$  arising from the splitting  $g \rightarrow \bar{q}_i q_i$ , we consider the next-to-leading-order (NLO) correction to the Drell-Yan process due to initial gluons, shown in Fig. 4.2.

Let  $s \equiv (p_1 + p_2)^2$ ,  $t \equiv (p_1 - p_3)^2$ , and  $u \equiv (p_2 - p_3)^2$  be the usual Mandelstam variables,

with  $s + t + u = Q^2$ . The differential cross section is

$$\begin{aligned} \frac{d\sigma_{g\bar{q}}^{(1)}}{dt} &= \frac{\pi\alpha\alpha_s}{3S} \frac{(4\pi\mu_D^4)^\epsilon}{\Gamma(1-\epsilon)} \sum_{i,j} C_{ij} \int_{Q^2}^S \frac{ds}{s^2} (g \otimes \bar{q}_j + \bar{q}_j \otimes g) \left(\frac{s}{S}\right) \int_{-\infty}^0 du \delta(s+t+u-Q^2) \\ &\quad \times \left(\frac{s}{tu}\right)^\epsilon \left[ (1-\epsilon) \left(\frac{s}{-t} + \frac{-t}{s}\right) - \frac{2uQ^2}{st} + 2\epsilon \right]. \end{aligned} \quad (4.4)$$

This expression manifestly shows the singular behavior near  $t = 0$ , which corresponds to the splitting of the initial gluon into a collinear quark-antiquark pair. In four dimensions there is a collinear singularity in the form of a simple pole at  $t = 0$ . As we move to  $4 - 2\epsilon$  dimensions,  $1/t$  becomes  $1/t^{1+\epsilon}$ , which is integrable when  $\text{Re } \epsilon < 0$ .

In order to absorb this collinear physics into the parton distribution functions, we define a factorization scheme, called the collinear scheme, as follows. First, we define the quantity  $\bar{\sigma}_{g\bar{q}}^{(1)}$  by keeping only the leading behavior  $1/t^{1+\epsilon}$  and imposing a cutoff  $-\mu^2$  on the integration over  $t$ :<sup>3</sup>

$$\bar{\sigma}_{g\bar{q}}^{(1)} \equiv \left[ \lim_{t \rightarrow 0} \left( (-t)^{1+\epsilon} \frac{d\sigma_{g\bar{q}}^{(1)}}{dt} \right) \right] \int_{-\mu^2}^0 dt \frac{1}{(-t)^{1+\epsilon}}. \quad (4.5)$$

We regard  $\mu$  as the factorization scale in this scheme.

We now perform the integration over  $t$  and obtain

$$\begin{aligned} \bar{\sigma}_{g\bar{q}}^{(1)} &= -\frac{\pi\alpha\alpha_s}{3S} \frac{1}{\epsilon\Gamma(1-\epsilon)} \left(\frac{4\pi\mu_D^4}{\mu^2}\right)^\epsilon \sum_{i,j} C_{ij} \int_{z_0}^1 \frac{dz}{z} (g \otimes \bar{q}_j + \bar{q}_j \otimes g) \left(\frac{z_0}{z}\right) \\ &\quad \times (1-z)^{-\epsilon} [1-\epsilon-2z(1-z)], \end{aligned} \quad (4.6)$$

---

<sup>3</sup>In four dimensions this amounts to keeping  $1/t$  times the residue of the collinear pole in  $d\sigma_{g\bar{q}}^{(1)}/dt$ .

where  $z \equiv Q^2/s$ . Expanding in powers of  $\epsilon$  gives

$$\begin{aligned} \bar{\sigma}_{g\bar{q}}^{(1)} &= \frac{2\pi\alpha\alpha_s}{3S}(1-\epsilon)\mu_D^{2\epsilon} \sum_{i,j} C_{ij} \int_{z_0}^1 \frac{dz}{z} (g \otimes \bar{q}_j + \bar{q}_j \otimes g) \left(\frac{z_0}{z}\right) \\ &\quad \times \left[ - \left( \frac{1}{\epsilon} - \gamma + \ln \frac{4\pi\mu_D^2}{\mu^2(1-z)} \right) P_{qg}(z) + z(1-z) \right], \end{aligned} \quad (4.7)$$

where  $P_{qg}(z) = \frac{1}{2}[z^2 + (1-z)^2]$  is the appropriate DGLAP splitting function.

Finally we rewrite the above cross section as

$$\bar{\sigma}_{g\bar{q}}^{(1)} = \frac{4\pi^2\alpha}{3S}(1-\epsilon)\mu_D^{2\epsilon} \sum_{i,j} C_{ij} (\delta q_i \otimes \bar{q}_j + \bar{q}_j \otimes \delta q_i)(z_0), \quad (4.8)$$

where

$$\delta q_i(x) = -\frac{\alpha_s}{2\pi} \int_x^1 \frac{dz}{z} g\left(\frac{x}{z}\right) \left[ \left( \frac{1}{\epsilon} - \gamma + \ln \frac{4\pi\mu_D^2}{\mu^2(1-z)} \right) P_{qg}(z) - z(1-z) \right]. \quad (4.9)$$

The correction  $\delta\bar{q}_j(x)$  to the antiquark distribution function, due to the process  $q_i g \rightarrow V q_j$ , is identical. These corrections are entirely absorbed into the parton distribution functions if we define  $q_i(x) = q_{0i}(x) + \delta q_i(x)$  and  $\bar{q}_j(x) = \bar{q}_{0j}(x) + \delta\bar{q}_j(x)$ , and calculate the LO cross section, Eq. (4.3), with  $q_i(x)$  and  $\bar{q}_j(x)$  in place of  $q_{0i}(x)$  and  $\bar{q}_{0j}(x)$ .

The total NLO correction, due to initial gluons, to the Drell-Yan cross section is [46]

$$\begin{aligned} \sigma_{g\bar{q}+qg}^{(1)} &= \frac{2\pi\alpha\alpha_s}{3S}\mu_D^{2\epsilon} \sum_{i,j} C_{ij} \int_{z_0}^1 \frac{dz}{z} (g \otimes \bar{q}_j + \bar{q}_j \otimes g + q_i \otimes g + g \otimes q_i) \left(\frac{z_0}{z}\right) \\ &\quad \times \left[ - \left( \frac{1}{\epsilon} - \gamma + \ln \frac{4\pi\mu_D^2 z}{Q^2(1-z)^2} \right) P_{qg}(z) + \frac{1}{4}(3 + 2z - 3z^2) \right], \end{aligned} \quad (4.10)$$

and, after the subtraction of  $\bar{\sigma}_{g\bar{q}}^{(1)}$  and  $\bar{\sigma}_{qg}^{(1)}$ , what remains is the explicit correction in the collinear scheme:

$$\begin{aligned} \sigma_{g\bar{q}+qg}^{(1)} - \bar{\sigma}_{g\bar{q}}^{(1)} - \bar{\sigma}_{qg}^{(1)} &= \frac{2\pi\alpha\alpha_s}{3S} \sum_{i,j} C_{ij} \int_{z_0}^1 \frac{dz}{z} (g \otimes \bar{q}_j + \bar{q}_j \otimes g + q_i \otimes g + g \otimes q_i) \left(\frac{z_0}{z}\right) \\ &\times \left[ P_{qg}(z) \ln \frac{Q^2(1-z)}{\mu^2 z} + \frac{1}{4}(1+2z-3z^2) \right]. \end{aligned} \quad (4.11)$$

Alternatively, this explicit correction can be computed easily in four dimensions, without regulating the collinear divergence. To achieve this, we simply write down the cross section and counterterm in four dimensions,

$$\begin{aligned} \sigma_{g\bar{q}+qg}^{(1)} - \bar{\sigma}_{g\bar{q}}^{(1)} - \bar{\sigma}_{qg}^{(1)} &= \frac{\pi\alpha\alpha_s}{3S} \sum_{i,j} C_{ij} \int_{Q^2}^S \frac{ds}{s^2} (g \otimes \bar{q}_j + \bar{q}_j \otimes g + q_i \otimes g + g \otimes q_i) \left(\frac{s}{S}\right) \\ &\times \left[ \int_{-s+Q^2}^0 dt \left( \frac{s}{-t} + \frac{-t}{s} - \frac{2Q^2(s-Q^2+t)}{s(-t)} \right) - \int_{-\mu^2}^0 \frac{dt}{-t} \left( s - \frac{2Q^2(s-Q^2)}{s} \right) \right], \end{aligned} \quad (4.12)$$

and rearrange terms:

$$\begin{aligned} \sigma_{g\bar{q}+qg}^{(1)} - \bar{\sigma}_{g\bar{q}}^{(1)} - \bar{\sigma}_{qg}^{(1)} &= \frac{\pi\alpha\alpha_s}{3S} \sum_{i,j} C_{ij} \int_{Q^2}^S \frac{ds}{s^2} (g \otimes \bar{q}_j + \bar{q}_j \otimes g + q_i \otimes g + g \otimes q_i) \left(\frac{s}{S}\right) \\ &\times \left[ \int_{-s+Q^2}^{-\mu^2} \frac{dt}{-t} \left( s - \frac{2Q^2(s-Q^2)}{s} \right) + \int_{-s+Q^2}^0 dt \left( \frac{-t}{s} + \frac{2Q^2}{s} \right) \right]. \end{aligned} \quad (4.13)$$

Both integrals in this expression are finite, and the result matches Eq. (4.11).

Now all that remains is to consider how to choose the factorization scale  $\mu$ . We advocate choosing  $\mu$  to be a scale which somehow characterizes the value of  $t$  where the collinear approximation  $d\sigma_{g\bar{q}+qg}^{(1)}/dt \propto 1/t$  (in four dimensions) ceases to hold, so that  $-t < \mu^2$  can be thought of as the ‘‘collinear region’’ and  $-t > \mu^2$  as the ‘‘noncollinear region’’. The quantity  $-t d\sigma_{g\bar{q}+qg}^{(1)}/dt$  approaches a constant as  $t \rightarrow 0$ , while at large values of  $-t$  it drops to 0, the suppression being caused by the delta function in Eq. (4.4), which requires that  $s+t \geq Q^2$ . A plot of this quantity resembles a plateau, and can be inspected visually in order to determine the appropriate value of  $\mu$ . However, before making this plot, we will

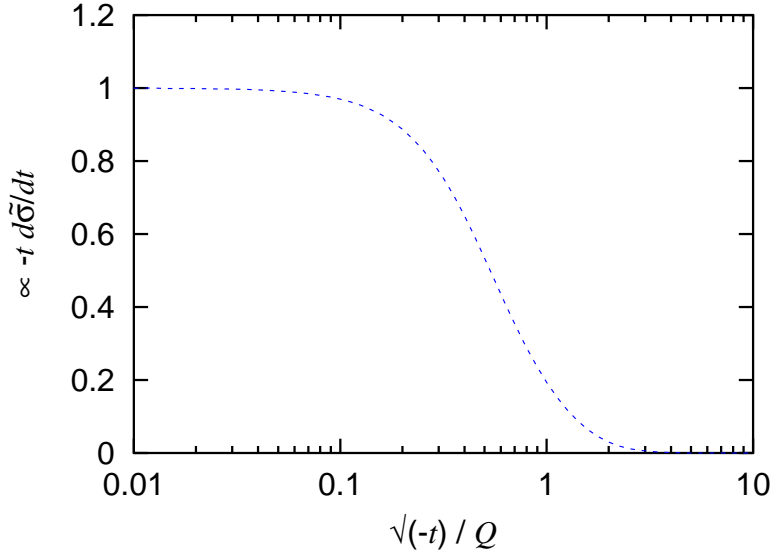


Figure 4.3: The quantity  $-t d\tilde{\sigma}_{g\bar{q}+qg}^{(1)}/dt$  defined in Eq. (4.14), normalized to its limiting value as  $t \rightarrow 0$ , for the case of real  $Z$ -boson production at the Tevatron. The curve passes through 0.5 when  $\sqrt{-t} = 0.53Q$ .

modify Eq. (4.4) by retaining in the integrand only those terms proportional to  $1/t$ , in order to match more closely our definition of  $\bar{\sigma}_{g\bar{q}}^{(1)}$  in Eq. (4.7). Thus, in Fig. 4.3, we plot the quantity

$$\begin{aligned}
 -t \frac{d\tilde{\sigma}_{g\bar{q}+qg}^{(1)}}{dt} &= \frac{\pi\alpha\alpha_s}{3S} \sum_{i,j} C_{ij} \int_{Q^2-t}^S \frac{ds}{s} (g \otimes \bar{q}_j + \bar{q}_j \otimes g + q_i \otimes g + g \otimes q_i) \left(\frac{s}{S}\right) \\
 &\quad \times \left[1 - \frac{2Q^2(s-Q^2)}{s^2}\right] \quad (4.14)
 \end{aligned}$$

for the case of real  $Z$ -boson production at the Tevatron ( $\sqrt{S} = 1.96$  TeV  $p\bar{p}$ ). We use the CTEQ6L1 parton distribution functions [51] here and in all subsequent plots. The right-hand side of Eq. (4.14) depends on  $t$  only in the limit of integration. This limit of integration is responsible for the suppression of  $-t d\tilde{\sigma}_{\text{init}}/dt$  at large  $-t$ . As  $-t$  increases,  $s$  is forced to increase, and the integrand falls off, in part because the partons must carry larger fractions of the hadrons' momenta.

There is some ambiguity in determining where the edge of the plateau is in Fig. 4.3. A

reasonable convention is to choose the value of  $t$  where the curve passes through 50% of its limiting value, indicating a factorization scale  $\mu = 0.53Q$  for real  $Z$ -boson production at the Tevatron.

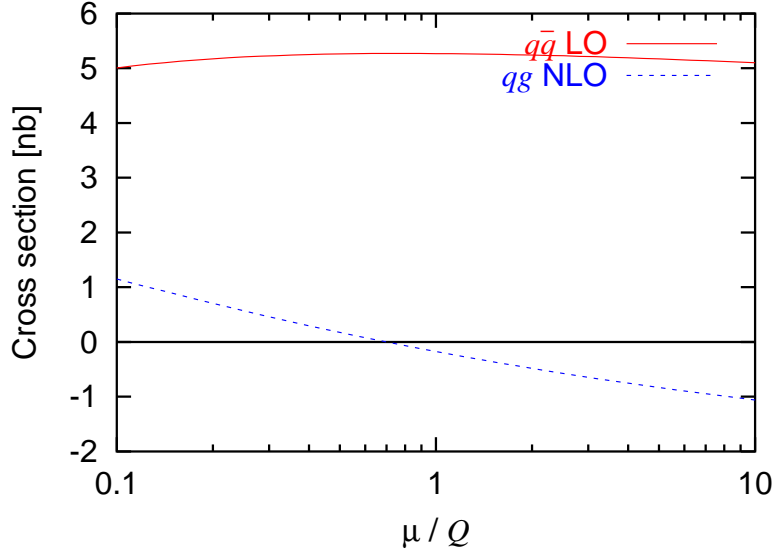


Figure 4.4: The factorization-scale dependence in the collinear scheme of the LO and initial-gluon NLO contributions to real  $Z$ -boson production at the Tevatron. The factorization scale indicated by the plateau is  $0.53Q$ .

Fig. 4.4 shows the factorization-scale dependence of the collinear-scheme NLO contribution to the cross section, given by Eq. (4.11), for the case of real  $Z$ -boson production at the Tevatron. This correction is quite small near the scale  $\mu = 0.53Q$ , which supports our argument for this scale. However, the correction shown in Fig. 4.4 is also quite small for  $\mu = Q$ , so we have not yet demonstrated the superiority of using a scale other than  $Q$ . This will become evident when we consider higher values of  $Q$  in Section 4.3.

### 4.2.2 Real and virtual gluons

Now consider the NLO correction due to gluon radiation, shown in Fig. 4.5. The differential cross section is given by

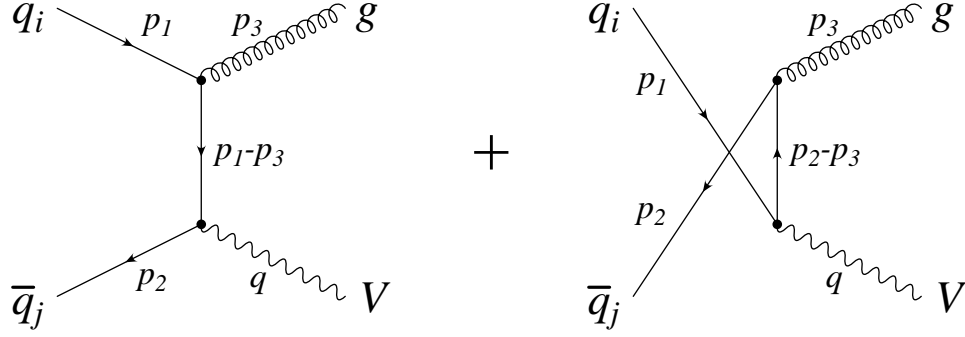


Figure 4.5: Correction to the production of an electroweak gauge boson  $V$  due to real gluon emission.

$$\begin{aligned} \frac{d\sigma_{\text{real}}}{dt} &= \frac{8\pi\alpha\alpha_s}{9S} \frac{(1-\epsilon)(4\pi\mu_D^4)^\epsilon}{\Gamma(1-\epsilon)} \sum_{i,j} C_{ij} \int_{Q^2}^S \frac{ds}{s^2} (q_i \otimes \bar{q}_j + \bar{q}_j \otimes q_i) \left(\frac{s}{S}\right) \int_{-\infty}^0 du \\ &\quad \times \delta(s+t+u-Q^2) \left(\frac{s}{tu}\right)^\epsilon \left[ (1-\epsilon) \left(\frac{t}{u} + \frac{u}{t}\right) + \frac{2sQ^2}{tu} - 2\epsilon \right], \quad (4.15) \end{aligned}$$

which in four dimensions has a singularity at  $t = 0$  from the initial quark emitting a collinear gluon, and another at  $u = 0$  from the initial antiquark emitting a collinear gluon. We focus on the  $t$ -channel singularity and, as before, keep only the leading term as  $t \rightarrow 0$ :

$$\begin{aligned} \bar{\sigma}_{\text{real}} &= -\frac{8\pi\alpha\alpha_s}{9S} \frac{1-\epsilon}{\epsilon\Gamma(1-\epsilon)} \sum_{i,j} C_{ij} \int_{z_0}^1 \frac{dz}{z} (q_i \otimes \bar{q}_j + \bar{q}_j \otimes q_i) \left(\frac{z_0}{z}\right) \\ &\quad \times \left(\frac{4\pi\mu_D^4}{\mu^2(1-z)}\right)^\epsilon \left[ (1-\epsilon)(1-z) + \frac{2z}{1-z} \right]. \quad (4.16) \end{aligned}$$

This integral is divergent in four dimensions, due to the presence of the term  $(1-z)^{-1-\epsilon}$ . This infrared singularity resides at the intersection of the two collinear singularities ( $t = u = 0$ ), and obscures the collinear behavior that we would like to extract. It is cancelled, however, by the infrared divergence from diagrams involving virtual gluons. We therefore turn our attention to these, beginning with the vertex correction shown in Fig. 4.6.

The inclusion of this diagram modifies the tree-level amplitude by the replacement  $\gamma^\mu \rightarrow$

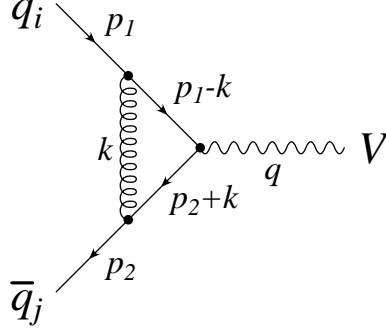


Figure 4.6: Vertex correction to the production of an electroweak gauge boson  $V$ .

$\gamma^\mu [1 + \delta F_1(Q^2)]$ , where

$$\gamma^\mu \delta F_1(Q^2) = -\frac{16}{3} \pi i \alpha_s \mu_D^{2\epsilon} \int \frac{d^{4-2\epsilon} k}{(2\pi)^{4-2\epsilon}} \frac{\gamma_\nu (\not{k} + \not{p}_2) \gamma^\mu (\not{k} - \not{p}_1) \gamma^\nu}{k^2 (k - p_1)^2 (k + p_2)^2}. \quad (4.17)$$

The loop integration is simplified by introducing two independent Feynman parameters  $x$  and  $y$  and shifting the loop momentum to  $\ell \equiv k - xp_1 + yp_2$ . The result is

$$\delta F_1(Q^2) = -\frac{64}{3} \pi i \alpha_s \mu_D^{2\epsilon} \int_0^1 dx \int_0^{1-x} dy \int \frac{d^{4-2\epsilon} \ell}{(2\pi)^{4-2\epsilon}} \times \frac{\frac{(1-\epsilon)^2}{2-\epsilon} \ell^2 - [1-x-y+(1-\epsilon)xy] Q^2}{(\ell^2 + xyQ^2)^3} \quad (4.18)$$

$$= \frac{2\alpha_s}{3\pi} \Gamma(1+\epsilon) \left( \frac{4\pi\mu_D^2}{-Q^2} \right)^\epsilon \int_0^1 dx \int_0^{1-x} dy \times (xy)^{-\epsilon} \left[ \frac{(1-\epsilon)(1-2\epsilon)}{\epsilon} + \frac{1}{x} + \frac{1}{y} - \frac{1}{xy} \right]. \quad (4.19)$$

The integrand contains terms proportional to  $x^{-1-\epsilon}$  and  $y^{-1-\epsilon}$ ; these correspond to collinear singularities at  $x = 0$  and  $y = 0$ . There is also a term proportional to  $(xy)^{-1-\epsilon}$ ; this is the infrared singularity which cancels against that of the real-gluon contribution. The term involving  $1/\epsilon$  is an ultraviolet divergence.

We must also include the correction due to wavefunction renormalization of the external quark lines, shown in Fig. 4.7. This involves the quark self-energy  $\Sigma(p)$ , which for mass-

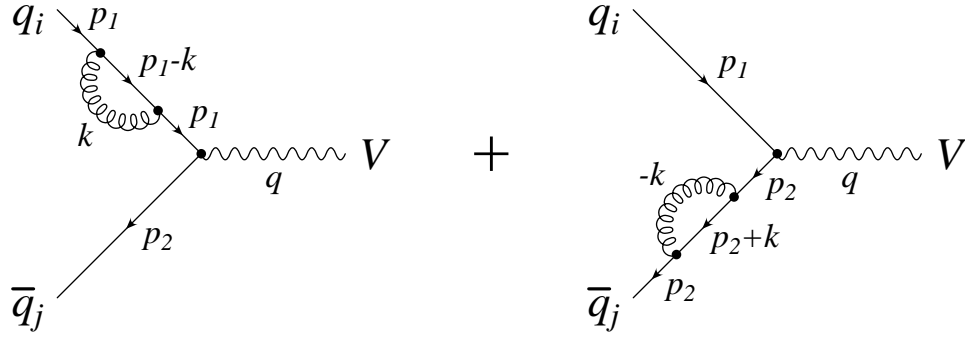


Figure 4.7: Wavefunction renormalization correction to the production of an electroweak gauge boson  $V$ .

less quarks takes the form  $\Sigma(p) = \Sigma'(p^2)\not{p}$ . The tree-level amplitude is modified by the multiplicative factor  $1/\sqrt{1 + \Sigma'(0)}$  for each external leg.

Let us first consider the correction to the incoming quark. The self-energy is

$$\Sigma(p_1) = \frac{32}{3}\pi i\alpha_s(1 - \epsilon)\mu_D^{2\epsilon} \int \frac{d^{4-2\epsilon}k}{(2\pi)^{4-2\epsilon}} \frac{\not{k} - \not{p}_1}{k^2(k - p_1)^2}. \quad (4.20)$$

This integral contains an ultraviolet divergence, which cancels against that of the vertex correction. It also contains a collinear divergence, which we want to express in a form that can be easily combined with those we have encountered in the vertex correction. The natural way to proceed with the calculation of  $\Sigma(p_1)$  is to introduce a single Feynman parameter  $x$ . This will not suffice for our present purposes; we need to introduce two independent Feynman parameters, as in the vertex correction. We can achieve this by multiplying by unity:

$$\Sigma(p_1) = \frac{32}{3}\pi i\alpha_s(1 - \epsilon)\mu_D^{2\epsilon} \int \frac{d^{4-2\epsilon}k}{(2\pi)^{4-2\epsilon}} \frac{(\not{k} - \not{p}_1)(k + p_2)^2}{k^2(k - p_1)^2(k + p_2)^2}. \quad (4.21)$$

The denominator now matches the denominator from the vertex correction, and we can therefore introduce matching Feynman parameters.

We can think of  $p_2$ , which has appeared out of nowhere, as the momentum of the incoming antiquark in  $q_i \bar{q}_j \rightarrow V$ . We take the antiquark and the vector boson to be on shell, i.e.  $p_2^2 = 0$  and  $(p_1 + p_2)^2 = Q^2$ , but  $p_1$  must be kept off shell for the moment.

As before we introduce Feynman parameters  $x$  and  $y$ , and shift the loop momentum to  $\ell \equiv k - xp_1 + yp_2$ :

$$\begin{aligned} \Sigma(p_1) = & \frac{64}{3} \pi i \alpha_s (1 - \epsilon) \mu_D^{2\epsilon} \int_0^1 dx \int_0^{1-x} dy \int \frac{d^{4-2\epsilon} \ell}{(2\pi)^{4-2\epsilon}} \frac{1}{[\ell^2 + xyQ^2 + x(1-x-y)p_1^2]^3} \\ & \times \left\{ \left[ \left( -1 + \frac{3-\epsilon}{2-\epsilon} x \right) \not{p}_1 + \left( \frac{1}{2-\epsilon} - \frac{3-\epsilon}{2-\epsilon} y \right) \not{p}_2 \right] \ell^2 \right. \\ & \left. - [(1-x)\not{p}_1 + y\not{p}_2] [x(1-y)Q^2 - x(1-x-y)p_1^2] \right\}. \quad (4.22) \end{aligned}$$

The presence of terms proportional to  $\not{p}_2$  may be surprising, but these terms integrate to zero and do not contain a collinear singularity. Thus they need trouble us no further. At this point we can read off the coefficient of  $\not{p}_1$  and set  $p_1^2 = 0$ .

$$\begin{aligned} \Sigma'(0) = & \frac{64}{3} \pi i \alpha_s (1 - \epsilon) \mu_D^{2\epsilon} \int_0^1 dx \int_0^{1-x} dy \int \frac{d^{4-2\epsilon} \ell}{(2\pi)^{4-2\epsilon}} \\ & \times \frac{\left( -1 + \frac{3-\epsilon}{2-\epsilon} x \right) \ell^2 - x(1-x)(1-y)Q^2}{(\ell^2 + xyQ^2)^3} \\ = & \frac{2\alpha_s}{3\pi} (1 - \epsilon) \Gamma(1 + \epsilon) \left( \frac{4\pi\mu_D^2}{-Q^2} \right)^\epsilon \int_0^1 dx \int_0^{1-x} dy (xy)^{-\epsilon} \\ & \times \left[ \frac{2(1-\epsilon)}{\epsilon} - \frac{3-2\epsilon}{\epsilon} x + \frac{1}{y} - \frac{x}{y} \right]. \quad (4.23) \end{aligned}$$

The terms involving  $1/\epsilon$  are the expected ultraviolet divergence. There is also a single collinear singularity, at  $y = 0$ .

The self-energy correction to the incoming antiquark line is completely analogous, but it is appropriate to interchange the parameters  $x$  and  $y$ . The order- $\alpha_s$  contribution to the  $q_i \bar{q}_j \rightarrow V$  amplitude due to virtual gluons is therefore equal to the tree-level amplitude times

the factor

$$\begin{aligned}
\Delta &\equiv \delta F_1(Q^2) - \frac{1}{2}\Sigma'(0) - \frac{1}{2}\Sigma'(0) \\
&= -\frac{\alpha_s}{3\pi}\Gamma(1+\epsilon)\left(\frac{4\pi\mu_D^2}{-Q^2}\right)^\epsilon \int_0^1 dx \int_0^{1-x} dy (xy)^{-\epsilon} \\
&\times \left[ \frac{2}{xy} - (1+\epsilon)\left(\frac{1}{x} + \frac{1}{y}\right) - (1-\epsilon)\left(\frac{x}{y} + \frac{y}{x}\right) \right. \\
&\quad \left. + \frac{2(1-\epsilon)}{\epsilon} - \frac{(1-\epsilon)(3-2\epsilon)}{\epsilon}(x+y) \right], \quad (4.24)
\end{aligned}$$

and the NLO contribution to the cross section is then

$$\begin{aligned}
\sigma_{\text{virt}} &= (2 \text{Re } \Delta)\sigma_{q\bar{q}}^{(0)} \\
&= -\frac{8\pi\alpha_s}{9S}(1-\epsilon)\Gamma(1+\epsilon) \text{Re} \left( \frac{4\pi\mu_D^4}{-Q^2} \right)^\epsilon \sum_{i,j} C_{ij}(q_i \otimes \bar{q}_j + \bar{q}_j \otimes q_i)(z_0) \\
&\times \int_0^1 dx \int_0^{1-x} dy (xy)^{-\epsilon} \left[ \frac{2}{xy} - (1+\epsilon)\left(\frac{1}{x} + \frac{1}{y}\right) - (1-\epsilon)\left(\frac{x}{y} + \frac{y}{x}\right) \right. \\
&\quad \left. + \frac{2(1-\epsilon)}{\epsilon} - \frac{(1-\epsilon)(3-2\epsilon)}{\epsilon}(x+y) \right], \quad (4.25)
\end{aligned}$$

This must be combined with the correction due to real-gluon emission to yield an infrared-finite result.

The hadronic real-gluon-emission cross section involves an integration over the Mandelstam variables  $s$ ,  $t$ , and  $u$ , subject to the constraint  $s + t + u = Q^2$ . There are collinear singularities at  $t = 0$  and at  $u = 0$ , and where the two meet there is an infrared singularity at  $s = Q^2$ . Similarly, the virtual-gluon cross section involves an integration over the Feynman parameters  $x$  and  $y$ , and for convenience we can introduce a third parameter  $z$ , constrained by  $x + y + z = 1$ . There are collinear singularities at  $x = 0$  and at  $y = 0$ , and where the two meet there is an infrared singularity at  $z = 1$ . The similarity between the two structures is

striking, and they can be made to match exactly by the mapping

$$x \rightarrow \frac{-u}{s}, \quad y \rightarrow \frac{-t}{s}, \quad z \rightarrow \frac{Q^2}{s}. \quad (4.26)$$

This mapping is illustrated in Fig. 4.8.

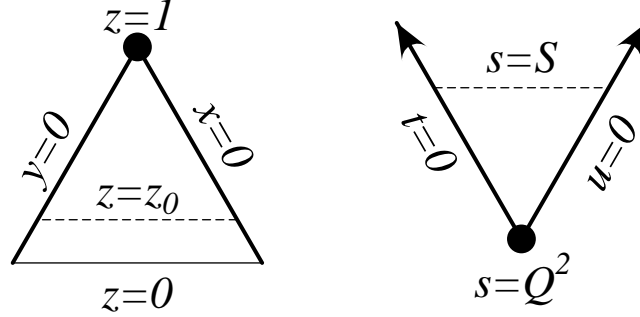


Figure 4.8: The region of Feynman-parameter space bounded by  $x = 0$ ,  $y = 0$ , and  $z = 0$  is mapped by Eq. (4.26) onto the region of Mandelstam-variable space bounded by  $s = \infty$ ,  $t = 0$ , and  $u = 0$ . The real-gluon contribution is bounded by  $s = S$  (or  $z = z_0$ ), while the virtual-gluon contribution extends all the way to  $z = 0$  (or  $s = \infty$ ). The heavy lines represent the collinear singularities, and the black dots represent the infrared singularity.

We thus change variables from  $x, y, z$  to  $s, t, u$ , using the relation

$$\begin{aligned} \int_0^1 dx \int_0^{1-x} dy &= \int_0^1 dx \int_0^1 dy \int_0^1 dz \delta(x + y + z - 1) \\ &= Q^2 \int_{Q^2}^{\infty} \frac{ds}{s^3} \int_{-\infty}^0 dt \int_{-\infty}^0 du \delta(s + t + u - Q^2). \end{aligned} \quad (4.27)$$

Thus we can write down the virtual-gluon differential cross section:

$$\begin{aligned}
\frac{d\sigma_{\text{virt}}}{dt} = & -\frac{8\pi\alpha\alpha_s}{9S}(1-\epsilon)\Gamma(1+\epsilon)\text{Re}\left(\frac{4\pi\mu_D^4}{-Q^2}\right)^\epsilon \sum_{i,j} C_{ij}(q_i \otimes \bar{q}_j + \bar{q}_j \otimes q_i) \left(\frac{Q^2}{S}\right) \\
& \times \int_{Q^2}^{\infty} ds \frac{Q^2}{s^3} \int_{-\infty}^0 du \delta(s+t+u-Q^2) \left(\frac{s^2}{tu}\right)^\epsilon \\
& \times \left[ \frac{2s^2}{tu} - (1+\epsilon) \left(\frac{s}{-t} + \frac{s}{-u}\right) - (1-\epsilon) \left(\frac{t}{u} + \frac{u}{t}\right) \right. \\
& \quad \left. + \frac{2(1-\epsilon)}{\epsilon} - \frac{(1-\epsilon)(3-2\epsilon)}{\epsilon} \frac{s-Q^2}{s} \right]. \quad (4.28)
\end{aligned}$$

In this equation the symbols  $s$ ,  $t$ , and  $u$ , while they have been designed to resemble Mandelstam variables, are not defined in terms of external momenta, but rather as particular combinations of Feynman parameters given by Eq. (4.26). In particular  $s \neq (p_1 + p_2)^2 = Q^2$ .

We now proceed in the same way as for real-gluon emission, focusing on the  $t = 0$  singularity and keeping only the leading terms as  $t \rightarrow 0$ .

$$\begin{aligned}
\bar{\sigma}_{\text{virt}} = & \frac{8\pi\alpha\alpha_s}{9S} \frac{1-\epsilon}{\epsilon} \Gamma(1+\epsilon) \text{Re}\left(\frac{4\pi\mu_D^4}{-\mu^2}\right)^\epsilon \sum_{i,j} C_{ij}(q_i \otimes \bar{q}_j + \bar{q}_j \otimes q_i)(z_0) \\
& \times \int_0^1 \frac{dz}{z} [z(1-z)]^{-\epsilon} \frac{z^2[3-z-\epsilon(1-z)]}{1-z}. \quad (4.29)
\end{aligned}$$

We now add Eqs. (4.16) and (4.29) to find

$$\begin{aligned}
\bar{\sigma}_{q\bar{q}}^{(1)} = & -\frac{8\pi\alpha\alpha_s}{9S} \frac{1-\epsilon}{\epsilon} \left(\frac{4\pi\mu_D^4}{\mu^2}\right)^\epsilon \sum_{i,j} C_{ij} \int_0^1 \frac{dz}{z} (1-z)^{-\epsilon} \\
& \times \left\{ \theta(z-z_0) \frac{1}{\Gamma(1-\epsilon)} (q_i \otimes \bar{q}_j + \bar{q}_j \otimes q_i) \left(\frac{z_0}{z}\right) \frac{1+z^2-\epsilon(1-z)^2}{1-z} \right. \\
& \quad \left. - \text{Re}(-1)^\epsilon \Gamma(1+\epsilon) (q_i \otimes \bar{q}_j + \bar{q}_j \otimes q_i)(z_0) z^{-\epsilon} \frac{z^2[3-z-\epsilon(1-z)]}{1-z} \right\}. \quad (4.30)
\end{aligned}$$

The infrared divergence,  $z \rightarrow 1$ , manifestly cancels between the real- and virtual-gluon contributions, up to terms of order  $\epsilon^2$  in the integrand, which yield finite terms after the

integration over  $z$ . The cancellation of the infrared divergence prior to integration is reminiscent of the work of Refs. [52, 53, 54].

We express this result in terms of the familiar “plus” distributions and expand in powers of  $\epsilon$ , obtaining

$$\begin{aligned} \bar{\sigma}_{q\bar{q}}^{(1)} &= \frac{2\pi\alpha\alpha_s}{3S}(1-\epsilon)\mu_D^{2\epsilon} \sum_{i,j} C_{ij} \int_{z_0}^1 \frac{dz}{z} (q_i \otimes \bar{q}_j + \bar{q}_j \otimes q_i) \left(\frac{z_0}{z}\right) \\ &\times \left[ - \left( \frac{1}{\epsilon} - \gamma + \ln \frac{4\pi\mu_D^2}{\mu^2} \right) P_{qq}(z) + \frac{4}{3}(1+z^2) \left( \frac{\ln(1-z)}{1-z} \right)_+ \right. \\ &\quad \left. + \left( \frac{4\pi^2}{3} - \frac{14}{3} \right) \delta(1-z) + \frac{4}{3}(1-z) \right], \quad (4.31) \end{aligned}$$

where  $P_{qq}(z) = \frac{4}{3}[(1+z^2)/(1-z)]_+$  is the DGLAP splitting function.

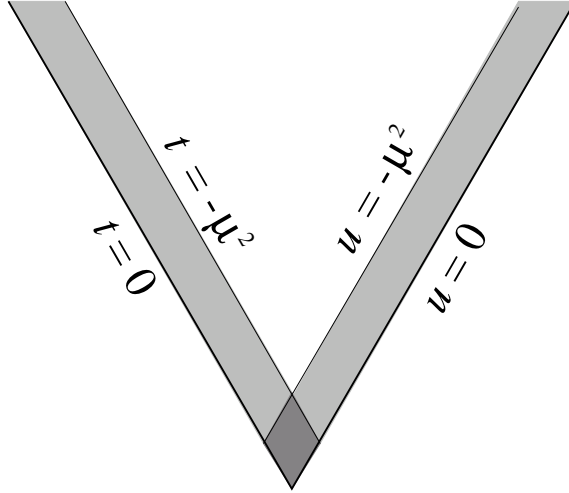


Figure 4.9: The counterterms corresponding to the  $t$ - and  $u$ -channel collinear singularities are formed by integrating over the shaded strips. We must be careful to avoid double-counting in the region where the two strips overlap.

The total real- and virtual-gluon cross section is given by [46]

$$\begin{aligned} \sigma_{q\bar{q}}^{(1)} &= \frac{2\pi\alpha\alpha_s}{3S}(1-\epsilon)\mu_D^{2\epsilon} \sum_{i,j} C_{ij} \int_{z_0}^1 \frac{dz}{z} (q_i \otimes \bar{q}_j + \bar{q}_j \otimes q_i) \left(\frac{z_0}{z}\right) \\ &\times \left[ -2 \left( \frac{1}{\epsilon} - \gamma + \ln \frac{4\pi\mu_D^4}{Q^2} \right) P_{qq}(z) + \frac{16}{3}(1+z^2) \left( \frac{\ln(1-z)}{1-z} \right)_+ \right. \\ &\quad \left. + \left( \frac{8\pi^2}{9} - \frac{32}{3} \right) \delta(1-z) - \frac{8}{3} \frac{1+z^2}{1-z} \ln z \right]. \end{aligned} \quad (4.32)$$

We must subtract from this expression two copies of  $\bar{\sigma}_{q\bar{q}}^{(1)}$  (corresponding to the two collinear singularities), which will be absorbed into the quark and antiquark distribution functions. However, in doing so we will have double-counted a finite contribution from the region where both  $t$  and  $u$  are near zero (see Fig. 4.9). We must therefore add the quantity

$$\begin{aligned} \bar{\bar{\sigma}}_{q\bar{q}}^{(1)} &\equiv \left[ \lim_{t,u \rightarrow 0} \left( (tu)^{1+\epsilon} \frac{d^2\sigma_{q\bar{q}}^{(1)}}{dt du} \right) \right] \int_{-\mu^2}^0 dt \int_{-\mu^2}^0 du \frac{1}{(tu)^{1+\epsilon}} \\ &= \frac{2\pi\alpha\alpha_s}{3S} \sum_{i,j} C_{ij} \int_{z_0}^1 \frac{dz}{z} (q_i \otimes \bar{q}_j + \bar{q}_j \otimes q_i) \left(\frac{z_0}{z}\right) \frac{8\pi^2}{9} \delta(1-z). \end{aligned} \quad (4.33)$$

Thus the explicit collinear-scheme NLO correction to the Drell-Yan cross section is

$$\begin{aligned} \sigma_{q\bar{q}}^{(1)} - 2\bar{\sigma}_{q\bar{q}}^{(1)} + \bar{\bar{\sigma}}_{q\bar{q}}^{(1)} &= \frac{2\pi\alpha\alpha_s}{3S} \sum_{i,j} C_{ij} \int_{z_0}^1 \frac{dz}{z} (q_i \otimes \bar{q}_j + \bar{q}_j \otimes q_i) \left(\frac{z_0}{z}\right) \\ &\times \left[ 2P_{qq}(z) \ln \frac{Q^2}{\mu^2} + \frac{8}{3}(1+z^2) \left( \frac{\ln(1-z)}{1-z} \right)_+ - \left( \frac{8\pi^2}{9} + \frac{4}{3} \right) \delta(1-z) \right. \\ &\quad \left. - \frac{8}{3} \frac{1+z^2}{1-z} \ln z - \frac{8}{3}(1-z) \right]. \end{aligned} \quad (4.34)$$

The collinear contribution absorbed into the quark distribution function is

$$\bar{\sigma}_{q\bar{q}}^{(1)} - \frac{1}{2}\bar{\bar{\sigma}}_{q\bar{q}}^{(1)} = \frac{4\pi^2\alpha}{3S}(1-\epsilon)\mu_D^{2\epsilon} \sum_{i,j} C_{ij} (\delta q_i \otimes \bar{q}_j + \bar{q}_j \otimes \delta q_i) \left(\frac{Q^2}{S}\right), \quad (4.35)$$

where

$$\delta q_i(x) = -\frac{\alpha_s}{2\pi} \int_x^1 \frac{dz}{z} q_i\left(\frac{x}{z}\right) \left[ \left( \frac{1}{\epsilon} - \gamma + \ln \frac{4\pi\mu_D^2}{\mu^2} \right) P_{qq}(z) - \frac{4}{3}(1+z^2) \left( \frac{\ln(1-z)}{1-z} \right)_+ - \left( \frac{8\pi^2}{9} - \frac{14}{3} \right) \delta(1-z) - \frac{4}{3}(1-z) \right]. \quad (4.36)$$

The correction  $\delta\bar{q}_j(x)$  to the antiquark distribution function is analogous.

Again, the explicit correction can be calculated directly by subtracting  $\bar{\sigma}_{q\bar{q}}^{(1)}$  before performing the integration, similarly to Eqs. (4.12) and (4.13). This obviates the need to regulate the collinear divergences. Furthermore, since Eq. (4.30) is manifestly infrared finite, there is no need to regulate the infrared divergences either. We checked that Eq. (4.34) is reproduced if we use dimensional regularization to regulate only the ultraviolet divergences.

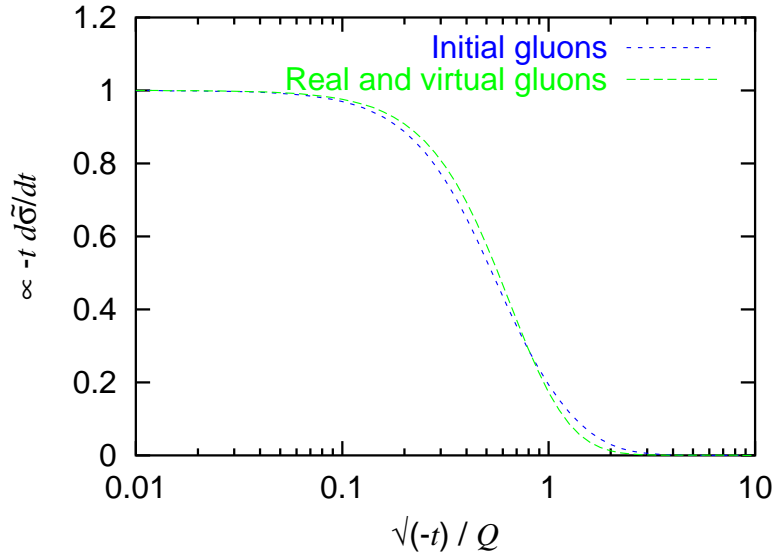


Figure 4.10: The quantities  $-t d\tilde{\sigma}_{g\bar{q}+qg}^{(1)}/dt$ , defined in Eq. (4.14), and  $-t d\tilde{\sigma}_{q\bar{q}}^{(1)}/dt$ , defined in Eq. (4.37), normalized to their respective limiting values as  $t \rightarrow 0$ , for the case of real  $Z$ -boson production at the Tevatron. The initial-gluon curve passes through 0.5 when  $\sqrt{-t} = 0.53Q$ , and the real- and virtual-gluon curve when  $\sqrt{-t} = 0.57Q$ .

In order to choose the factorization scale, we must construct the analogous quantity to

Eq. (4.14). Retaining only terms proportional to  $1/t$  in Eqs. (4.15) and (4.28), we obtain

$$-t \frac{d\tilde{\sigma}_{q\bar{q}}^{(1)}}{dt} = \frac{8\pi\alpha\alpha_s}{9S} \sum_{i,j} C_{ij} \int_{Q^2-t}^{\infty} \frac{ds}{s} \left[ \theta(S-s)(q_i \otimes \bar{q}_j + \bar{q}_j \otimes q_i) \left(\frac{s}{S}\right) \frac{s^2 + Q^4}{s(s-Q^2)} \right. \\ \left. - (q_i \otimes \bar{q}_j + \bar{q}_j \otimes q_i) \left(\frac{Q^2}{S}\right) \frac{Q^4(3s-Q^2)}{s^2(s-Q^2)} \right]. \quad (4.37)$$

This quantity is plotted, along with  $-t d\tilde{\sigma}_{g\bar{q}+qg}^{(1)}/dt$ , in Fig. 4.10. The factorization scale indicated by the real- and virtual-gluon plateau is  $0.57Q$ , about the same as that indicated by the initial-gluon plateau.

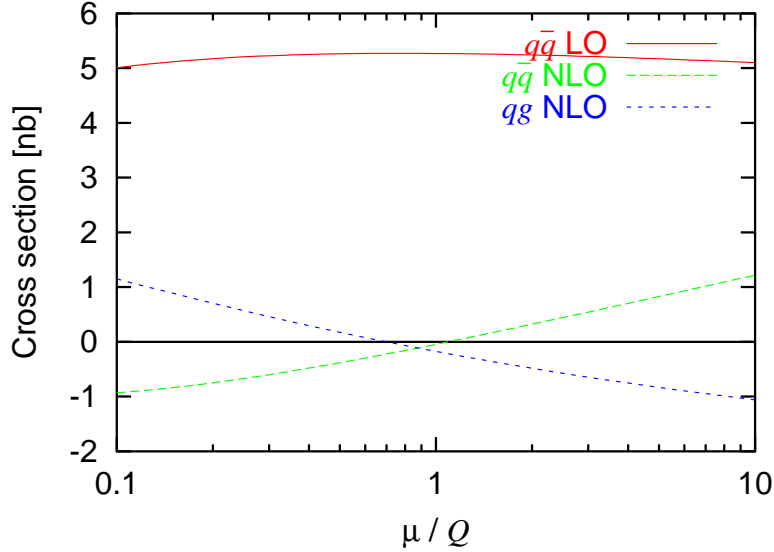


Figure 4.11: The factorization-scale dependence in the collinear scheme of the LO and NLO contributions to real  $Z$ -boson production at the Tevatron. The factorization scales indicated by the plateaux are  $0.53Q$  for initial gluons and  $0.57Q$  for real and virtual gluons.

Fig. 4.11 shows the factorization-scale dependence of both NLO corrections to the Drell-Yan cross section in the collinear scheme. At  $\mu \approx Q/2$ , the correction due to real and virtual gluons is very small, about -7% of the LO cross section. This correction is even smaller at  $\mu \approx Q$ , essentially vanishing. However, there is no reason to expect the correction to vanish near the appropriate factorization scale; it is enough that it is small, indicating a convergent perturbation series.

### 4.3 Results

In this section we show the factorization-scale dependence of the LO and NLO contributions to the Drell-Yan cross section, in the collinear scheme, for several values of  $Q$  and  $\sqrt{S}$ . In some cases the initial-gluon correction has been multiplied by a large factor in order to make it more visible.

Fig. 4.12 shows the case of virtual  $Z$ -boson production at the CERN Large Hadron Collider (LHC) ( $\sqrt{S} = 14$  TeV  $pp$ ), with  $Q = 650$  GeV. This value of  $Q$  has been chosen so that the ratio  $Q/\sqrt{S}$  is the same as for the case of real  $Z$ -boson production at the Tevatron, presented in Fig 4.11. The factorization scales indicated by the plateaux are about the same as in that case, still in the vicinity of  $\mu \approx Q/2$ . Again, both NLO corrections are very small near this scale.

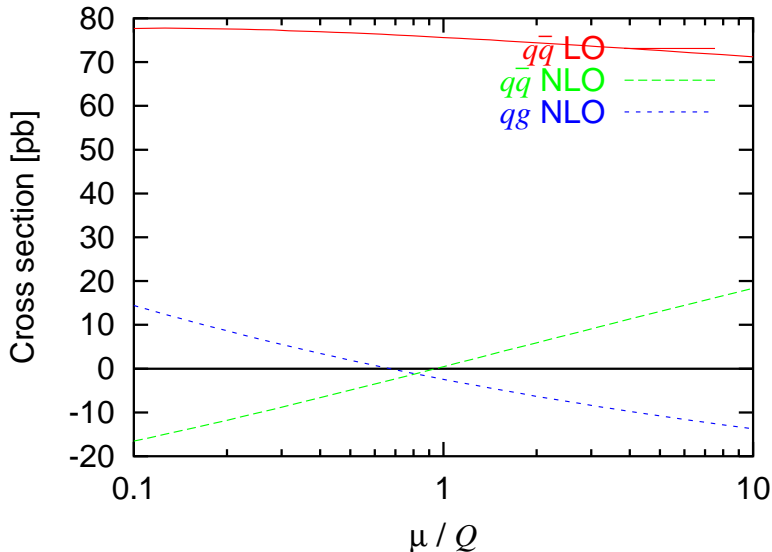


Figure 4.12: The factorization-scale dependence in the collinear scheme of the LO and NLO contributions to virtual  $Z$ -boson production at the LHC, with  $Q = 650$  GeV. The factorization scales indicated by the plateaux are  $0.52Q$  for initial gluons and  $0.61Q$  for real and virtual gluons.

Fig. 4.13 shows the case of virtual  $Z$ -boson production at the Tevatron, with  $Q = 280$  GeV. The factorization scales indicated by the initial-gluon plateau ( $0.44Q$ ) and by

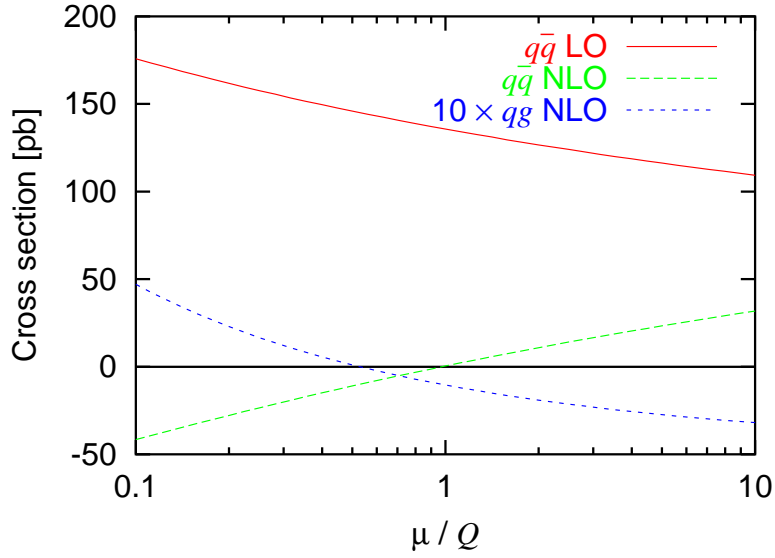


Figure 4.13: The factorization-scale dependence in the collinear scheme of the LO and NLO contributions to virtual  $Z$ -boson production at the Tevatron, with  $Q = 280$  GeV. The factorization scales indicated by the plateaux are  $0.44Q$  for initial gluons and  $0.64Q$  for real and virtual gluons.

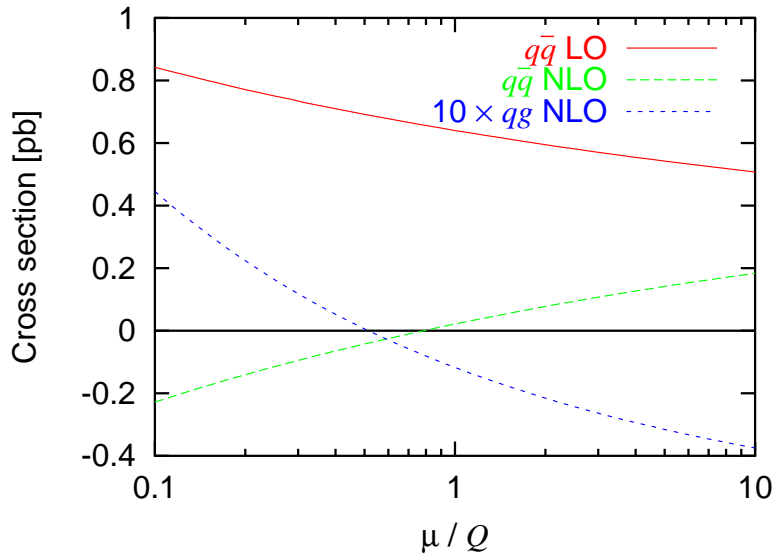


Figure 4.14: The factorization-scale dependence in the collinear scheme of the LO and NLO contributions to virtual  $Z$ -boson production at the LHC, with  $Q = 2$  TeV. The factorization scales indicated by the plateaux are  $0.43Q$  for initial gluons and  $0.62Q$  for real and virtual gluons.

the real- and virtual-gluon plateau ( $0.64Q$ ) differ more than in the case of real  $Z$ -boson production, but are close enough that both corrections are very small for  $\mu \approx Q/2$ . Fig. 4.14 shows the case of virtual  $Z$ -boson production at the LHC, with  $Q = 2$  TeV. The ratio  $Q/\sqrt{S}$  is the same in Figs. 4.13 and 4.14, and the behavior of the NLO corrections is very similar.

In Figs. 4.15–4.20 we show the factorization-scale dependence of the virtual  $Z$ -boson production cross section for increasingly high values of  $Q$ , at both the Tevatron and the LHC. As  $Q/\sqrt{S}$  increases, the factorization scale indicated by the real- and virtual-gluon plateau decreases slowly, while that indicated by the initial-gluon plateau decreases somewhat more rapidly. As the scale indicated by the initial-gluon plateau decreases, we observe a corresponding decrease in the scale at which the initial-gluon correction is minimized, which supports our argument for this scale choice. In Figs. 4.19 and 4.20, the two scales differ by nearly a factor of 2, and this difference is reflected in the plots; the initial-gluon correction is very small for  $\mu \approx Q/4$ , while the real- and virtual-gluon correction is very small for  $\mu \approx Q/2$ . When choosing a single factorization scale, it is necessary to compromise between these two values. Since the initial-gluon correction is dwarfed by the real- and virtual-gluon correction, for practical purposes one should choose the scale indicated by the real- and virtual-gluon plateau,  $\mu \approx Q/2$ .

In Figs. 4.21 and 4.22, we examine Drell-Yan production of a virtual photon in a fixed-target experiment with a beam energy of 800 GeV ( $\sqrt{S} = 38.8$  GeV  $pp$ ). Once again, the NLO corrections are small if the factorization scale is chosen according to the plateaux. Fig. 4.22 in particular illustrates the importance of this choice: if one instead chose  $\mu = Q$ , the NLO correction due to real and virtual gluons would equal 35% of the LO cross section.

## 4.4 Discussion

The expansion parameter in perturbative QCD is  $\alpha_s/\pi \approx 0.04$  (for renormalization scales near the  $Z$  mass), so it is reasonable to expect QCD radiative corrections to be of this

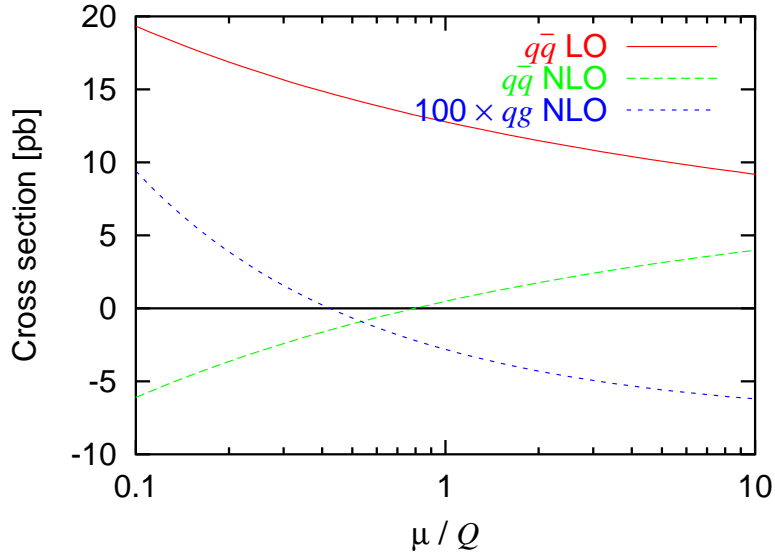


Figure 4.15: The factorization-scale dependence in the collinear scheme of the LO and NLO contributions to virtual  $Z$ -boson production at the Tevatron, with  $Q = 490$  GeV. The factorization scales indicated by the plateaux are  $0.37Q$  for initial gluons and  $0.63Q$  for real and virtual gluons.

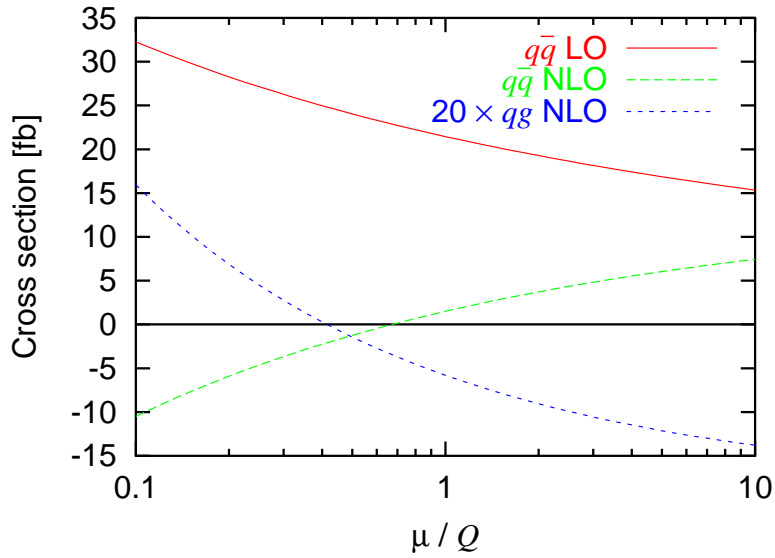


Figure 4.16: The factorization-scale dependence in the collinear scheme of the LO and NLO contributions to virtual  $Z$ -boson production at the LHC, with  $Q = 3.5$  TeV. The factorization scales indicated by the plateaux are  $0.37Q$  for initial gluons and  $0.58Q$  for real and virtual gluons.

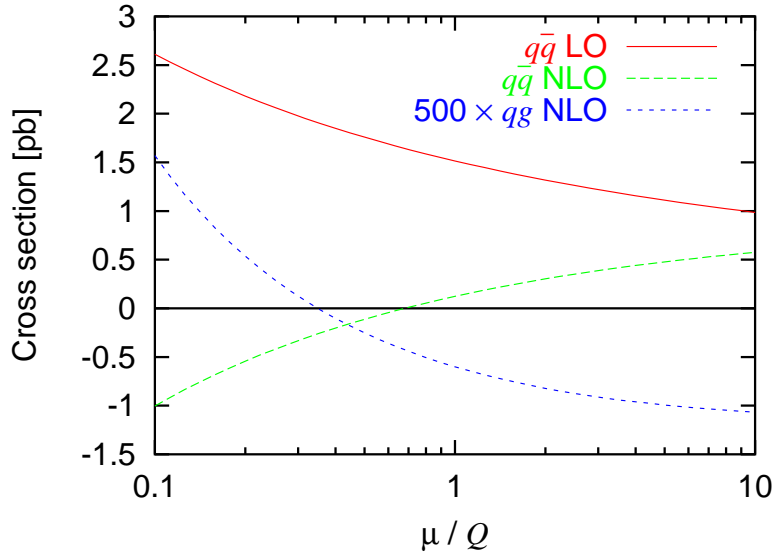


Figure 4.17: The factorization-scale dependence in the collinear scheme of the LO and NLO contributions to virtual  $Z$ -boson production at the Tevatron, with  $Q = 700$  GeV. The factorization scales indicated by the plateaux are  $0.33Q$  for initial gluons and  $0.58Q$  for real and virtual gluons.

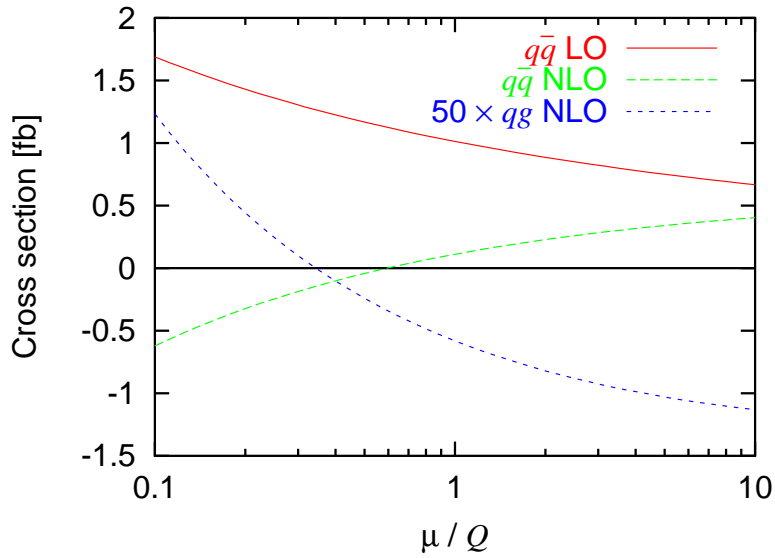


Figure 4.18: The factorization-scale dependence in the collinear scheme of the LO and NLO contributions to virtual  $Z$ -boson production at the LHC, with  $Q = 5$  TeV. The factorization scales indicated by the plateaux are  $0.32Q$  for initial gluons and  $0.53Q$  for real and virtual gluons.

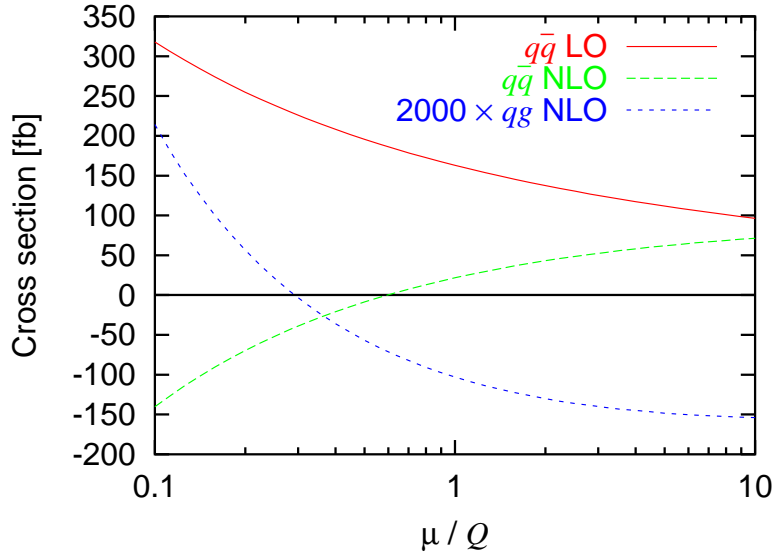


Figure 4.19: The factorization-scale dependence in the collinear scheme of the LO and NLO contributions to virtual  $Z$ -boson production at the Tevatron, with  $Q = 910$  GeV. The factorization scales indicated by the plateaux are  $0.28Q$  for initial gluons and  $0.53Q$  for real and virtual gluons.

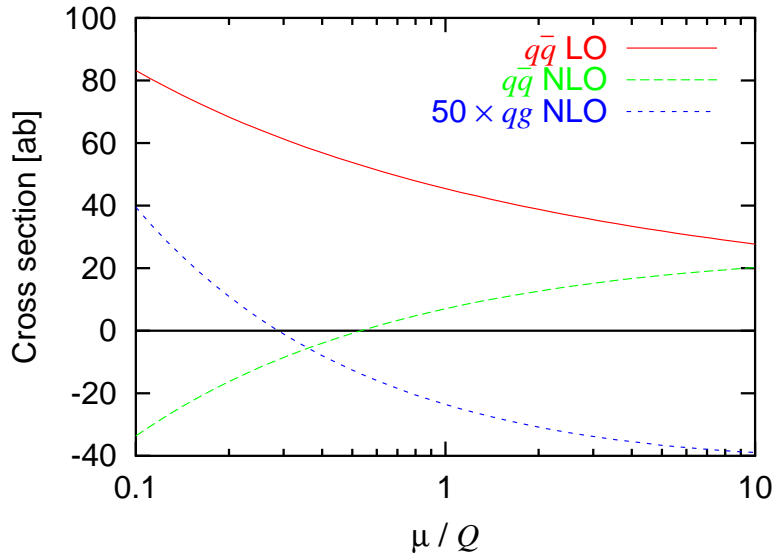


Figure 4.20: The factorization-scale dependence in the collinear scheme of the LO and NLO contributions to virtual  $Z$ -boson production at the LHC, with  $Q = 6.5$  TeV. The factorization scales indicated by the plateaux are  $0.28Q$  for initial gluons and  $0.49Q$  for real and virtual gluons.

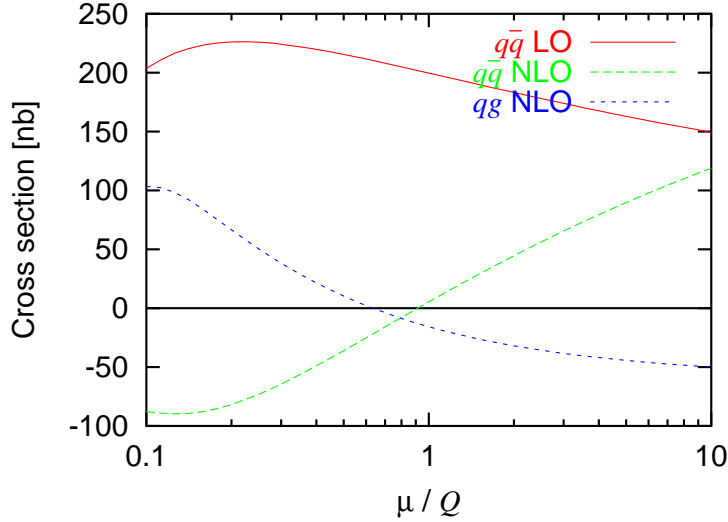


Figure 4.21: The factorization-scale dependence in the collinear scheme of the LO and NLO contributions to virtual photon production in  $pp$  collisions at  $\sqrt{S} = 38.8$  GeV, with  $Q = 5$  GeV. The factorization scales indicated by the plateaux are  $0.48Q$  for initial gluons and  $0.64Q$  for real and virtual gluons.

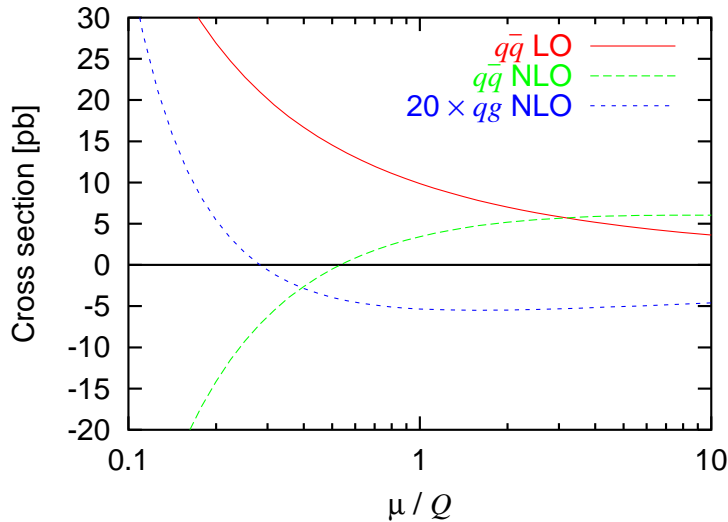


Figure 4.22: The factorization-scale dependence in the collinear scheme of the LO and NLO contributions to virtual photon production in  $pp$  collisions at  $\sqrt{S} = 38.8$  GeV, with  $Q = 20$  GeV. The factorization scales indicated by the plateaux are  $0.27Q$  for initial gluons and  $0.48Q$  for real and virtual gluons.

order. Indeed, this is exactly the size of the NLO correction to  $e^+e^- \rightarrow q\bar{q}$ , one of the classic processes of QCD. However, for QCD corrections to hadron-hadron processes, we have become accustomed to much larger radiative corrections, of order 20–100%. The size of the correction is dependent on the factorization scale, so there is always some assumption about the appropriate factorization scale when one quotes the size of the radiative correction.

In this paper we have introduced the collinear factorization scheme, and argued for a method to choose the factorization scale in that scheme. We applied this to the Drell-Yan process, and found that the NLO corrections are very small, less than 10%, for a wide variety of machine energies and values of the vector-boson invariant mass  $Q$ . The factorization scale indicated by our method is  $\mu \approx Q/2$  in the collinear scheme. This is not necessarily the correct scale in other factorization schemes, such as the popular  $\overline{\text{MS}}$  scheme.

The lack of large radiative corrections for a given factorization scale (for a given scheme) supports that choice of factorization scale as being appropriate. When calculated to all orders in perturbation theory, the cross section is independent of the factorization scale. In practice one is limited to low orders in perturbation theory, so one seeks a choice of factorization scale that yields a rapid convergence of the perturbation series.

To be more precise, we must consider what one means by the size of the radiative corrections. The only definition that is scheme-independent, at least formally to any given order in perturbation theory, is as follows. The LO calculation should be performed with LO parton distribution functions, the NLO calculation with NLO parton distribution functions, and so on. Since we are working in the collinear scheme, we should be using collinear-scheme parton distribution functions at NLO, which are not available. Thus, what we have shown in this paper is that the explicit NLO corrections to the Drell-Yan process are small in the collinear scheme. There remains an additional correction that results from passing from LO to NLO parton distribution functions. Until a NLO set of collinear-scheme parton distribution functions is available, we cannot know the size of this correction.

There is a surprising aspect to our results. It is well known that the Drell-Yan process,

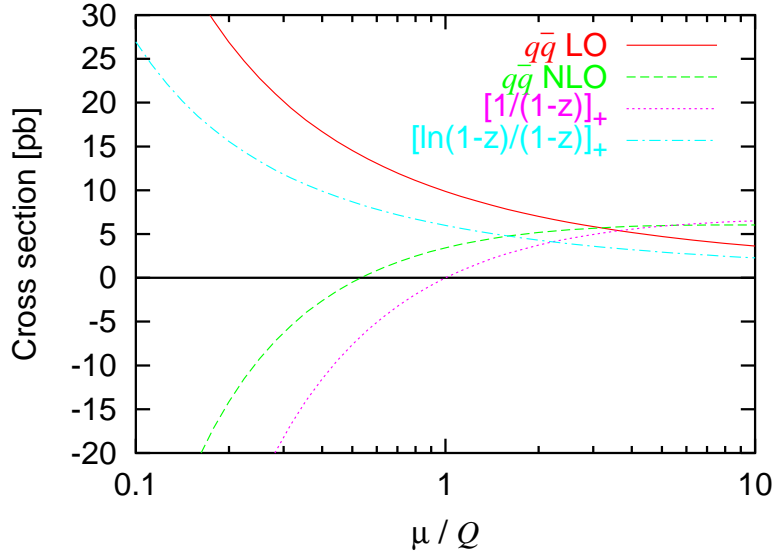


Figure 4.23: The factorization-scale dependence in the collinear scheme of the LO and real- and virtual-gluon NLO contributions to virtual photon production in  $pp$  collisions at  $\sqrt{S} = 38.8$  GeV, with  $Q = 20$  GeV. The terms proportional to  $[1/(1-z)]_+$  and  $[\ln(1-z)/(1-z)]_+$  are plotted separately. The factorization scale indicated by the real- and virtual-gluon plateau is  $0.48Q$ .

like all hadron-hadron scattering processes, is afflicted by large “threshold” logarithms that degrade the convergence of the perturbation series [55]. These correspond to the terms proportional to  $[\ln(1-z)/(1-z)]_+$  and  $[1/(1-z)]_+$  [implicit in  $P_{qq}(z)$ ] in the real- and virtual-gluon emission correction [see Eq. (4.34)]. Although such terms are present in the collinear scheme, they are of opposite sign (for  $\mu \approx Q/2$ ), and largely cancel. The net result is that the NLO correction is very small, even for  $Q$  of order half the center-of-mass energy, where such logarithms are particularly large. In contrast, for  $\mu = Q$  the term proportional to  $[1/(1-z)]_+$  vanishes [since it is multiplied by  $\ln(Q/\mu)$ ], leaving a large correction from the  $[\ln(1-z)/(1-z)]_+$  term. For example, this term dominates the NLO correction at  $\sqrt{S} = 38.8$  GeV,  $Q = 20$  GeV (see Fig. 4.23) for  $\mu = Q$ , resulting in a 35% correction to the LO cross section.

# References

- [1] F. Maltoni, T. McElmurry and S. Willenbrock, Phys. Rev. D **72**, 074024 (2005) [arXiv:hep-ph/0505014].
- [2] D. A. Dicus and S. Willenbrock, Phys. Rev. D **39**, 751 (1989).
- [3] Z. Kunszt and F. Zwirner, Nucl. Phys. B **385**, 3 (1992) [arXiv:hep-ph/9203223].
- [4] C. Kao and N. Stepanov, Phys. Rev. D **52**, 5025 (1995) [arXiv:hep-ph/9503415].
- [5] J. Dai, J. F. Gunion and R. Vega, Phys. Lett. B **345**, 29 (1995) [arXiv:hep-ph/9403362].
- [6] J. Dai, J. F. Gunion and R. Vega, Phys. Lett. B **387**, 801 (1996) [arXiv:hep-ph/9607379].
- [7] E. Richter-Was and D. Froidevaux, Z. Phys. C **76**, 665 (1997) [arXiv:hep-ph/9708455].
- [8] V. D. Barger and C. Kao, Phys. Lett. B **424**, 69 (1998) [arXiv:hep-ph/9711328].
- [9] D. Choudhury, A. Datta and S. Raychaudhuri, arXiv:hep-ph/9809552.
- [10] C. S. Huang and S. H. Zhu, Phys. Rev. D **60**, 075012 (1999) [arXiv:hep-ph/9812201].
- [11] M. Drees, M. Guchait and P. Roy, Phys. Rev. Lett. **80**, 2047 (1998) [Erratum-ibid. **81**, 2394 (1998)] [arXiv:hep-ph/9801229].
- [12] M. Carena, S. Mrenna and C. E. Wagner, Phys. Rev. D **60**, 075010 (1999) [arXiv:hep-ph/9808312].
- [13] J. L. Diaz-Cruz, H. J. He, T. Tait and C. P. Yuan, Phys. Rev. Lett. **80**, 4641 (1998) [arXiv:hep-ph/9802294].
- [14] C. Balazs, J. L. Diaz-Cruz, H. J. He, T. Tait and C. P. Yuan, Phys. Rev. D **59**, 055016 (1999) [arXiv:hep-ph/9807349].
- [15] C. Balazs, H. J. He and C. P. Yuan, Phys. Rev. D **60**, 114001 (1999) [arXiv:hep-ph/9812263].
- [16] D. Dicus, T. Stelzer, Z. Sullivan and S. Willenbrock, Phys. Rev. D **59**, 094016 (1999) [arXiv:hep-ph/9811492].
- [17] ATLAS Collaboration, Technical Design Report, CERN-LHCC-99-15.

- [18] M. Carena *et al.*, Report of the Tevatron Higgs Working Group, arXiv:hep-ph/0010338.
- [19] T. Affolder *et al.* [CDF Collaboration], Phys. Rev. Lett. **86**, 4472 (2001) [arXiv:hep-ex/0010052].
- [20] J. Campbell, R. K. Ellis, F. Maltoni and S. Willenbrock, Phys. Rev. D **67**, 095002 (2003) [arXiv:hep-ph/0204093].
- [21] F. Maltoni, Z. Sullivan and S. Willenbrock, Phys. Rev. D **67**, 093005 (2003) [arXiv:hep-ph/0301033].
- [22] R. V. Harlander and W. B. Kilgore, Phys. Rev. D **68**, 013001 (2003) [arXiv:hep-ph/0304035].
- [23] S. Dittmaier, M. Krämer and M. Spira, Phys. Rev. D **70**, 074010 (2004) [arXiv:hep-ph/0309204].
- [24] S. Dawson, C. B. Jackson, L. Reina and D. Wackerroth, Phys. Rev. D **69**, 074027 (2004) [arXiv:hep-ph/0311067].
- [25] S. Dawson, C. B. Jackson, L. Reina and D. Wackerroth, arXiv:hep-ph/0408077.
- [26] J. Campbell *et al.*, in *Les Houches 2003: Physics at TeV Colliders*, arXiv:hep-ph/0405302.
- [27] V. Abazov [D0 Collaboration], arXiv:hep-ex/0504018.
- [28] D. Acosta *et al.* [CDF Collaboration], arXiv:hep-ex/0412006.
- [29] J. Campbell, R. K. Ellis, F. Maltoni and S. Willenbrock, Phys. Rev. D **69**, 074021 (2004) [arXiv:hep-ph/0312024].
- [30] V. M. Abazov *et al.* [D0 Collaboration], arXiv:hep-ex/0410078.
- [31] M. A. Aivazis, J. C. Collins, F. I. Olness and W. K. Tung, Phys. Rev. D **50**, 3102 (1994) [arXiv:hep-ph/9312319].
- [32] J. C. Collins, Phys. Rev. D **58**, 094002 (1998) [arXiv:hep-ph/9806259].
- [33] M. Krämer, Nucl. Phys. Proc. Suppl. **135**, 66 (2004) [arXiv:hep-ph/0407080].
- [34] A. D. Martin, R. G. Roberts, W. J. Stirling and R. S. Thorne, Eur. Phys. J. C **23**, 73 (2002) [arXiv:hep-ph/0110215].
- [35] A. D. Martin, R. G. Roberts, W. J. Stirling and R. S. Thorne, Phys. Lett. B **531**, 216 (2002) [arXiv:hep-ph/0201127].
- [36] T. Plehn, Phys. Rev. D **67**, 014018 (2003) [arXiv:hep-ph/0206121].
- [37] E. Boos and T. Plehn, Phys. Rev. D **69**, 094005 (2004) [arXiv:hep-ph/0304034].

- [38] R. Hamberg, W. L. van Neerven and T. Matsuura, Nucl. Phys. B **359**, 343 (1991) [Erratum-ibid. B **644**, 403 (2002)].
- [39] P. J. Rijken and W. L. van Neerven, Phys. Rev. D **52**, 149 (1995) [arXiv:hep-ph/9501373].
- [40] R. V. Harlander and W. B. Kilgore, Phys. Rev. Lett. **88**, 201801 (2002) [arXiv:hep-ph/0201206].
- [41] T. Stelzer, Z. Sullivan and S. Willenbrock, Phys. Rev. D **56**, 5919 (1997) [arXiv:hep-ph/9705398].
- [42] A. Chuvakin, J. Smith and W. L. van Neerven, Phys. Rev. D **61**, 096004 (2000) [arXiv:hep-ph/9910250].
- [43] L. Trentadue and G. Veneziano, Phys. Lett. B **323**, 201 (1994).
- [44] J. M. Campbell and R. K. Ellis, Phys. Rev. D **62**, 114012 (2000) [arXiv:hep-ph/0006304].
- [45] J. Kubar-André and F. E. Paige, Phys. Rev. D **19**, 221 (1979).
- [46] G. Altarelli, R. K. Ellis and G. Martinelli, Nucl. Phys. B **157**, 461 (1979).
- [47] G. Sterman, *An Introduction to Quantum Field Theory* (Cambridge University Press, Cambridge, England, 1993), p. 377.
- [48] F. Maltoni, T. McElmurry, R. Putman, and S. Willenbrock, in preparation.
- [49] J. C. Collins, ANL-HEP-CP-90-58, in *Proceedings of the 25th Rencontre de Moriond: High Energy Hadronic Interactions*, Les Arcs, France, Mar 11-17, 1990, ed. J. Trân Thanh Vân (Editions Frontières, Gif-sur-Yvette, France, 1990), p. 123.
- [50] J. Alwall and J. Rathsman, JHEP **0412**, 050 (2004) [arXiv:hep-ph/0409094].
- [51] J. Pumplin, D. R. Stump, J. Huston, H. L. Lai, P. Nadolsky and W. K. Tung, JHEP **0207**, 012 (2002) [arXiv:hep-ph/0201195].
- [52] D. E. Soper, Phys. Rev. Lett. **81**, 2638 (1998) [arXiv:hep-ph/9804454].
- [53] D. E. Soper, Phys. Rev. D **62**, 014009 (2000) [arXiv:hep-ph/9910292].
- [54] Z. Nagy and D. E. Soper, JHEP **0309**, 055 (2003) [arXiv:hep-ph/0308127].
- [55] G. Sterman, Nucl. Phys. B **281**, 310 (1987).

# Author's Biography

Thomas James McElmurry was born in Madison, Wisconsin, on June 4, 1979, to Brian and Nancy McElmurry. It was a Monday morning, and there have been many more in the years since then. He was raised in Mounds View, Minnesota, and graduated from Irondale High School in 1997. He attended Bethel College in Arden Hills, Minnesota, earning bachelor's degrees in Physics and Mathematics, and graduating *summa cum laude* in 2001. He loved every minute of it, even if he occasionally didn't realize it at the time. In August 2001, he began his graduate studies in the Department of Physics at the University of Illinois at Urbana-Champaign, hoping to unlock all the secrets of the universe, but he'll settle for a Ph.D. He wonders what the future will bring, and hopes it will bring it at a convenient time.